Exploring Sensory Function and Evolution in the Crustacean Visual System

Ana Patricia Parracho Filipe Ramos

Numéro national de thèse : 2017LYSEN091

THESE de DOCTORAT DE L'UNIVERSITE DE LYON

Opérée par

L'ECOLE NORMALE SUPERIEURE DE LYON

Ecole Doctorale N° 340,

Biologie Moléculaire, Intégrative et Cellulaire

Discipline : Science de la vie

Soutenue publiquement le 18/12/2017, par :

Ana Patrícia PARRACHO FILIPE RAMOS

Exploring sensory function and evolution in the crustacean visual system

Étude des fonctions sensorielles et de l'évolution du système visuel des crustacés

---

Devant le jury composé de :

Averof, Michalis Dr.	*École Normale Supérieure de Lyon*	*Directeur de thèse*
Stollewerk, Angelika Prof.	*Queen Mary University of London*	*Rapporteure*
Casares Fernandez, L.Fernando Dr.	*Université Pablo de Olavide, Séville*	*Rapporteur*
Salecker, Iris Prof.	*The Francis Crick Institute, London*	*Examinatrice*
Abderrahman, Khila Dr.	*École Normale Supérieure de Lyon*	*Examinateur*

Abstract

The wide diversity of eye designs present in arthropods makes them a unique group for studying the diversity and evolution of the visual system. However, most of our knowledge on the development and the neural architecture of the visual system comes from few model organisms. My project aims to contribute to the study of the diversity and evolution of the arthropod visual system by studying the eye of the crustacean *Parhyale hawaiensis*; focusing on its development, neuroarchitecture and function. In particular, my work aims to characterize the structure of the visual system, to map the connections between photoreceptors and optic lobe and to understand the functional adaptations of the eye, in relation to the eyes of other arthropods.

A description of the basic anatomy of the visual system was performed by means of electron microscopy, immunostainings and by generating transgenic reporter lines. I found that *Parhyale* has an apposition-type compound eye composed of around 8 (in hatchlings) to 50 (in adults) ommatidia. Each ommatidium is formed by 5 photoreceptor cells (R1-R5).

Two opsins were found to be encoded in the genome and transcriptomes of *Parhyale*, named Ph-Opsin1 and Ph-Opsin2. Ph-Opsin 1 is most closely related to the long-wavelength opsins of crustaceans and insects, whereas Ph-Opsin2 is most closely related to crustacean mid-wavelength opsins. In situ hybridization showed that these *Parhyale* opsins are exclusively expressed in the retina. Using the genome sequence as a guide, I cloned upstream regulatory sequences from each opsin genes and generated transgenic reporters that recapitulate the expression patterns of Ph-Opsin1 and Ph-Opsin2. As a result, two stable transgenic lines were generates: Ph-Ops1::GFP-CAAX and Ph-Ops2::mKate-CAAX. These reporters revealed that each opsin is expressed in a different subset of photoreceptor cells: R1-R4 express Ph-Opsin1 while R5 expresses Ph-Opsin2.

Immunostainings with antibodies directed against acetylated-tubulin, as well live imaging of the two transgenic lines, showed that photoreceptor cells send long projections from the retina to the optic lobe. Unlike *Drosophila* and other crustaceans, where the optic lobe is distinct from the central brain and located close to the retina, in *Parhyale* the optic lobe seems to be located away from the retina and closer to the central brain. Three optic

neuropils were identified: the lamina, the medulla and a deeper neuropil which is possibly the lobula or lobula plate. The opsin-driven reporters allowed me to follow the axonal projections of the photoreceptors into the brain, revealing that all photoreceptors project to the lamina. This differs from what has been shown in dipterans and crustaceans, where at least one photoreceptor per ommatidium projects to the medulla.

To perform a more detailed study of photoreceptor projections into the optic lobes, a Brainbow-like stochastic cell marking method is currently being adapted to label the photoreceptors and brain. This tool, still in development, will allow me to differentiate individual photoreceptor projections and to gain insights into the processing of visual signals.

Electron microscopy showed that the rhabdomeres of two pairs of photoreceptors, R1+R3 and R2+R4, are orthogonally aligned to each other in each ommatidium, and that the rhabdom does not rotate. These features render the photoreceptors intrinsically sensitive to specific directions of light polarisation and are typical of ommatidia involved in polarised light detection. Therefore, I tried to understand whether and how *Parhyale* respond to polarised light by means of behavioural experiments. I developed two experimental setups (a T-maze and an escape arena), to address whether *Parhyale* have phototactic and polarotactic responses and whether they show other behavioural responses triggered by light polarisation. The data I have collected suggest that *Parhyale* are phototactic to dim white light but show no response to polarised light in these specific experimental assays. Potential problems with these behavioural assays are discussed.

Finally I show that the eye of *Parhyale* quickly adapts to different conditions of light intensity. This is achieved by movement of the shielding pigment granules, located inside the photoreceptor cells and by morphological changes of the photoreceptor basal membrane.

This project is pioneering the study of the visual system in *Parhyale*. It is the first time that genetic tools have been introduced to study the crustacean visual system. It establishes *Parhyale* as a powerful experimental system for in vivo studies of compound eye development and axonal targeting, a field currently dominated by studies in a single species of fruitfly.

Sommaire

La grande variété de morphologie de l'appareil visuel chez les arthropodes en fait un groupe unique pour l'étude de la diversité et l'évolution du système visuel. Cependant, la plupart de nos connaissances sur le développement et l'architecture neurale du système visuel provient de quelques organismes modèles. Mon projet vise à contribuer à l'étude de la diversité et de l'évolution du système visuel des arthropodes en étudiant l'œil du crustacé *Parhyale hawaiensis*; axé sur son développement, sa neuro-architecture et sa fonction. En particulier, mon travail vise à caractériser la structure du système visuel, à cartographier les connexions entre les photorécepteurs et le lobe optique et à comprendre les adaptations fonctionnelles de l'œil, par rapport aux yeux des autres arthropodes.

Une description de l'anatomie de base du système visuel a été réalisée au moyen de la microscopie électronique, par immunomarquage et par la production de lignées de transgénique. J'ai trouvé que *Parhyale* possède un œil composé de type apposition composée d'environ 8 (chez les nouveau-nés) à 50 (chez les adultes) ommatidies. Chaque ommatidie est formée par 5 cellules photoréceptrices (R1-R5).

Nous avons trouvé que deux opsines étaient codés dans le génome et transcriptome de *Parhyale*, nommés Ph-Opsin1 et Ph-Opsin2. Ph-Opsin1 est plus proche à des opsines des crustacés et des insectes avec une longue longueur d'onde (LWS), tandis que Ph-Opsin2 est plus étroitement apparenté aux opsines de longueur d'onde moyenne (MWS) des crustacés. L'*hybridation in situ* a montré que ces opsines *Parhyale* sont exclusivement exprimés dans la rétine. En utilisant la séquence génomique comme guide, j'ai cloné des séquences régulatrices en amont de chaque gène d'opsine et généré des rapporteurs transgéniques qui récapitulent les patterns d'expression de Ph-Opsin1 et de Ph-Opsin2. Par conséquent, deux lignées transgéniques stables ont été générées: Ph-Ops1:: GFP-CAAX et Ph-Ops2:: mKate-CAAX. Ces rapporteurs ont révélé que chaque opsine est exprimée dans un sous-ensemble différent de cellules photoréceptrices: R1-R4 exprime Ph-Opsin1 tandis que R5 exprime le Ph-Opsin2.

Les immunostainings avec des anticorps dirigés contre la tubuline acétylée, ainsi que l'imagerie des deux lignées transgéniques, ont montré que les cellules photoréceptrices envoient de longues projections depuis la rétine au lobe optique. Contrairement à *Drosophila* et aux autres crustacés, où le lobe optique est distinct du cerveau central et est situé près de la rétine, dans *Parhyale* le lobe optique semble être situé loin de la rétine et plus près du cerveau central. Trois neuropiles optiques ont été identifiés: la lamina, la medulla et un neuropile plus profond qui est probablement la lobula plate ou la lobula. Les rapporteurs opsines m'ont permis de suivre les projections axonales des

photorécepteurs dans le cerveau, révélant que tous les photorécepteurs se projettent dans la lamina. Ceci diffère de ce qui a été montré chez les diptères et les crustacés, où au moins un photorécepteur par ommatidie projette ses axones dans la medulla.

Pour effectuer une étude plus détaillée des projections des photorécepteurs dans les lobes optiques, une méthode de marquage stochastique des cellules (comme la technique 'Brainbow') est actuellement en cours d'adaptation pour marquer les photorécepteurs et le cerveau. Cet outil, encore en développement, me permettra de différencier les projections individuelles des photorécepteurs et d'acquérir des connaissances sur le traitement des signaux visuels.

La microscopie électronique a montré que les rhabdomères des deux paires de photorécepteurs, R1 + R3 et R2 + R4, sont orthogonalement alignés les uns aux autres dans chaque ommatidie, et que le rhabdome ne tourne pas. Ces caractéristiques rendent les photorécepteurs intrinsèquement sensibles aux directions spécifiques de la lumière polarisée; ces caractéristiques sont typiques des ommatidies impliquées dans la détection de la lumière polarisée. Par conséquent, j'ai essayé de comprendre comment réagît *Parhyale* à la lumière polarisée, au moyen d'expériences comportementales. J'ai développé deux configurations expérimentales (un T-Maze et une arène d'évasion), pour répondre à la question de savoir si *Parhyale* ont des réponses phototactiques et polarotactiques et si elles montrent d'autres réactions comportementales déclenchées par la polarisation de la lumière. Les données que j'ai recueillies suggèrent que *Parhyale* sont phototactiques pour la lumière blanche mais ne montrent aucune réponse à la lumière polarisée dans ces essais expérimentaux. Les problèmes potentiels liés à ces tests de comportement sont discutés.

Enfin, je montre que l'œil de *Parhyale* s'adapte rapidement à différentes conditions d'intensité lumineuse. Ceci est obtenu par le mouvement des granules de pigments, situés à l'intérieur des cellules photoréceptrices, et par des changements morphologiques de la membrane basale du photorécepteur.

Ce projet est pionnier dans l'étude du système visuel chez *Parhyale*. C'est la première fois que des outils génétiques ont été introduits pour étudier le système visuel de crustacés. Il établit *Parhyale* comme un puissant système expérimental pour des études in vivo de développement des yeux composé et de ciblage axonal du system visuel, un champ actuellement dominé par des études sur une seule espèce de mouche.

Acknowledgments

4 years of PhD wouldn't have been possible without the contribution of many people, professionally and personally. It has been a long, sometimes tortuous, road and I couldn't be more grateful to those who gave me the strength to keep going.

My first thank you goes to Michalis. Thanks for the opportunity of working and learning with you. For being always there in desperate times, for the support and enthusiasm. For giving me the needed liberty to carry on this project.

To my thesis committee members, Abdou and Iris. I'm not sure if I could have asked for a more supportive committee. A special thanks to Iris for the patience in sitting next to me in front of a computer, trying to understand the *Parhyale* optic lobe.

Few people need to be thanked for their participation in this project. Namely Dan-Eric Nilsson, Ola Gustafsson and Carina Rasmussen, who made the TEM imaging possible. Also a thank you to Nicola Labert for the histology preparations. A special thanks to François Lapraz (and Max Telford) for the precious help (and step by step guide) with the opsin phylogeny.

To the Averof lab, for the support, discussions and coffees. An enormous thank you to Nikos who taught me everything about *Parhyale*, and to Marco who, literally, spent these last 4 years by my side, listening to my complaints and offering coffee. I'm still surprised how you managed to restrain yourself, even with so many spoons around. A big thank you to Jana for embarking on the (frustrating) *in situ* project.

To the Neptune 'family'. So many things shared along these years, so many places visited and wonderful times spent. It has been a pleasure to share with you this long road. I can only hope that we manage to meet again.

To my 'Lyon Is The Best' crew, Meli, Emilia, Ian, Marco, Leiore, Nikos, Mari, Lorenzo and Rodrigo, plus new additions Pierre, Federica, and Roberto. You have made my life in Lyon possible. So many moments that no words would do them justice. Emilia and Mari thanks for… being. To Guillaume, for being always ready to show me how important research is. Pour mes chères colocataires, pour toute la convivialité et mots de support pendant l'écriture de cette thèse.

To my dearest friends Bia, Ana, Miguel, Magda, Vitinho, for being there despite the distance.

E finalmente um obrigado à famelga, pelo apoio incondicional.

Merci, Obrigada, Grazie, Gracias, Eskerrik asko, Ευχαριστούμε, Danke.

Table of Contents

In the study of this membrane I for the first time felt my faith in Darwinism weakened, being amazed and confounded by the supreme constructive ingenuity revealed not only in the retina […] of the vertebrates but even in the meanest insect eye.

Santiago Ramón y Cajal

Recollections of My Life (1898), 576.

Preamble

1. General introduction to visual systems

Eyes are probably the most exciting sensory organs that we possess. They are found in most animals; and are one of the features that distinguish animals from plants, fungi and unicellular organisms.

But what do you need to build an eye? If we think about a digital camera there are 3 main structures that contribute to the final image: the lenses, a sensor that captures the light and an electronic body that processes and transmits the information in a readable manner to the user. An eye has the same basic components: lenses to guide the light, a sensor composed of photoreceptor cells which contain light-sensing molecules, and a processor, consisting of the brain structures dedicated to the processing of the visual scene (referred to as the optic lobes). This comparison leads to the following definition of an eye: Any dioptric apparatus that focuses light on photoreceptor neurons, which convey information to retinotopically organized neural centres (Strausfeld et al., 2016).

Visually guided behaviours have shaped the evolution of eyes: more demanding behaviours (for example detection of fast moving objects or the need to discriminate colours) required more complex visuals systems. On the other hand, visual ecology – i.e. the ways by which eyes contribute to the animal's life style – has shaped evolution of the ecosystem, influencing how animals find their food, how they escape from becoming someone else's food, how they find their way back home, how they mate, etc. In other words, it contributes to shaping the fitness.

Eye Evolution

Most of the eye types that we know today arose during the Cambrian period, around 550 Mya. The oldest eye fossils found, which date from this period, already show a high level of complexity and there is no fossil evidence on earlier types of eye, making hard to predict the course of eye evolution. However, visual structures with different levels of complexity, adapted to the animal's needs, can nowadays be found through the animal kingdom, giving a hint on how could have the eyes evolve. This comparative view has led to a model on eye evolution, based in four stages (Fig. 0-1) (Nilsson, 2009).

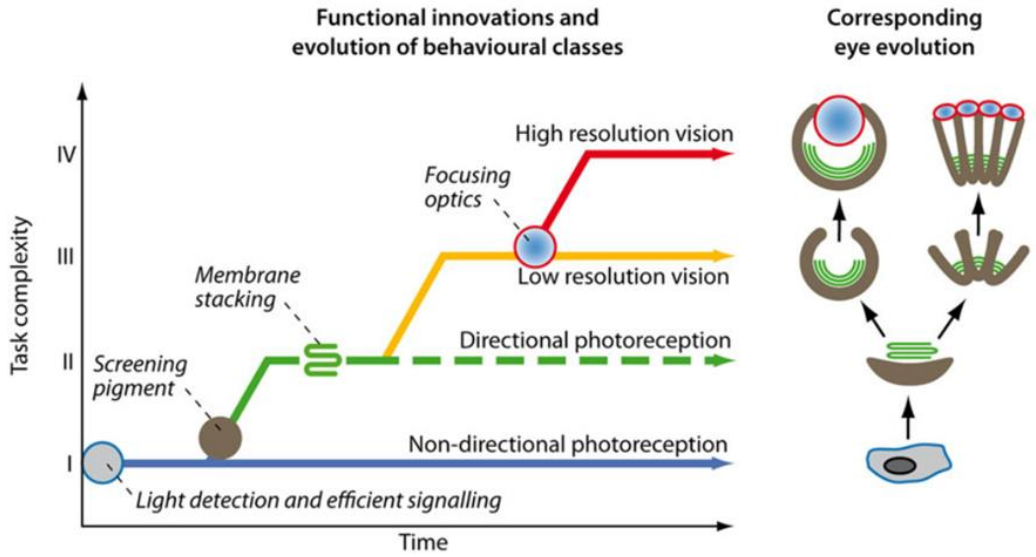

Fig. 0-1 Four stages of eye evolution – Major functional innovations during eye evolution allowed the organisms to perform increasingly complex tasks (from Nilsson, 2009)

The first step to build an eye is to couple a light sensing molecule, the opsin, to a signalling system, thus forming a photoreceptor. This simple coupling, found for example in sea urchin and sea star larvae, gives the animal the opportunity to monitor ambient light intensity, which can provide information for day/night rhythms or position in the substrate/water column. The addition of a shielding pigment, which blocks light from certain directions, gives the animals the capability to know where the light is coming from, allowing for phototactic behaviour. True vision of low and high resolution arises from the multiplication of directional photoreceptors and addition of dioptric apparatus, which provides animals with spatial vision and the ability to form images.

Evolution of photoreceptors

Photoreceptor neurons carry the opsins and transmit the information that they produce to the brain. Photoreceptor cells involved in vision acquired a morphological modification which allowed them to hold a large quantity of opsin molecules, crucial for efficient detection of light: a large expansion of the cell membrane on the apical side of the cell, which forms multiple layers arranged perpendicularly to the expected direction of the incoming light. This modification was accomplished in 2 ways, giving rise to the 2 types

of visual photoreceptors known: the rhabdomeric photoreceptors and the ciliary photoreceptors. The first type presents bundles of microvilli, extending parallel to each other, while the second type carries stacks of membrane derived from cilia. In both types, these stacks of membranes hold the transmembrane opsin molecules.

Camera eyes and compound eyes

The multiplication of photoreceptors, during the course of eye evolution, gave rise to the two major types of eyes seen in animals: camera eyes and compound eyes (Fig. 0-2).

Camera eyes are characterized by the presence of a single optical unit that focuses the image into an underlying layer of photoreceptive cells that compose the retina. These eyes are mostly present in vertebrates but can also be found in molluscs, annelids, crustaceans (copepods), cnidarians, arachnids and insects (as ocelli and larval eyes). Despite this widespread distribution, camera eyes don't have a single origin but arose by convergent evolution in the different animal groups. The most striking example of convergent camera eyes is that of the octopus eye which, compared to the vertebrate eye, presents a different kind of photoreceptor cell (rhabdomeric vs ciliary) and a retina with a different structure (photoreceptors having opposite orientations with respect to the incoming light).

Compound eyes, on the other hand, are formed by repetitive structures, the ommatidia. Each ommatidium, which is tubular in shape, is composed of an optic apparatus that guides light to rhabdomeric photoreceptor cells that lay beneath.

Compound eyes are the most common eyes in the animal kingdom, but are mostly found in arthropods. Some annelids and bivalve molluscs also present compound eyes, but in a more rudimentary form.

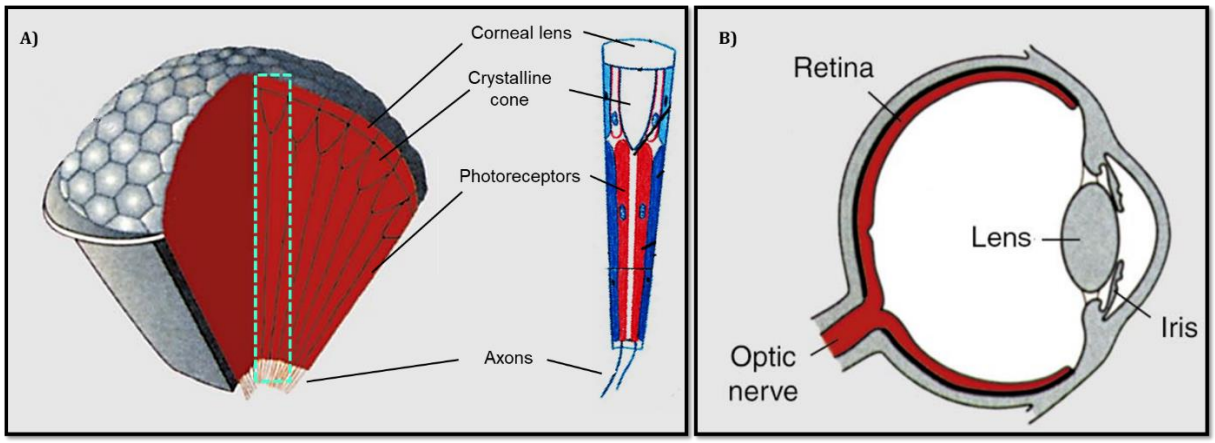

Fig. 0-2 Two major types of eyes - A) Compound eyes are formed by repetitive units, the ommatidia, which contain the lens (corneal lens and crystalline cone) and the rhabdomeric photoreceptors which connect to the brain. **B)** Camera eyes have a single lens that focus the light into the retina, composed by the photoreceptors and interneurons. *Adapted from* (Gehring and Ikeo, 1999)

Opsins and spectral sensitivity

The capacity of an animal to adapt the visual system to its needs and to the environment that surrounds him, is intrinsically related to the spectral sensitivity given by the opsin.

Opsins are members of the G protein coupled receptors, composed of 7 transmembrane helices, which activate internal signal transduction pathways. They are covalently bound to an UV sensitive chromophore (usually a retinal) at lysine residue of the 7th helix. The connection of the opsin to the chromophore will shift its absorbance spectrum towards the red. Fine tuning of the spectral sensitivity is then determined by specific amino acids present in the opsin, at the side chains of the binding pocket.

Based on phylogenetic analysis of opsin sequences, we can distinguish 4 major classes of opsins in the animal kingdom (Porter et al., 2012a):

- C- opsins, present in ciliary photoreceptors
- Cnidopsins, present only in cnidarians and ctenophores
- R-opsins, present in rhabdomeric photoreceptors
- Group 4 opsins, less characterized opsins, including retinal G-protein-coupled receptor neuropsins and peropsins.

The most common types of opsins are the C and R opsins. They differ in their modes of function: when activated by light, C-opsins cause the hyperpolarisation of the cell, followed by a G_T signalling cascade, whereas R-opsins depolarize and have a G_q signalling transduction pathway.

For 3 of these 4 groups we can find members of all animal taxa, suggesting that multiple lineages of opsins were already present in the last common metazoan.

Opsins are expressed in a wide variety of tissues and cell types, and not all are used for image formation. Examples include the pinopsins and parapinopsin (C-opsins), found in the pineal organ of birds, lizards and lamprey, peropsin, expressed in the bee's brain, melanopsins (R-opsins), which are present in the vertebrate retina but are responsible for setting of the circadian rhythms rather than image formation (Do et al., 2009) and the R-opsins expressed in the tube feet of sea urchins(Lesser et al., 2011).

Visual opsins can be separated into 3 classes, based on their absorbance spectra: long-wavelength (LWS), middle-wavelength (MWS) and short-wavelength (SWS), corresponding to green-yellow, blue and UV absorbance spectra respectively (Fig. 0-3).

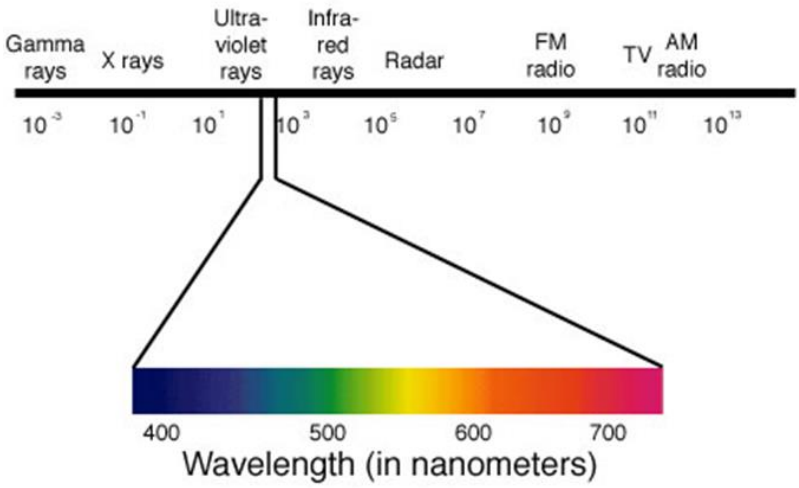

Fig. 0-3 The electro-magnetic spectrum Visible light has a frequency from ~400 to ~750 nm

2. Vision in arthropods

Arthropods have the widest diversity of eye designs in the animal kingdom making this an exceptional group for studying eye evolution. The panoply of species, their wide range of habitats and diverse modes of living are reflected in the number of eye designs present, revealing the importance of the visuals system to the adaptation of the animals to their habitats.

In extant arthropods, we can find 4 main types of eyes (reviewed in (Nilsson and Kelber, 2007; Strausfeld et al., 2016)):

- Compound retinas with fixed number of photoreceptors per ommatidium and lenses formed by crystalline cone cells
    - Typical in insects, crustaceans and scutigeromorphs (Myriapoda)
- Large corneal eyelets surmounting a varying number of stacked photoreceptors
    - Found in myriapods (except Scutigeromorpha)
- Compound retinas with variable numbers of photoreceptors and corneal lenses
    - Found in Xiphosuran eyes
- Single lens eyes
    - Found in Chelicerates (except Xiphosura)

The earliest compound eyes found in the fossil record belonged to radiodontans, a lineage belonging to the arthropod stem group, whose emergence preceded arthropodization. Radiodontans are considered to be the largest predators during the Cambrian. They possessed enormous compound apposition eyes, with up to 16000 facets (Cong et al., 2014; Paterson et al., 2011).

The finding of radiontan compound eyes in the Cambrian, supports the position that high resolution apposition compound eyes, with isomorphic ommatidia and a fixed number of photoreceptor cells, are the ground pattern organization for arthropods (Strausfeld et al., 2016). From that ancestral state, we see significant conservation in crustaceans and insects, and radical divergence in chelicerates (including single lens eyes of arachnids) and myriapods (except scutigeromorphs).

The architecture of the visual system has been extensively used to reconstruct the phylogenetic relationships between arthropods. The first theory that insects and malacostracan crustaceans would share a common ancestor was based on comparisons of their retinal structures by E. Ray Lankester in 1904.

While there is an ongoing debate on the phylogenetic relationships of different arthropod groups, recent studies point clearly towards a shared ancestor of insects and crustaceans, giving rise to the monophyletic group Pancrustacea. The interrelationships within this group are still controversial (Fig. 0-4) (Budd and Telford, 2009; Cong et al., 2014; Legg et al., 2013; Regier et al., 2010).

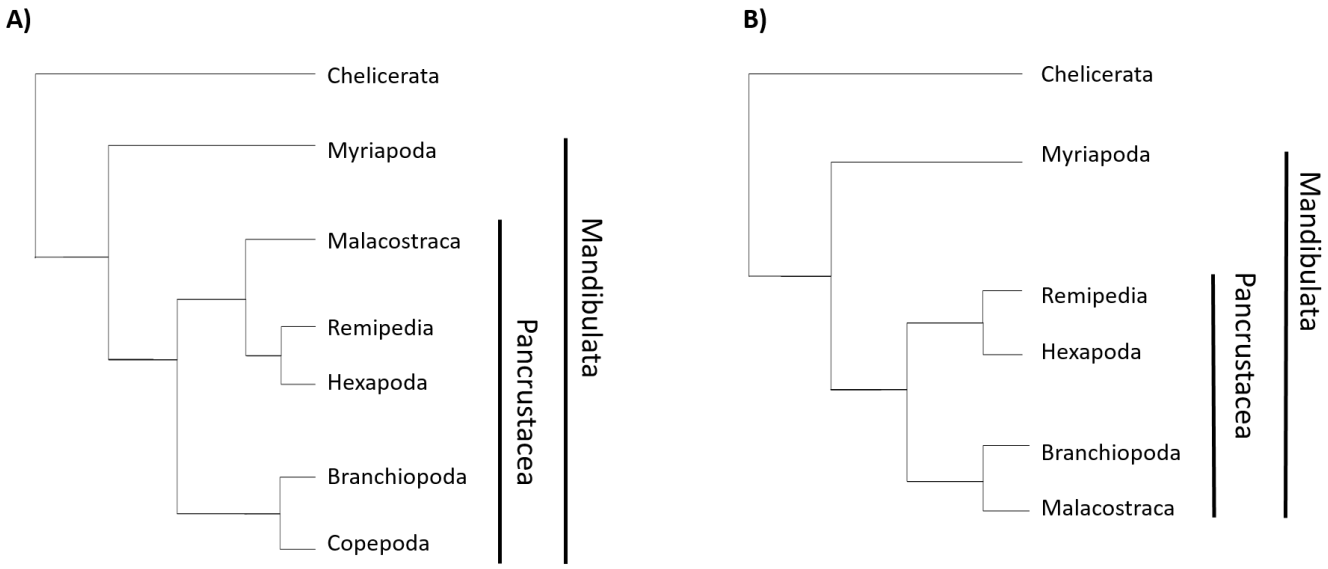

Fig. 0-4 Arthropod phylogeny – Two of the current views on arthropod phylogeny based in Legg et al. 2013 (A) and Regier et al. 2010 (B)

Despite the long-lasting interest in the study of arthropod eyes, most of our knowledge on the development and neural architecture of the visual system comes from few model organisms, usually hexapods. The most profound knowledge we have comes from *Drosophila melanogaster*, where genetic/molecular tools allow for a careful study the architecture of the visual system and on the molecular players that give rise to it.

The visual systems of crustaceans have been studied largely in the context of ecology and neuro-physiology, but not in a scale comparable to hexapods. Contributions on the development of crustacean eyes are still scarce and largely descriptive. Part of the reason for this is the lack of model organisms suitable for genetic manipulation. This scenario has been changing recently with the adaptation of the small crustacean *Parhyale hawaiensis* to the lab life.

3. *Parhyale* hawaiensis

Life cycle

Parhyale is a small malacostracan crustacean of the order Amphipoda.

The generation time of *Parhyale* is approximately 2 to 3 months at 26ºC and animals will continue to grow throughout their lifetime (from ~1 to ~10mm in lenght). Reproduction is continuous throughout the year, as long as the conditions are favourable. For reproduction, the male grabs the female, forming a couple, until oviposition and fertilisation of the eggs. The fertilized eggs are carried by the female in a brood pouch, situated ventrally between the thoracic appendages. Hundreds of eggs at 1-cell stage can be obtained daily from anesthetized females for injections. Once the embryos hatch, they are released from the brood pouch and sexual maturation will be reached after ~7 weeks.

Parhyale has a direct development; the duration of embryogenesis is 10-12 days at 26ºC and developmental stages have been described(Browne et al., 2005). Early cell lineage is stereotypical (a common feature of malacostracan embryos (Dohle and Scholtz, 1988; Dohle et al., 2004)): the first cleavage separates left from right side for most of the ectodermal and mesodermal tissues and at the 8-cell stage each blastomere will contribute to a single germ cell layer (Gerberding, 2002; Wolff and Gerberding, 2015). This characteristic allowed for studies on germ layer specification and compensation during development (Alwes et al., 2011; Gerberding, 2002; Price et al., 2010) and limb regeneration (Alwes et al., 2016; Konstantinides and Averof, 2014). Cell divisions and migration during gastrulation are also described (Alwes et al., 2011; Chaw and Patel, 2012).

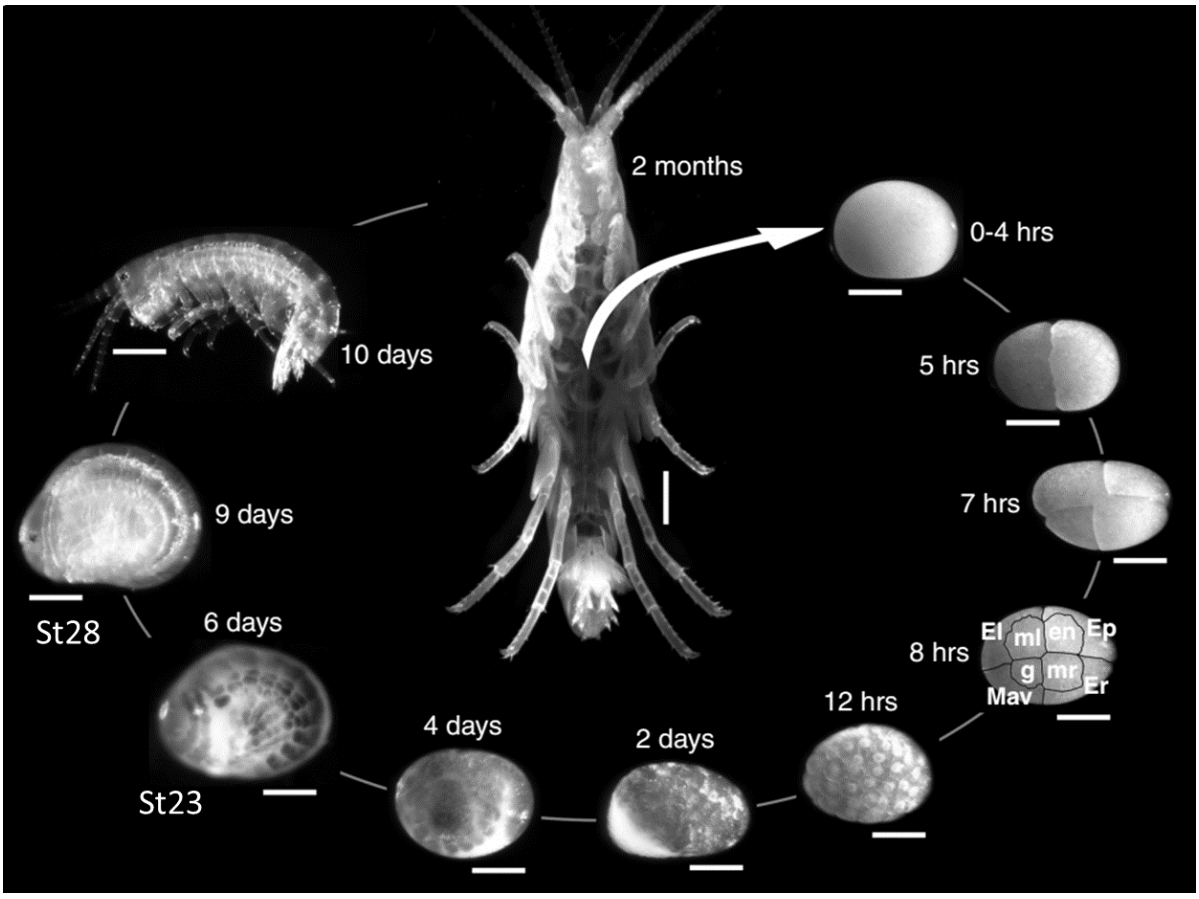

Fig. 0-5 *Parhyale hawaiensis* life cycle – Adult *Parhyale* reach sexual maturation at around 2-3 months. Embryogenesis lasts 10 days at 26ºC. Embryos at one cell stage can be retrieved from dormant females and cultured in sea water. 8 hours after fertilization the egg underwent a total of three cleavages, giving rise to 4 micromeres and 4 macromeres with restricted cell fates: **El**, **Er** and **Ep** give rise to left, right and posterior ectoderm, respectively; **Mav** gives rise to the anterior and visceral mesoderm; **ml**, **mr** originate the left and right mesoderm; **en** gives rise to the endoderm and **g** to the germline. After 9 days, at stage 28, the eyes present a red pigmentation. All scale bars are 200 µm except in the adult female that is 1000 µm. A*dapted from* (Stamataki and Pavlopoulos 2016). Stages after (Browne et al., 2005), early cell lineage from (Gerberding 2002).

Habitat

The colonies that inhabit the labs around the world today, have all come from a single population, found in the filtration system of the John G. Shedd Aquarium in Chicago in 1997. The original source of that population is unknown.

In nature, *Parhyale* is distributed worldwide in tropical areas, in intertidal and shallow waters such as mangroves or rocky shores. Sighting records include the Lizard Islands (Australia), the Canary Islands, Trinidad, south-eastern Brazil, Fiji Islands. Frequent changes in salinity, temperature and turbidity in these habitats have produced a robust species that can be easily kept in the lab.

Behaviour studies on circadian clocks show some evidence for an increased activity of *Parhyale* during the night (B. Hunt PhD thesis), peaking at sunrise and sunset hours.

Working with Parhyale

Parhyale was introduced to the lab by Brown and Patel in late 1990s. It has been used as a research model for almost 20 years, with a community of researchers engaged in developing new experimental tools in this species. Transgenesis (Pavlopoulos and Averof, 2005), gene misexpression (Pavlopoulos et al., 2009), gene knockdown(Liubicich et al., 2009; Özhan-Kizil et al., 2009), CRISPR/Cas9-mediated gene editing(Martin et al., 2016) , a sequenced genome and other genomic and transcriptomic resources (Blythe et al., 2012; Kao et al., 2016; Nestorov et al., 2013; Parchem et al., 2010; Zeng et al., 2011) are available in this species.

These tools and the fact that crustaceans are a sister group to hexapods, make *Parhyale* an attractive organism to compare with *Drosophila* and to make inferences about the evolution of developmental, morphological and physiological traits.

One of the most impressive features of *Parhyale* is its amenability for live imaging. The transparency of the embryos and of the adult cuticle allows imaging and cell tracking in embryonic, juvenile and adult stages for several days (examples in Fig. 0-6). Stunning examples are the reconstruction of the cell lineages underlying limb outgrowth using light-sheet microscopy (Wolff et al., 2017) and in the study of cell dynamics during limb regeneration (Alwes et al., 2016). Combining this characteristic with the possibility of transgenesis makes *Parhyale* a powerful organism for studying development, regeneration and cell behaviour in real time.

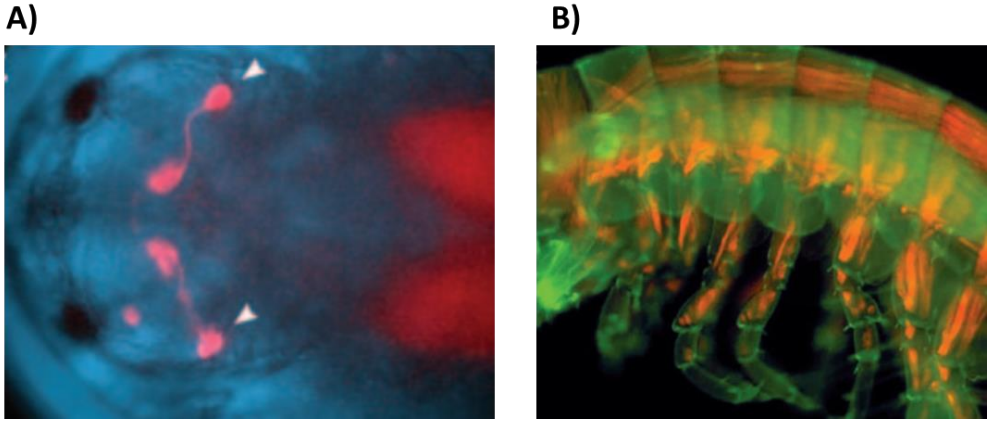

Fig. 0-6 Live imaging in *Parhyale* – A) Head of a *Parhyale* embryo seen from the dorsal side, showing dsRed expression driven by the 3xP3 regulatory sequence (white arrows) **B)** Trunk of a *Parhyale* juvenile, showing dsRed expression driven by the Ph-MuscleSpecific regulatory regions. *From* (Pavlopoulos 2005)

Despite the established genetic tools, many others which are routinely used in other model organisms (such as zebrafish and *Drosophila*) have failed to work in *Parhyale*. Namely we are still missing a constitutive/ubiquitous promoter despite several trials with endogenous and viral promoters (N. Konstantinides PhD thesis and A. Pavlopoulos personal communication). Also using the Cre/lox and Flp/FRT recombination systems, often employed to generate cell mosaics, proved unfruitful (N. Konstantinides PhD thesis and M. Grillo personal communication).

Cell specific markers are also still missing. One of the reasons for this is the difficulty in exploring the *Parhyale*'s genome for regulatory regions, due to the large intergenic regions. A gene-trapping approach has been established in *Parhyale* (Kontarakis et al., 2011), and few gene-trap screens have been conducted in the lab, yielding a few gene-trap lines. However, more often than expected, many of these lines proved to be unstable, both in maintenance of the trap and survival rates.

4. Purposes of the project

The diversity seen in arthropod visual systems is achieved by modifications on the optical properties of the eye and neuroanatomy. Processing of information is dependent on the connections established between the eye and the brain and within the optic neuropils.

In arthropods, the knowledge on visual information processing has been largely driven by studies in a few model organisms, and principally *Drosophila*. The development of molecular, genetic and imaging tools in this model organism has provided great insight on the development, the neuroanatomy and sensory processing in the visual system. Outside the diptera clade, most of the studies on arthropod visual systems have relied on the usage of more classical techniques, such as transmitted electron microscopy, electrophysiology and unspecific/stochastic labelling of neuronal cells (e.g. Golgi staining). This is due, in part, on the difficulty applying modern molecular, genetic and imaging tools to non-model organisms.

Studies in *Drosophila* have been giving us an enormous amount of knowledge on the function of the arthropod visual system, however the lack of other organisms where genetic and imaging tools can be applied leads to a lack of knowledge on the diversity of how the visual system develops and functions, and, consequently, on its evolution. The need for new arthropod models to study the visual system has, therefore, become very important.

Parhyale has proven to be a reliable model organism where genetic and imaging tools can be applied. This provides the opportunity to compare crustacean and dipteran visual

systems in greater depth, and gain insights on the diversity and evolution of the visual system development, structure and function.

I started this project with two main (related) objectives: 1) To explore the visual system of *Parhyale*, focusing on a description of the eye structure, neuroarchitecture and function; 2) to develop genetic tools that allow us to label different neuronal cell types, helping to identify (and possibly manipulate in the future) different components of the visual system, starting from the primary visual sensors, the photoreceptors cells.

PART 1

A DESCRIPTION OF THE *PARHYALE* VISUAL SYSTEM

I. Introduction

I.1 - The compound eye

The compound eye is formed by an array of multiple repetitive units, the ommatidia. Each of these units collects/senses lights from a small region in space, therefore a larger number of ommatidia results in higher image resolution. In each ommatidium we can find an optic apparatus composed of one or more lenses – usually an outer cuticular lens (or corneal lenses) and an inner lens formed by the cone cells (crystalline cone) – lying over a cluster of photoreceptor cells and their light sensing structures (the rhabdomeres). The cluster of rhabdomeres in each ommatidium is called a rhabdom; when the rhabdomeres are tightly clustered together, it is said to be a 'fused' rhabdom, when they are separated it is said to be 'open' (Fig. I-1). Open rhabdoms are found in fruit flies and house flies, while bees, mosquitos, beetles and most crustaceans have fused rhabdoms. In insects, the transition from close to open rhabdom seems to be associated with the expression of the gene *Spacemaker* (*spam*), which is only found in the eyes of insects with open rhabdom. Knock out (KO) of *spam* in insects with open rhabdom leads to a fused rhabdom. The opposite happens when *spam* is overexpressed in insects with a fused rhabdom (Zelhof et al., 2006).

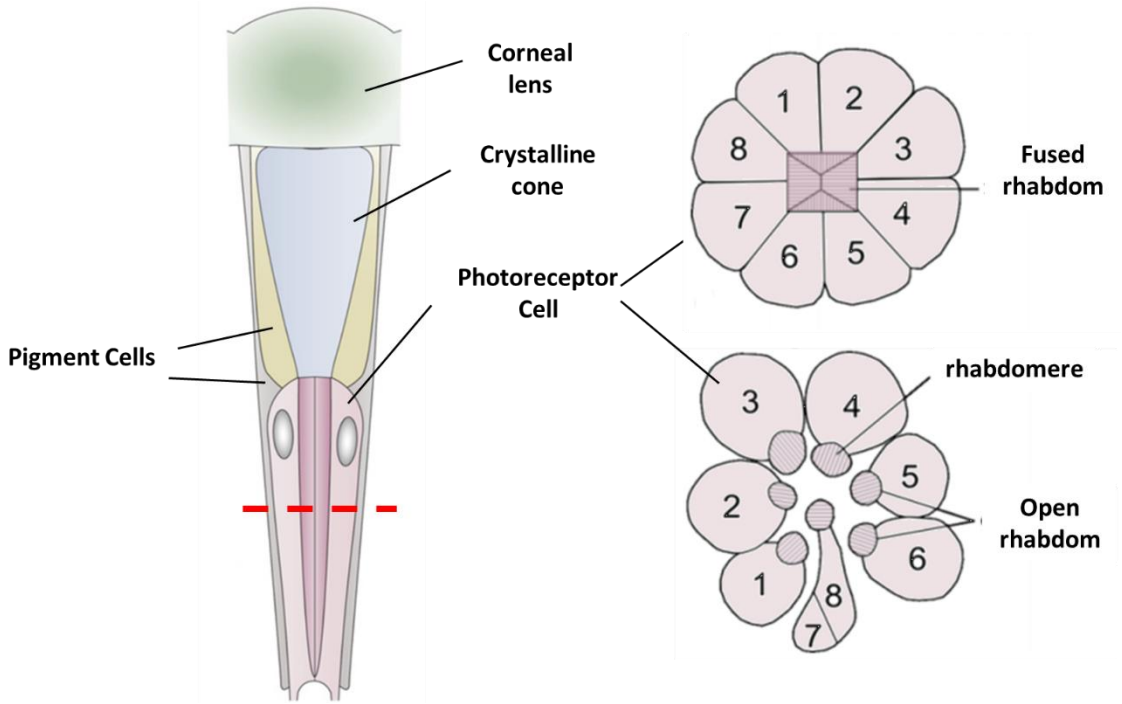

Fig. I-1 The ommatidium – Schematic representation of a typical hexapod ommatidium with 8 photoreceptor cells and either an open or a fused rhabdom. *Adapted from* (Dan-E.Nilsson 2013) *and* (Karman S. 2012)

In addition to the light focusing and sensing apparatus, pigment cells, containing granules of reflective or shielding pigment also make part of the ommatidium. This pigment, which can also be found inside the photoreceptor cells, is crucial to control the influx of light into the rhabdom, as I will discuss in Part 2 of this thesis.

Many specific modifications of this architecture occur across the arthropods.

I.1.A - Three types of compound eyes

The diversity seen in compound eyes comes from variations in the number of ommatidia, in the optic apparatus and in the neural wiring. These changes influence the resolution and sensitivity of the eye and are adapted to the animals' needs within a specific habitat (for example, vision in water vs air or night vs day)

On the basis of changes in the optical arrangement and neural wiring, we can distinguish 3 main types of compound eyes: Apposition, superposition and neural superposition eyes(reviewed in(Cronin et al., 2014)) (Fig. I-2)

Apposition compound eyes

Apposition eyes are present in most diurnal insects and crustaceans. In apposition compound eyes the photoreceptors lie right beneath the lenses (crystalline cones) and extend until the proximal part of the retina. When the light enters the ommatidium through he crystalline cones, the rhabdom serves as a light guide, causing multiple reflections that will make the light to travel down until the most proximal tip. To avoid scattering of light between ommatidia, each ommatidium is surrounded by sleeves of light-absorbent screening pigments

The field of view of each ommatidium is defined by the acceptance angle, which is determined by the shape and size of the lenses. The final image perceived consists of a set of pixels, each detected by one ommatidium.

Superposition compound eyes

The main differences of superposition eyes, compared to apposition eyes, is the fact that each ommatidium is not separated by shielding pigment and the rhabdom is separated from the crystalline cone by an optically homogeneous "clear zone".

Due to this arrangement, and to remarkable specializations of the crystalline cones, light rays entering several facets can be focused on each single rhabdom.

Since each photoreceptor receives light from many facets, the sensitivity of the eye is boosted, making the superposition eyes a common design in insects and crustaceans active under dim light conditions, such as nocturnal moths or deep sea crustaceans. However, the increase in sensitivity has costs: the absence of a shielding pigment results in decreased contrast and spatial resolution. Some species manage to overcome this trade off by employing additional specializations, allowing them to see colours at night and to follow the dim polarisation pattern of the moon light.

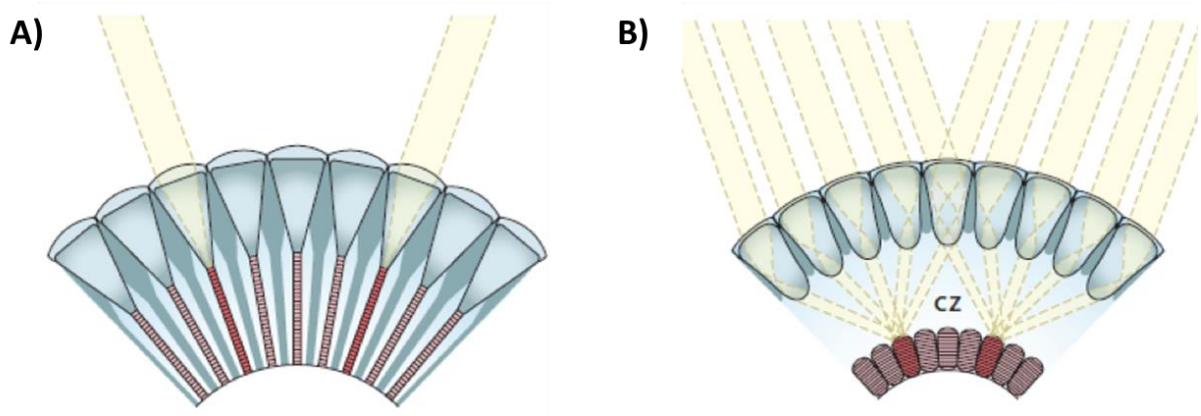

Fig. I-2 Apposition and Superposition compound eyes – A) In apposition compound eyes rhabdoms are in close contact with the crystalline cone cell and each ommatidia is separated from the others by shielding pigments. Each ommatidia will form a single pixel of the final image. **B)** In superposition eyes, each rhabdom, which is separated from the crystalline cone cells by a clear zone (CZ), receives light focused by several lenses. From Dan-E.Nilsson.

Neural superposition eyes

Neural superposition eyes are part of the apposition eye type, but differ by having an open rhabdom, resolving the light that enters each crystalline cone on the separate rhabdomeres. Thus, the photoreceptors within an ommatidium receive light from a slightly different point in space. Conversely, individual photoreceptors in neighbouring ommatidia receive light from exactly the same point in space; the signals of these photoreceptors are combined (superimposed) in the optic lobe, hence the name neural superposition.

Usually apposition eyes have a better resolving power than superposition eyes due to the pigment that separates each ommatidium. However, this architecture also leads to lower sensitivity. Neural superposition eyes can overcome the problem, since this design can result in a seven-fold increase in sensitivity (Kirschfeld, 1972).

I.2 - Photoreceptors and ommatidia structure

The cellular composition of ommatidia varies considerably when we look at the different taxa across arthropods.

The number of photoreceptor cells per ommatidium in insects and crustaceans is usually 8, but it can be as high as 10 in insects, or as low as 5 in crustaceans (reviewed in(Oakley, 2003). Important differences are also seen in the arrangement of the photoreceptors and in their spectral sensitivity. These changes can affect the sensibility of the animal to colours or to light polarisation (discussed in the Part 2 of this thesis).

In *Drosophila* for example, we can find a total of 8 photoreceptors per ommatidium and an open rhabdom. The 6 outer photoreceptors – R1 to R6 – span the entire length of the ommatidium, while the other two – R7 and R8 – rest in between the outer photoreceptors (therefore are called inner photoreceptors) and span only half of the length of the ommatidium. R7 is located distally, with R8 laying below (reviewed in Clandinin and Zipursky, 2002). The bee *Apis mellifera* has a fused rhabdom with 9 photoreceptors; of these, 8 have the same size and span the entire length of the ommatidium, whereas the 9th is a smaller cell and locates proximally (Varela, 1969).

A more complex structure is seen in butterflies, which have a so-called tiered rhabdom. Each ommatidium carries 9 photoreceptors. The distal part is a fused rhabdom with contributions from only 4 photoreceptor cells, R1-4, while the proximal part is a fused rhabdom with contributions from R5-R8. As in bees, R9 is a very small photoreceptor located proximally, and has little contribution to the rhabdom (Arikawa, 2003). Tiered receptors can also be found in stomatopod crustaceans (Cronin and Marshall, 1989b).

Crabs, which have a similar structure to most other malacostran crustaceans, have a fused rhabdom formed by 8 photoreceptors. R1-R7 span the entire length of the rhabdom, while R8 sits on top, just below the cone cell (Stowe, 1977).

Fig. I-3 shows schemes for several types of ommatidia found in insects and crustaceans that can serve as a reference.

Photoreceptors also vary in the way they send their axonal projections to the part of the brain responsible for the processing of the visual stimuli, the optic lobe.

In flies, R1-R6 send projections to the first neuropil of the optic lobe – the lamina – and, therefore, have short fibers. R7 and R8 on the other hand have long projections that will cross the lamina and reach the second optic neuropil, the medulla (reviewed in Clandinin and Zipursky, 2002). Bees and butterflies have a similar arrangement with R3 to R8 projecting to the lamina, while R1, R2 and R9 project to the medulla (therefore 3 long fibers instead of 2) (Sommer and Wehner, 1975; Takemura et al., 2005; Varela, 1970). In

crabs and crayfish only R8 projects to the medulla, and R1-R7 project to the lamina (Nässel, 1976; Stowe, 1977).

A recent study was able to show that R1 and R2 of butterflies are specified similarly to R7 in *Drosophila* (expressing Prospero), while R9 is specified similarly to *Drosophila* R8 (expressing Senseless). These findings suggest that butterfly R1 and R2 are homologous to *Drosophila* R7, while R9 is homologous to *Drosophila* R8 (Perry et al., 2016).

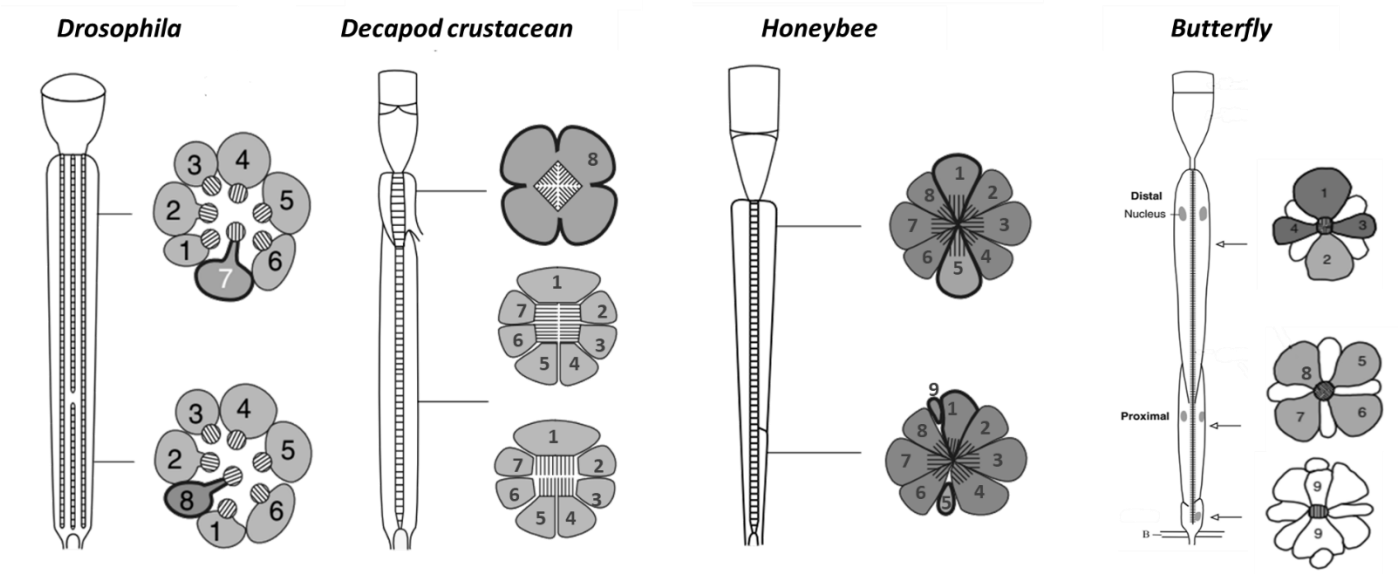

Fig. I-3 Ommatidia types in pancrustaceans – *Drosophila* has a total of 8 photoreceptor per ommatidium, being R7 and R8 smaller and contribute to only half of the total rhabdom length. In malacostracan crustaceans we can usually find 7 photoreceptor than contribute to almost the entire length of the rhabdom, plus an 8th photoreceptor only present at the distal part of the ommatidium. In honeybees 8photoreceptor compose the rhabdom; a 9th, small cell is present only at the proximal part. Butterflies have a tiered rhabdom in which the distal and proximal part are composed by 2 different sets of photoreceptor; a 9th smaller cell is present only at the proximal tip. *Adapted from* (A. Kelber and M. Henze 2013 *and* A. Kelber 2016)

I.2.A - Visual pigments of compound eyes

The spectral sensitivities of the visual opsins found in different animals often correlate with the spectral distribution of the light in their environment. While an insect subjected to bright day light is presented with all the visible light spectrum, marine or fresh water animals will be exposed to a narrower range of wavelengths, since long and very short wavelengths are mostly absorbed by water, and their intensity decreases rapidly with depth (reviewed in Cronin, 2006).

Phylogenetic analysis of arthropod R-opsins suggest that the ancestral pancrustacean eye had 4 visual opsin genes – LWS2, MWS1, MWS2 and SWS. Across pancrustacean evolution,

these ancestral genes were repeatedly duplicated, lost or have seen their expression change from one type of eye to another (Henze et al., 2015).

This dynamic evolution has resulted in mono, di, tri and tetra chromatic eyes, present in pancrustaceans.

Drosophila has 6 opsins in the visual system – Rh1 to Rh6. Outer photoreceptors R1 to R6 express Rh1, a blue- green (MWS) absorbing visual pigment, while R7 can express either Rh3 or Rh4 (both UV absorbing) and R8 expresses Rh5 or Rh6 (blue and green respectively). Rh2 is only expressed in the ocelli (Hardie, 1985, 1986).

Fly ommatidia can therefore differ from each other, resulting in a retinal mosaic in which we can find 2 types of ommatidia, stochastically distributed across the eye: 'yellow' ommatidia, where R7 expresses Rh4 and R8 expresses Rh6, and 'pale' ommatidia with R7 expressing Rh3 and R8 expressing Rh5 (Hardie, 1985, 1986).

Retinal mosaics are common in insects (for example, bees have 3 ommatidial types (Wakakuwa et al., 2005)) but can also occur in crustaceans, with the most extreme example found in the mantis shrimp (Cronin and Marshall, 1989b; Marshall, 1988). Besides retinal mosaics related to colour, the retina can be often regionalized, with specific areas bearing certain ommatidial types in order to perform a specific function. This is the case of the "dorsal rim area" and 'ventral eye" in *Drosophila*, which specialize in the detection of polarised light, as discussed in the part 2 of the thesis (Wernet et al., 2012).

Most crustaceans possess only 2 opsins, a MWS expressed in R1-R7 and a SWS expressed in R8 (Marshall et al., 2003). There are however exceptions; we can find deep sea crustaceans with only one opsin, or others, like Daphnia, with 4 opsins (Smith and Macagno, 1990). Again, the most extreme case is seen in stomatopods, which have as many as 15 opsins (Porter et al., 2012b). The crayfish *Procambarus clarkii* has been shown to express different types of opsins depending on the time of the year (reviewed in (Cronin and Hariyama, 2002)).

It should also be noted that, despite the normal situation of having one rhodopsin per photoreceptor, we can also find cases where 2 opsins are expressed in the same cell. Examples include the crab *Hemigrapsus sanguineos* (Sakamoto et al., 1996) and some photoreceptors in butterfly eyes (Arikawa, 2003). We can also find cases where different photoreceptors are sensitive to different wavelengths even though they express the same rhodopsin. This is achieved, by the presence of different screening pigments in the ommatidium (carotenoids, ommochromes and/or pteridines), which give the eye their characteristic colour. They are used as optic filters and that constrain the spectral

sensitivity of the photoreceptor. Examples include butterflies(Arikawa, 2003), house flies(Hardie, 1986) and stomatopods (Cronin et al., 2001).

Therefore, it is difficult to deduce the spectral sensitivity of a given photoreceptor based solely on which opsin is expressed.

I.3 - Visual information processing – the optic lobe

Despite their small brains, arthropods are capable of performing complex visual tasks fast and reliably: search for food and mating partners, fight conspecifics, and avoid obstacles and predators.

The part of the brain responsible for visual information processing is collectively called the optic lobe. In arthropods, it consists of a number of neuropils which lie externally to the protocerebrum.

In pancrustaceans we can identify 4 to 5 neuropils that compose the pathway for visual information processing: lamina, medulla (outer and inner medulla in insects), lobula and lobula plate.

Each of these parts contains an ordered representation of the external space – a retinotopic map. Particular operations (spatial/temporal filtering, motion and colour detection) are processed in series or in parallel in the different layers. This ordered processing of information is a requisite for later operations that will translate into behaviours (reviewed in Strausfeld et al., 2006).

Visual processing starts when light reaches the photoreceptor cells within the ommatidia. There, light information will be transduced into neuronal signals. Photoreceptors receiving light from the same point in space, converge their axons to the same location within the first synaptic neuropil – the lamina – forming a column called the optic cartridge. While short photoreceptor fibers terminate there, long photoreceptor fibers cross the lamina and terminate in the medulla.

Each cartridge is placed in the lamina in a retinotopic manner. Thus the number of cartridges corresponds to the number of facets (ommatidia) present in the eye. In addition to photoreceptors, each cartridge also includes second order neurons, which establish connections within the cartridge and between cartridges (within or outside the neuropil).

In pancrustacean optic lobes we find two chiasmas, where the axons connecting consecutive neuropils cross each other: between the lamina and the medulla, and between the medulla and the lobula (Sinakevitch et al., 2003). The crossing of axons causes the inversion of the order of cartridges, and therefore of the retinotopic map. Chiasms are an evolutionary novelty of the pancrustacean optic lobes, not being found in

other arthropods, and are a consequence of the mode of development of the neuropils (Strausfeld, 2005).

The best studied arthropod optic lobe is undoubtedly that of *Drosophila*. It has given us valuable information on how visual information is computed in the brain. I will therefore use it as an example to introduce visual information processing.

I.3.A - Visual information processing – lessons from the fly

Flies have neural superposition compound eyes, in which each ommatidium is composed of 8 photoreceptor cells. Due to the open rhabdom, photoreceptors from the same ommatidium do not receive light form the same point in space. Instead, any given point is "seen" by individual photoreceptors residing in 7 neighbouring ommatidia (Fig. I-4 C). The signals received by these 7 photoreceptors converge in individual cartridges of the lamina (R1-R6) and the medulla (R7 and R8).

In addition, cartridges in the lamina contain neuronal processes from monopolar cells (L1 to L5), C2, C3 and T1 neurons, plus amacrine cells. L1 and L2 are the main post-synaptic targets of R1-R6 and have been shown to play a crucial role in motion detection. Some of those lamina interneurons leave the lamina cartridges and form connections in the medulla; in particular, L3 connects directly to the R7 and R8 axonal projections (reviewed in Zhu, 2013).

Medulla cartridges are far more complex than lamina ones, consisting of processes from around 60 neurons. Those will project either within the medulla (some connecting the outer with the inner medulla) or towards the deeper neuropils – the lobula and lobula plate (Fischbach and Dittrich, 1989).

The lobula plate contains wide-field tangential cells that integrate signals from hundreds of R1-R6 pathways. It is in this neuropil where computation of optic flow direction seems to take place. The lobula is the least studied neuropil; it is thought to be sensitive to object features such as orientation, texture and colour (Strausfeld and Lee, 1991).

Finally, visual projection neurons connect the medulla, lobula and lobula plate to the central brain. These play a dual role, conveying information from the retina to the central brain and also sending command signals back from the central brain to the optic lobe.

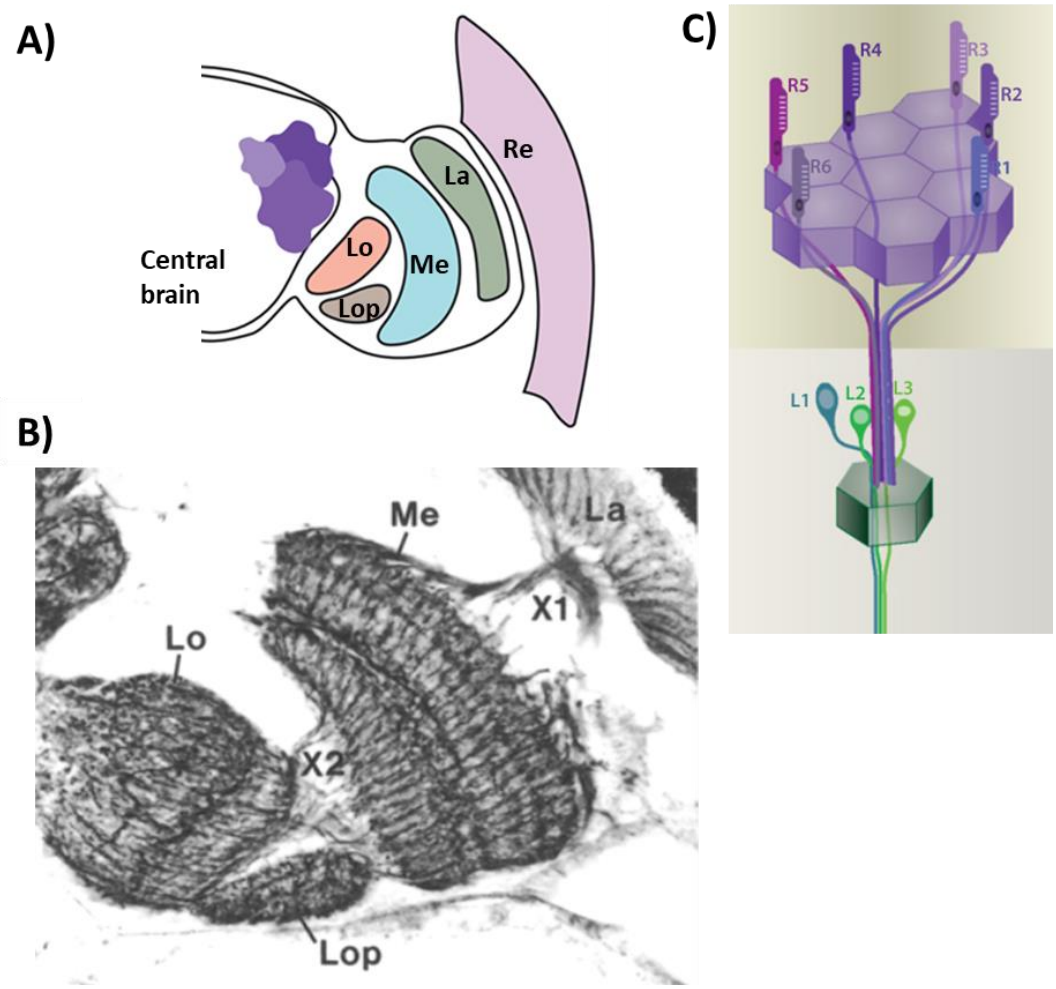

Fig. I-4 Structure of the *Drosophila* optic lobe – **A)** Scheme of the *Drosophila* optic lobe showing the retina **Re,** lamina **La**, medulla **Me**, lobula **Lo** and lobula plate **Lop; B)** Golgi staining of a *Drosophila* optic lobe showing the 5 neuropils and the chiasms (**X1** and **X2**) that connect them. *From* (Fischbach and Dittrich, 1989) **C)** Scheme of the connections between R1-R6 and the lamina. Each lamina cartridge receives input from a single photoreceptor of different, neighbouring ommatidia. *Adapted from* (R. Sanes and S. Zipursky 2010)

Colour and motion

Colour vision is the ability to discriminate between light stimuli of different spectral composition, independently of their relative intensity. It is used to detect, recognise and discriminate objects. It is mediated by colour opponent (or coding) neurons, which receive opposing inputs (excitatory and inhibitory) from receptors of different spectral types (Chittka et al., 1992; KELBER et al., 2003).

In the fly medulla, intricate connections involving interneurons connected to R7 and R8 axonal projections (which have a different spectral sensitivity) point towards being part of a pathway of colour opponent neurons. Therefore, the medulla is often regarded as the neuropil responsible for the first stages of colour information processing, being fed information from R7 and R8 – the chromatic pathway.

R1-R6 have the same spectral sensitivity and make part of the achromatic pathway, providing information on motion (rather than colour), which is primarily processed at the lamina by L1 and L2 neurons.

This separation between colour and motion processing is not, however, strict. Studies on the ultrastructure of R7/R8 axons showed the existence of synapses between those and lamina monopolar neurons in the medulla, and also the existence of gap junctions and synapses between R7/R8 and R6 axons in the lamina(Shaw, 1984; Shaw et al., 1989; Takemura et al., 2008; Zheng et al., 2006). A more recent study confirmed that R7/R8 signals improve motion discrimination and adjust the sensitivity of the optomotor response (Wardill et al., 2012). These input signals are included in the motion detection circuit through interaction of R7/R8 axons with lamina monopolar cells in the medulla but also through the gap junctions between R7/R8 and R6 axons.

Conversely, it has been shown that blockage of L3 lamina monopolar cells (which connect R1-R6 in the lamina to R7-R8 in de medulla) impairs bright blue/green discrimination. This suggests that, in the medulla, there is colour opponent processing between R1-R6 and R7-R8 (Garbers and Wachtler, 2016; Schnaitmann et al., 2013a).

I.3.B - Optic lobe evolution in Arthropods

The arrangement of 4 optic neuropils is found in most pancrustaceans, independently of the type of compound eye that they use. There are however some exceptions in crustaceans and insects that underwent secondary loss or reduction of one or two neuropils. For example, branchiopod crustaceans, like *Artemia* and *Daphnia*, possess only 2 optic neuropils: a lamina, directly connected to the retina, and a tectum-like deeper neuropil. Both are connected to each other by uncrossed retinotopic axons (Harzsch and Glötzner, 2002; Nässel et al., 1978). The latter neuropil is thought to be homologous to the pancrustacean lobula plate (Strausfeld et al., 2016). In addition, the size of the lobula plate varies considerably when comparing different crustaceans, and it can be very small in many decapods(Sinakevitch et al., 2003).

Myriapods present only two optic neuropils and, both receive input from the retina. Axons connecting the two neuropils seem to cross each other, suggesting the presence of a

chiasma (Sombke and Harzsch, 2015). Similarly, xiphosurans have two optic neuropils connected through a potential chiasm (Harzsch et al., 2006).

Fossils of the euarthropod Radiondata brain show stout optic nerves associated with 2 enlarged areas, suggesting that this extinct arthropod stem group also possessed only 2 optic neuropils (Cong et al., 2014).

Taken together, these observations suggest that the ground pattern of the arthropod visual system comprises an apposition compound eye connected to two nested optic neuropils, a condition still seen today in Myriapods. The addition of two additional optic neuropils, the medulla and lobula, plus the chiasma that connects them, represents an evolutionary novelty of the pancrustacean clade (Strausfeld, 2005; Strausfeld et al., 2016).

I.4 - Purposes of Part 1

Despite the many studies on crustacean visual systems, we are still lacking models were genetic tools can be applied in a similar way has in *Drosophila. Parhyale* is therefore an opportunity to study visual system evolution within the Pancrustacea clade.

This part of the project, which composes the major part of my thesis, is dedicated to the description of the *Parhyale* visual system, providing an essential basis for future works.

II. Results

II.1 - Structure and growth of Parhyale eyes

Parhyale have been in the lab for almost 20 years but there are still no descriptive studies on the anatomy and neural connectivity of their eyes. I therefore started my project with a basic description on the structure of the *Parhyale* eye.

Parhyale has an apposition compound eye with 5 photoreceptors per ommatidium

Parhyale adults have one pair of dark, kidney-shaped compound eyes, located laterally in the head. As seen from the surface of the eye, the facets are arranged in rows, have a round shape and are surrounded by a white reflective pigment (Fig. II-1 A). This pattern is seen in almost all animals, with few exceptions where facets seem to have more irregular shapes (Fig. II-1 B). Around 5% of the animals (rough estimate) show this arrangement which may be due to a developmental defect. Scanning Electron Microscopy (SEM) images of *Parhyale*'s juveniles (data by T. Pavlopoulos and M. Averof) reveal that the cuticle above the eyes is smooth and facets are not perceptible, indicating that the cuticle is not specialized to work as a lens (Fig. II-1 C).

To further characterize the fine structure of the eye, adult heads were fixed and prepared for Transmitted Electron Microscopy (TEM). EPON-embedded samples were sectioned in semi-thin (2μm) or ultra-thin (50nm) sections and analysed with a light and transmission electron microscope respectively. Data from serial, longitudinal and transversal, semi-thin sections were collected from at least 6 different animals. For longitudinal and transversal ultra-thin sections a total of 2 animals was used (Fig. II-2 A and B, respectively). To complement the information given by the semi- and ultra-thin sections, thick sections (100μm - 300 μm) of adult heads were stained with DAPI and imaged with a confocal laser scanning microscope.

In semi-thin sections, stained with toluidine blue, each ommatidium is seen separated from the others by densely packed dark vesicles, the shielding pigment granules. The rhabdom, which has a cone shape, lays just below the dioptric apparatus (or lens, stained in dark blue) (Fig. II-1 D). The pigment-shielded ommatidia, with rhabdoms in close proximity to the lenses, are characteristic of apposition compound eyes.

The lens is formed by 2 crystalline cone cells ((Fig. II-1 E-E'). I was not able to observe the nuclei of these two cells, neither the nuclei of the 2 accessory crystalline cone cells that have been described for amphipods (Hallberg and Nilsson, 1980).

Longitudinal sectioning shows that the eye has two distinct parts: a more distal one, comprising the lens and rhabdoms; and a proximal region, comprised mainly of nuclei.

Very few nuclei are seen at the distal part of the eye, suggesting that photoreceptor nuclei are positioned at the proximal region. This separation has been noted before in amphipods (Hallberg and Nilsson, 1980) and a fenestrated membrane was described separating the 2 regions. The presumed position of the fenestrated membrane is partially marked in the figures, at the proximal end of the rhabdom (Fig. II-1D-F).

In TEM sections, rhabdoms are distinguished by their densely packed microvilli, surrounded by electron dense vesicles (shielding pigment granules). These vesicles present different TEM contrasts (white arrow heads in Fig. II-2 C) which correspond to different pigment types (probably ommochromes and carotenoids). There are no cell membranes separating the microvilli from the pigment granules, indicating that pigment granules are enclosed within the photoreceptor cells. The reflective white pigment, which appears as empty vesicles, remains outside of the photoreceptor cells, presumably within reflective pigment cells that surround the ommatidia. No dark pigment granules were found outside the photoreceptor cells.

Transversal sections of the ommatidia show a rhabdom with a rayed (star-like) shape, composed of five photoreceptor cells, named R1 to R5 (Fig. II-2 D-D'). The rhabdomeres are in close contact with each other. In all the sections observed, R1 – R4 have a similar size while R5 is considerably smaller than the others, possessing a diminutive rhabdomere. The microvilli of R1 and R3 are oriented in parallel to each other and orthogonally to R2 and R4. Interdigitation of the rhabdomeres was not seen in any of the longitudinal sections (>4 sections) (Fig. II-2 E).

Photoreceptor cells extend until the most distal part of the eye, surrounding the lens. Cytoplasmic extensions are seen between the photoreceptor and the lens (Fig. II-2 F). Some photoreceptors from neighbouring ommatidia seem to contact each other via membrane extensions (red arrows in Fig. II-2 G). It was not possible to determine, in general, which and how many photoreceptors show this connection.

From these results we can conclude that *Parhyale* has an apposition compound eye, with 5 photoreceptors per ommatidium. The rhabdom is fused, and, unlike other crustaceans, there is no interdigitation of the rhabdomeres.

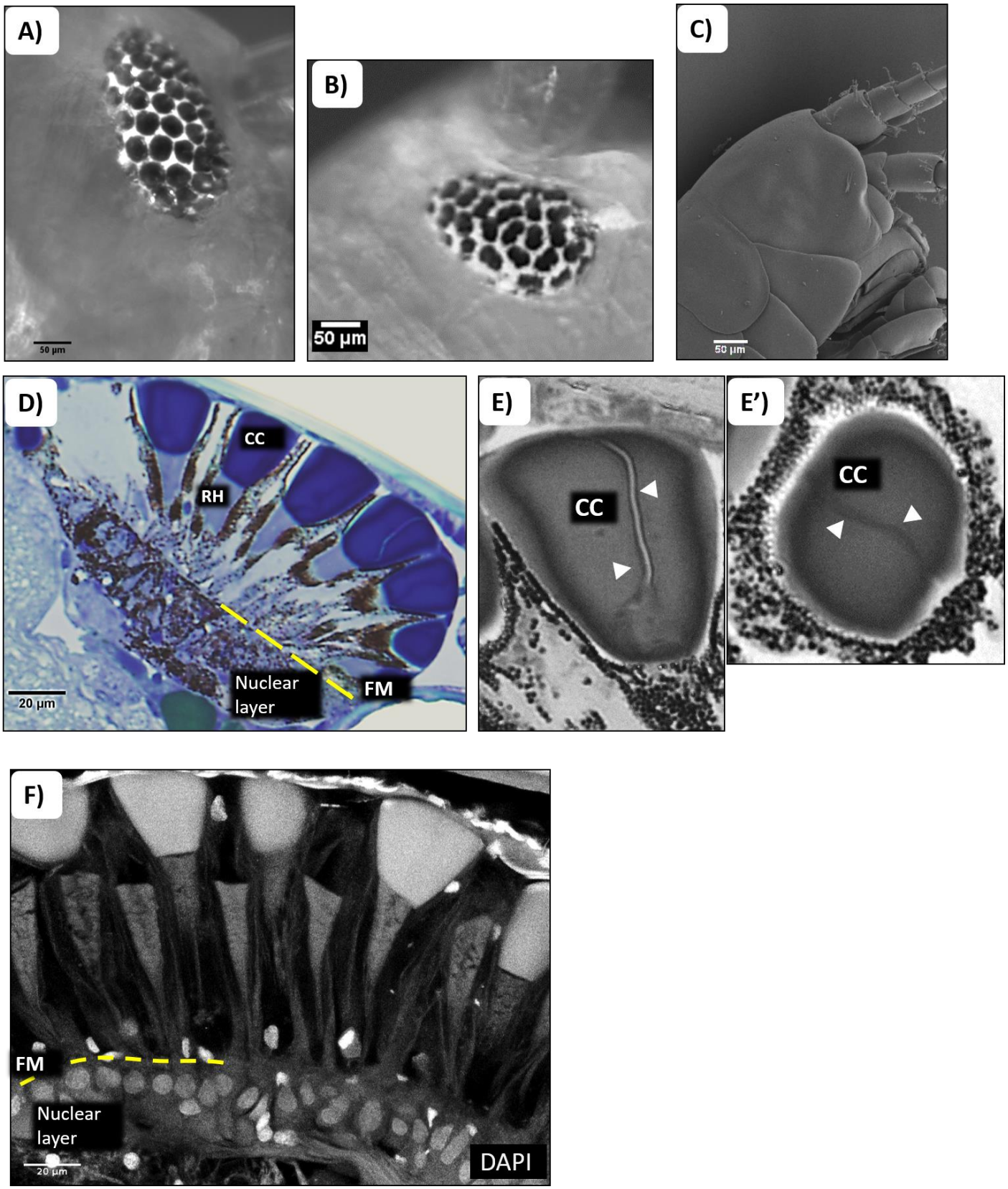

Fig. II-1 General features of *Parhyale* adult eyes – A) detailed view of a *Parhyale* compound eye. Facets are arranged in rows. **B)** Few animals carry ommatidia with irregular facets **C)** SEM of the head. The cuticle above the eye is smooth in the surface and facets are not perceptible. **D)** Longitudinal semi-thin plastic section stained with toluidine blue, showing the apposition eye of *Parhyale*. **E-E')** Detail of the dioptric apparatus composed by two cone cells, in semi-thin plastic sections. Arrowheads point to the separation between the two cells **F)** DAPI staining of the eye, showing the nuclei beneath the fenestrated membrane. **CC-** crystalline cone cell **RH-** rhabdom **FM-** fenestrated membrane

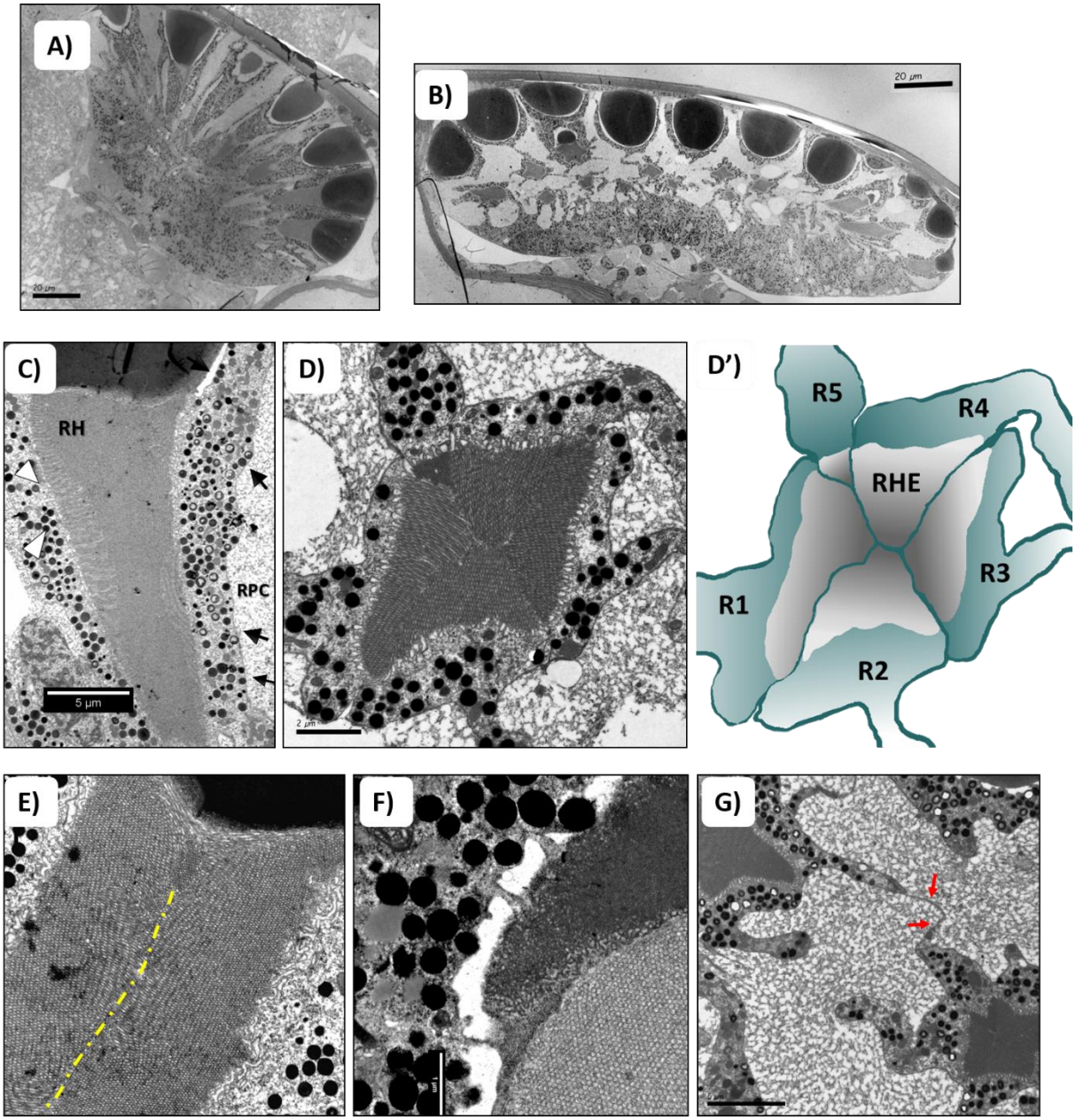

Fig. II-2 TEM details of adult *Parhyale* eyes – A-B) Longitudinal and transversal TEM sections of the *Parhyale* eye; **C)** Longitudinal TEM section of a single rhabdom. White arrowheads point to the different pigment granules, black arrows point to the photoreceptor cell membrane. **D-D')** TEM Cross section of a rhabdom and respective scheme. Each ommatidium is composed of 5 photoreceptor cells with a fused rhabdom. **E)** Longitudinal TEM section through a rhabdom. The yellow line marks the meeting point between two opposing rhabdomeres; **F)** Cytoplasmic **c**onnections between a photoreceptor cell and a crystalline cone cell **G)** Connections between 2 photoreceptor cells from neighbouring ommatidia. **RH-** rhabdom **RHE-** rhabdomere **RPC –** reflective pigment cell.

Eyes keep growing during the life time of Parhyale

From the moment they hatch to the end of their life, *Parhyale* keep growing with each molt. The size of their body increases, allowing for a rough estimate of their age based on body size. Alongside the body, the eyes also keep growing.

In embryos, the eyes are first visible at around stage 26 (S26) (Browne et al., 2005), when 3 lenses are perceptible. A red pigment is first visible at S27, where also 6 smaller, less developed ommatidia can be seen surrounding the older trio of lenses. 24h later, at S27-28, the white reflecting pigment can be seen surrounding the ommatidia. The aligned rows start to be distinguishable in 1 month old animals (Fig. II-3 B).

To document how much the eyes change, I quantified the number of ommatidia, as well the dimensions of each eye, in different aged animals (body size was used as a proxy for age) (Fig. II-3 A). Young hatchlings present around 8 ommatidia per eye, and this number steadily increases, reaching 50 ommatidia in the oldest adults (a 6x increase in ommatidia number). In the same animals, the length of an eye can increase 7x from ~0.037 mm to ~0.27 mm and the width of the eye increases by 6x from 0.026mm to 0.16mm. Considering the "kidney" shape of the eye, the total area was calculated as an ellipse, which varies from around 800µm2 to 34000µm2, a 40x increase.

During growth, the surface area of each ommatidium also increases from 7-12 µm in hatchlings to 20-30 µm in adults (based in measurements from 2 hatchlings and 2 adults), which corresponds to ~6x increase in the surface of the ommatidium.

Based on these results, we can estimate that the increase in the area of the eye is mostly due to an increase in both ommatidial size and number.

A)

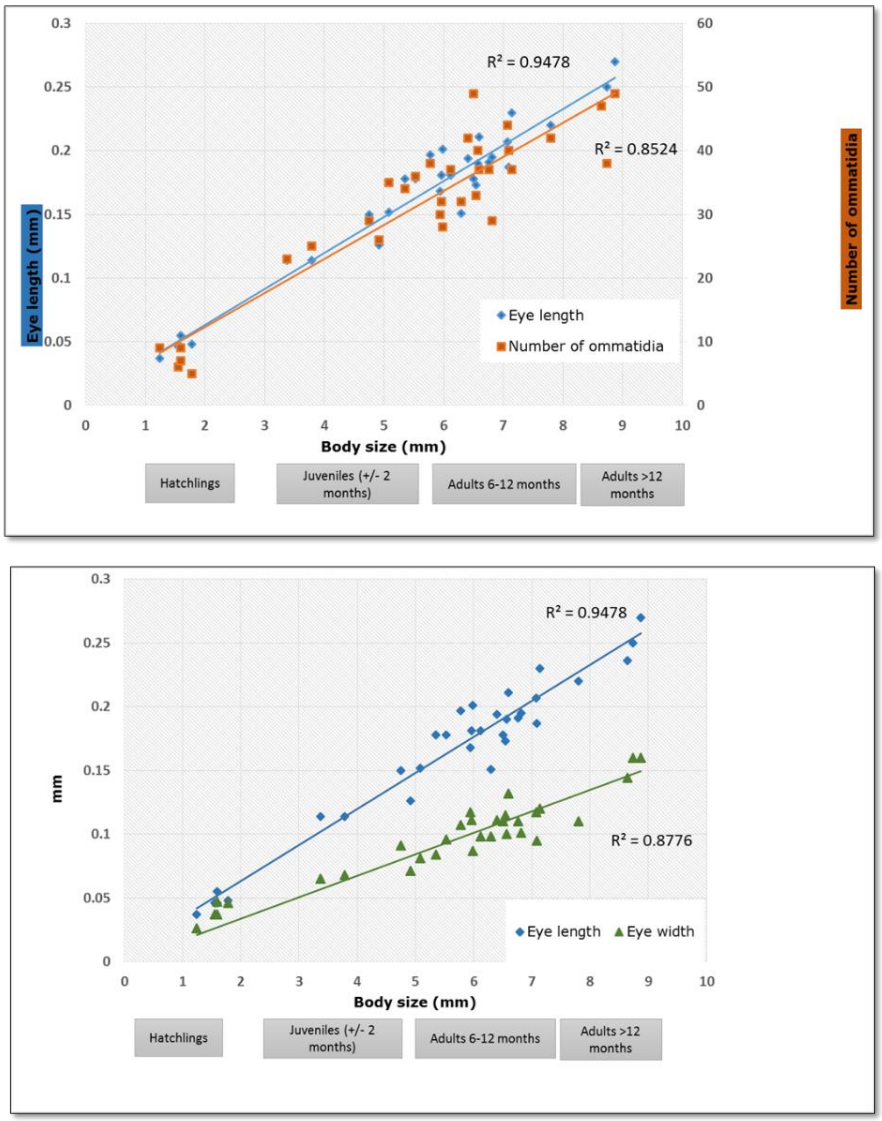

B)

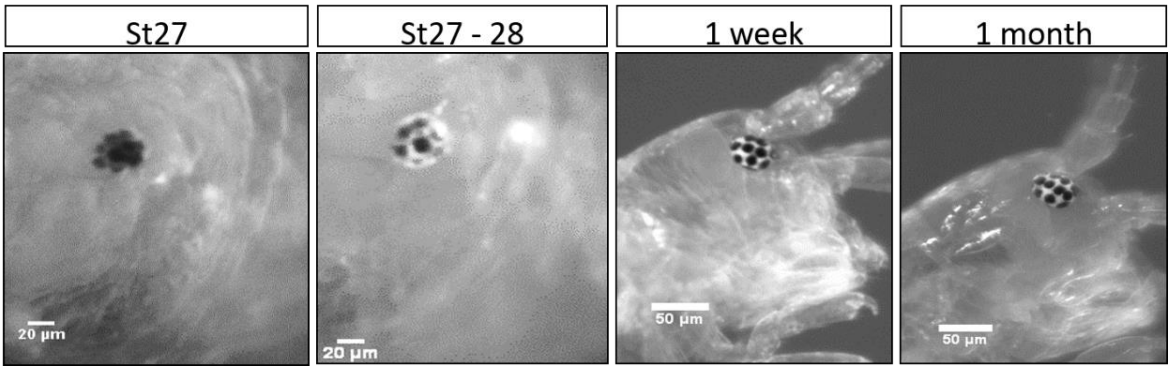

Fig. II-3 New ommatidia are added during the life time of *Parhyale* - A) quantification of the number of ommatidia and eye size vs body size. Adult animals can have up to 50 ommatidia per eye, while hatchlings have around 8 ommatidia. **B)** Eye development from embryos to 1 month old hatchlings. At stage27 embryos have 3 big ommatidia surrounded by 6 less developed ones. The alignment pattern of into rows only starts to be distinguishable in one month old animals.

II.2 - Photoreceptor types

Two Opsins are expressed in the eyes of Parhyale

Eyes couldn't function without opsins, which give an identity to the photoreceptors by defining the wavelength to which they are sensitive. To identify the number of opsins present in *Parhyale* I searched for opsin homologues in their transcriptome. *Drosophila* RH1 protein sequence was used as a reference as a query in BLAST searches of embryonic (Zeng et al., 2011) and head transcriptomes (courtesy of B. Hunt and E. Rosato). Sequences that produced strong BLAST hits were aligned to arthropod protein sequences. Two sequences were found, named Ph-Opsin1 and Ph-Opsin2, which produced a good protein alignment with representatives of the crustacean and insect opsin classes (Fig. II-4 A). Sequences of the two opsins were found in both transcriptomes, however the Ph-Opsin2 complete transcript was only found in the head transcriptome.

To determine to which spectral classes *Parhyale* opsins could belong to, I performed a phylogenetic analysis using a protein sequence dataset used previously for the molecular characterization of crustacean visual opsins (Porter et al., 2007). The data set was chosen because: 1) it included most of the crustacean visual opsins sequenced; 2) for most of the species, the wavelength of maximal absorbance (λmax) for each opsin is known, allowing to group the opsins according to their spectral class. A few additional protein sequences (sequenced more recently) were added to the original dataset from *Daphnia magna* and *Hyalella Azteca* (however the λmax for these proteins is not known). A total of 71 sequences was used, including sequences used as outgroups: vertebrate opsins, human melatonin and a human G coupled receptor. A table with all accession numbers can be found in Material and Methods.

The Maximum Likelihood tree produced shows that Ph-opsin1 clusters within the Crustacean LWS group, while Ph-opsin2 clusters with a known MWS crustacean opsin (Fig. II-5). From these results I suggest that Ph-Opsin1 belongs to the LWS clade, and Ph-Opsin2 is more closely related with MWS opsins. The sensitivities of Ph-Opsin1 and Ph-Opsin2 are likely to resemble those of LWS and MWS opsin clades, respectively, however this assumption could only be confirmed by measuring the λmax for each opsin.

To confirm where the two Ph-Opsin genes are expressed I performed an In Situ Hybridization. The procedure was performed in embryos from S26 to S27-28 and in adult heads, where the cuticle was manually removed. In embryos older than S28 it is not possible to perform in situs due to cuticle deposition, which, unlike in the adults, is not possible to remove.

For both opsins, strong signal is observed in the eyes of embryos and adults (Fig. II-4 B). Ph-Opsin1 gives a stronger signal than Ph-Opsin2. For both opsins, expression is seen at

S26, but is stronger at S27-28, when the eyes are more developed. At this stage the photoreceptor axons are also labelled, especially for Ph-Opsin1 (for Ph-Opsin2 the labelling of the axons is very faint, possibly due to the overall weaker signal). In adults it was not possible to see labelled axons, possibly due to incomplete probe penetration.

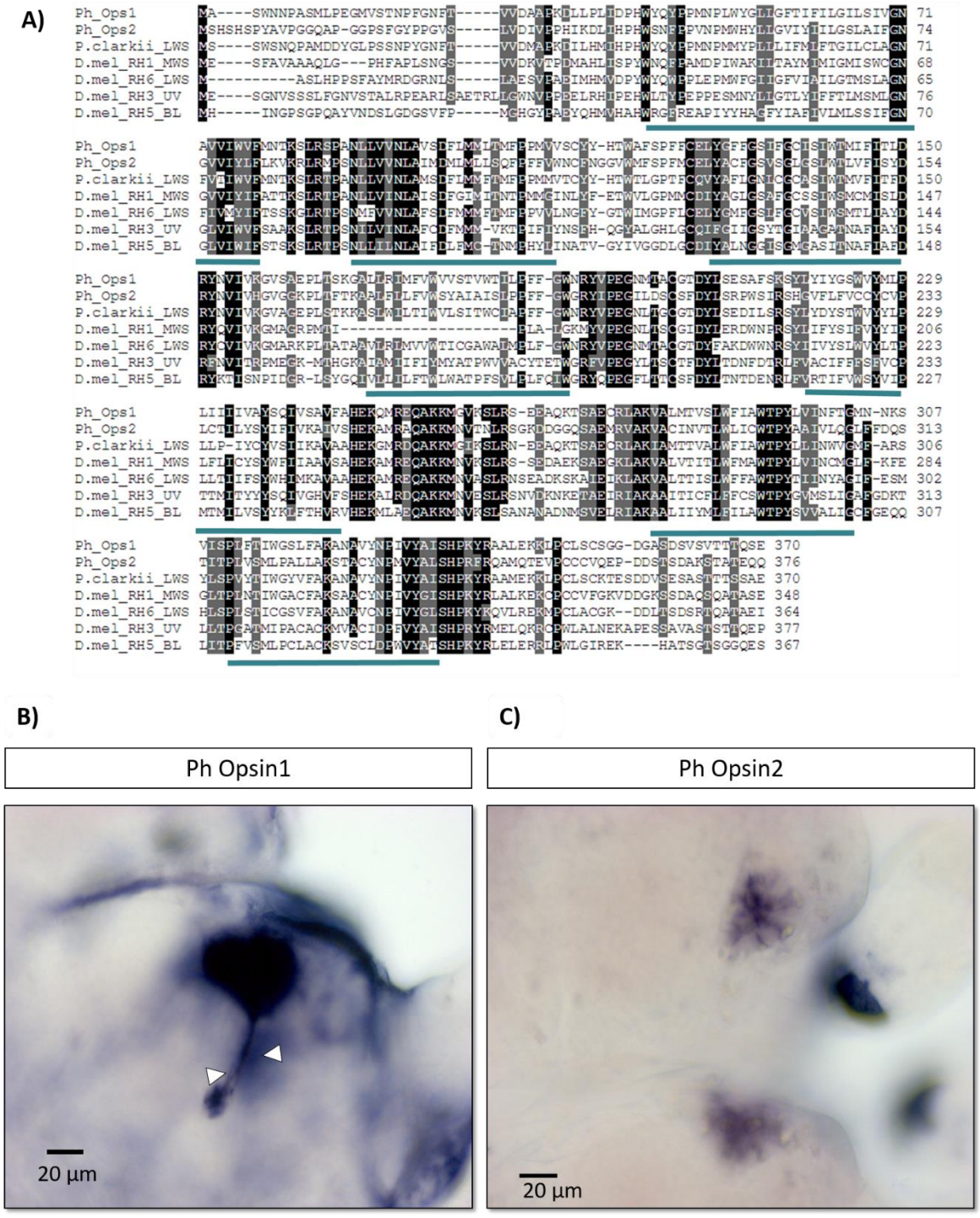

Fig. II-4 *Parhyale* opsins – A) Protein alignment of the two *Parhyale* opsins (Ph-ops1 and Ph-Ops2) found in the transcriptome against several *Drosophila* and crayfish sequences. A black background indicates identical amino acids, and a grey background similar ones. Underlined regions indicate the seven helix structure, characteristic of the opsin proteins. **B)** *In Situ Hybridization* for Ph-Ops1 and **C)** Ph-Ops2 in embryos at S27-28. Opsin expression is only detectable in the eyes and in the photoreceptor cell axons (arrowheads)

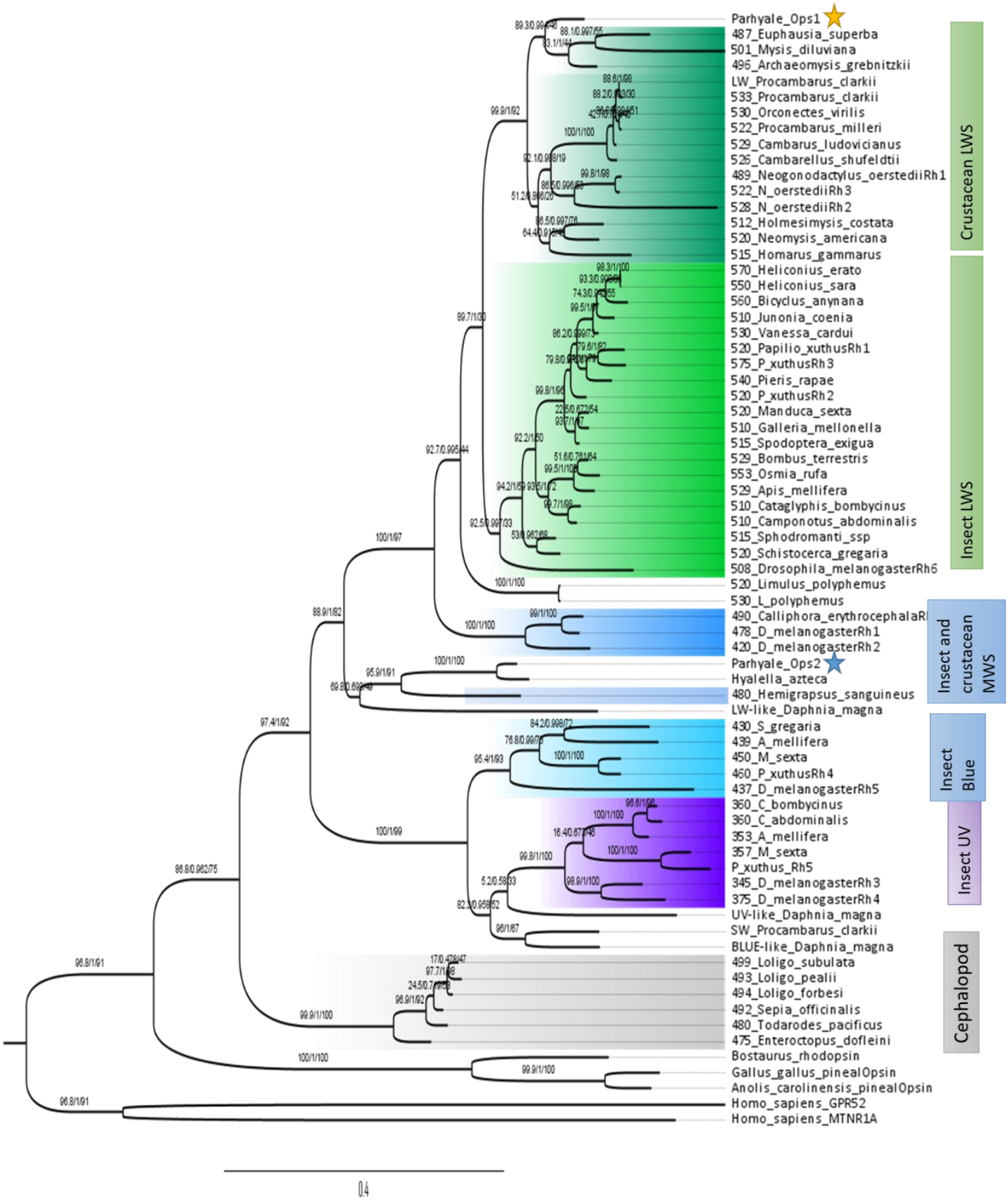

Fig. II-5 Arthropod and Cephalopod Opsin Phylogeny – Phylogenetic tree based on maximum Likelihood analysis of 405 a.a. residues. Numbers at the nodes indicate bootstrap scores of 100 replicates. The maximum wavelength sensitivity of each opsin is given before the species name (when described in the literature). Ph-Ops1 falls in the crustacean LWS cluster.

Ph-Opsin1 is expressed in R1-R4 and Ph-Opsin2 in R5

In situ hybridization gave a poor resolution and didn't allow to distinguish opsin expression in each photoreceptor. To find stable markers for the different photoreceptor types that could allow for live imaging of embryos and adults, and to clearly label photoreceptor projections, I created two transgenic lines using the Cis-Regulatory Elements (CRE) of the two opsin genes.

To find potential CRE sequences I used the published *Parhyale* genome (Kao et al., 2016). Ph-Opsin1 and Ph-Opsin2 transcripts were aligned with the genome to identify untranscribed upstream regions and intron/exon boundaries. Splice donor and acceptor sites were identified using a splice predictor algorithm. To test the ability of the different upstream regions to drive expression of fluorescent proteins, reporter constructs were cloned into a plasmid containing a 3xP3 promoter (3xP3::dsRed/GFP) (Pavlopoulos and Averof, 2005). In *Parhyale* 3xP3 drives expression in two small spots at the lateral sides of the head, allowing to confirm transgenesis in embryos from S27 on. For insertion of the construct into the genome, the Minos transposon was used as vector (Pavlopoulos and Averof, 2005). Most of the positive G0 embryos were kept to establish stable transgenic lines, while other 5 embryos were live imaged with a confocal microscope.

For Ph-opsin1, I cloned a genomic region which included the 5'UTR plus 1.5kb upstream. To have an insight on if fluorescent protein localization would have an influence on the final signal, the genomic region was used to drive expression of cytosolic EGFP and a membrane targeted mKateCAAX, separated by a T2A cleaving peptide ((Fig. II-6 A). Upon injection and analysis of G0 embryos, I could conclude that this region is sufficient to drive expression of both fluorescent proteins in the eyes of *Parhyale* embryos from S27 on (same stage when 3xP3 expression starts) and was kept through adulthood.

The small size and transparency of the embryos allowed to image individual ommatidia (Fig. II-6 D). The rhabdom is recognisable by the rayed structure as seen in TEM sections. The EGFP signal was found diffused throughout the photoreceptor cells and although the rhabdom could be distinguished, it was hard to discriminate from the cytoplasm. On the other hand, the signal from mKateCAAX was much stronger and sharper in the rhabdoms allowing to fully discriminate their morphology. Photoreceptor cell membranes (besides microvilli) were also clearly labelled, however the signal from the rhabdoms is so strong that it prevents a good imaging of the photoreceptor membranes at the distal part of the eye. The rayed structure resembles the one seen for R1-R4 cells, in TEM sections.

For Ph-Opsin2 I first cloned genomic regions including the 5'UTR plus 1.5, 2.5 and 5 kb upstream, to drive expression of mKateCAAX. Neither of these regions was able to drive expression of the fluorescent protein in the embryos or early hatchlings. Therefore I prepared a new construct which included the first intron of the opsin sequence, since it

may also contain regulatory regions. The final construct includes a genomic region 1.5kb upstream of the 5'UTR, the first exon, including the translation start site, the first intron and part of the second exon (Fig. II-6 C). The fluorescent protein, mKateCAAX, was cloned after the second exon, in frame with the opsin open reading frame. The T2A cleaving peptide was included to ensure that stability and localization of the fluorescent protein was not affected by the N-terminus of the opsin sequence. This region was able to drive expression of mKateCAAX in the eyes: it is seen first at late embryogenesis, just before embryos hatch (S29), and persists trough adulthood.

Embryos at S29 already present involuntary muscle movements, and the eyes have a strong red colour, due to shielding pigment deposition, which is autofluorescent in the red channel. Nevertheless, live imaging of the eyes in G0 embryos injected with the Ph-Opsin2 CRE at S29, revealed a strong signal in photoreceptor cells. The rayed structure of the rhabdom, as seen for Ph-Opsin1, was not observed. Instead, a single oval shape was seen per ommatidium (Fig. II-6 E). This morphology resembles the morphology of R5, as seen in TEM sections.

After confirming the ability of the two CRE's to drive expression of reporter proteins in the photoreceptor cells of *Parhyale*, I established two stable transgenic lines: Ph-Ops1::EGFPCAAX and Ph-Ops2::mKateCAAX.

To clearly identify in which photoreceptors each opsin was expressed, Ph-Ops1 and Ph-Ops2 stable transgenic lines were crossed and double transgenic embryos (around 5) were imaged (Fig. II-6 F'). The rayed and oval shaped structures were again observed in the ommatidia (for EGFP and mKate respectively) and I could conclude that the signal from the two reporters does not overlap. Given the shape of the rhabdomeres labelled with the reporters and the non-overlapping signal, I conclude that Ph-Opsin1 is expressed in R1-R4 and Ph-Opsin2 in R5. To understand weather the rhabdomeres of the two photoreceptor types extend throughout the total height of the rhabdom – instead of being preferentially located distally (near the lens) or proximally – optical sections were taken from distal to proximal positions of the retina (Fig. II-6 F). Signal from both reporters was found throughout the Z-stacks, indicating that all rhabdomeres are present through the entire length of the rhabdom

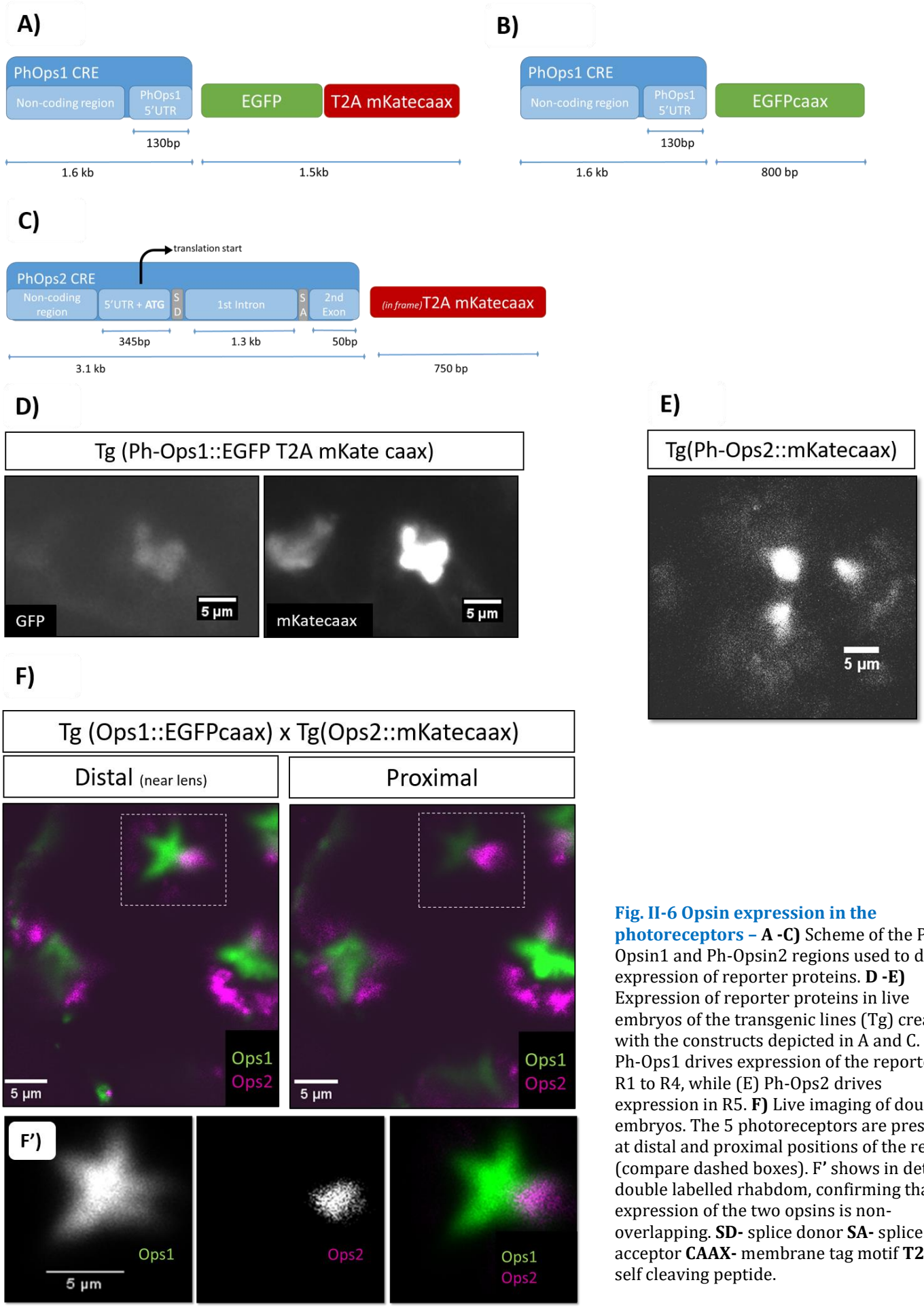

Fig. II-6 Opsin expression in the photoreceptors – A -C) Scheme of the Ph-Opsin1 and Ph-Opsin2 regions used to drive expression of reporter proteins. **D -E)** Expression of reporter proteins in live embryos of the transgenic lines (Tg) created with the constructs depicted in A and C. (D) Ph-Ops1 drives expression of the reporter in R1 to R4, while (E) Ph-Ops2 drives expression in R5. **F)** Live imaging of double tg embryos. The 5 photoreceptors are present at distal and proximal positions of the retina (compare dashed boxes). F' shows in detail a double labelled rhabdom, confirming that the expression of the two opsins is non-overlapping. **SD-** splice donor **SA-** splice acceptor **CAAX-** membrane tag motif **T2A-** self cleaving peptide.

II.3 - Optic lobe structure

Information perceived by photoreceptor cells in the retina is processed at the optic lobe, which in arthropods is composed of distinct neuropils, i.e. synaptic dense regions surrounded by cell bodies. In hexapods the neuropils are named lamina, medulla, lobula and lobula plate. While the nomenclature of the neuropils is well established for this group (Ito et al., 2014), the same isn't true for crustaceans and other arthropods, where the same neuropil can receive different names depending on the study.

In this part of my thesis I will use the nomenclature proposed by Sandeman (Sandeman et al., 1992)for decapod crustaceans, with a few changes proposed by Harzsch (Harzsch and Hansson, 2008), which relate this nomenclature to the one of hexapods. According to Sandeman, the brain of decapods is divided into a protocerebrum, deuterocerebrum and tritocerebrum. The optic lobe is part of the protocerebrum and is composed by three neuropils: the first, the lamina, lays just after the retina, followed by the second neuropil, the external medulla, and the third neuropil, the medulla interna. A terminal medulla is described as being part of the lateral protocerebrum. Harzsch designates the external and internal medulla as medulla and lobula, respectively.

Besides their relative position, the lamina and medulla also present a columnar arrangement of their axons, representing the retinotopic map. Chiasmas are present between lamina-medulla and medulla-lobula.

This nomenclature is based on morphological characters, and does not necessarily imply a homology or common function of the neuropils.

The retina connects to the optic lobe via an elongated optic nerve

The *Parhyale* brain has never been described in detail. To gain insight on the general structure of the brain and, more specifically, of the optic lobe, I performed immunostainings with acetylated tubulin antibody in S27-28 embryos. This stage was chosen due to the fact that embryos are small and transparent enough to allow imaging of the entire brain, and they show already a well developed eye.

In Z-stack projections of stained embryos (Fig. II-7) it is possible to distinguish the eye, from which the axons of photoreceptor cells are seen projecting into the brain. These axons converge to an axonal bundle outside the retina, the optic nerve, which extends considerably until it reaches the first neuropil. The convergence of photoreceptor axons and the formation of a unique axon bundle is also seen in adult retinas, dissected and immunostained for acetylated-tubulin (Fig. II-8).

A second and third neuropil are also distinguishable in these stainings (details in Fig. II-7). The first and second neuropil present axons arranged in a columnar shape, and are

connected through a chiasm. Based on these observations, I suggest that the 1st and 2nd neuropil correspond to the lamina and medulla, respectively. Interestingly, the lamina is not positioned in close proximity to the eye, as usually seen in hexapods for example.

A second chiasm, between the 2nd and 3rd neuropils is not noticeable. Therefore it is not possible to conclude whether the 3rd neuropil corresponds to the lobula.

Imaging the adult brain proved to be more difficult. The fact that the optic lobe is positioned far away from the retina and connected to it by an axon bundle (as seen in embryos) made it hard to capture the optic neuropils and their connections in thin sections of the brain. Staining of adult whole mount heads is possible, but the thickness of the tissue (>300μm) limits penetration of the antibody and does not allow to image the entire brain. I also tried to perform brain dissections, but too often the eye would detach from the brain, thus preventing a clear recognition of the neuropils.

To overcome these problems I performed immunostainings with acetylated-tubulin antibody on thick vibratome sections (150-300 μm) through the *Parhyale* adult brain. Despite the thickness of these sections, I could visualize the entire optic lobe, optic nerve and retina in the same section only in 2 animals. In Z-stack projections of the stained tissue (Fig. II-9) we can again recognize the optic nerve that connects the retina to the optic lobe, forming below the nuclear layer of the eye. Three neuropils are clearly distinguishable, laying very close to each other. A chiasm can be identified between the lamina and medulla (arrowhead in Fig. II-9 C), but not between the medulla and the 3rd neuropil. Unlike embryos, the columnar arrangement of the axons in the first two neuropils is not perceptible in these preparations.

The optic nerve of adult *Parhyale* offered us two unexpected observations: first, we can see two rows of nuclei along the optic nerve (red arrows in Fig. II-9 B); second the axons that form the nerve seem to cross each other. The later can be seen in more detail in Fig. II-9 D (red arrows), which shows optical sections at different tissue depths: groups of axons can be distinguished connecting the ventral part of the retina to the dorsal side of the lamina; the opposite is seen in deeper regions of the nerve.

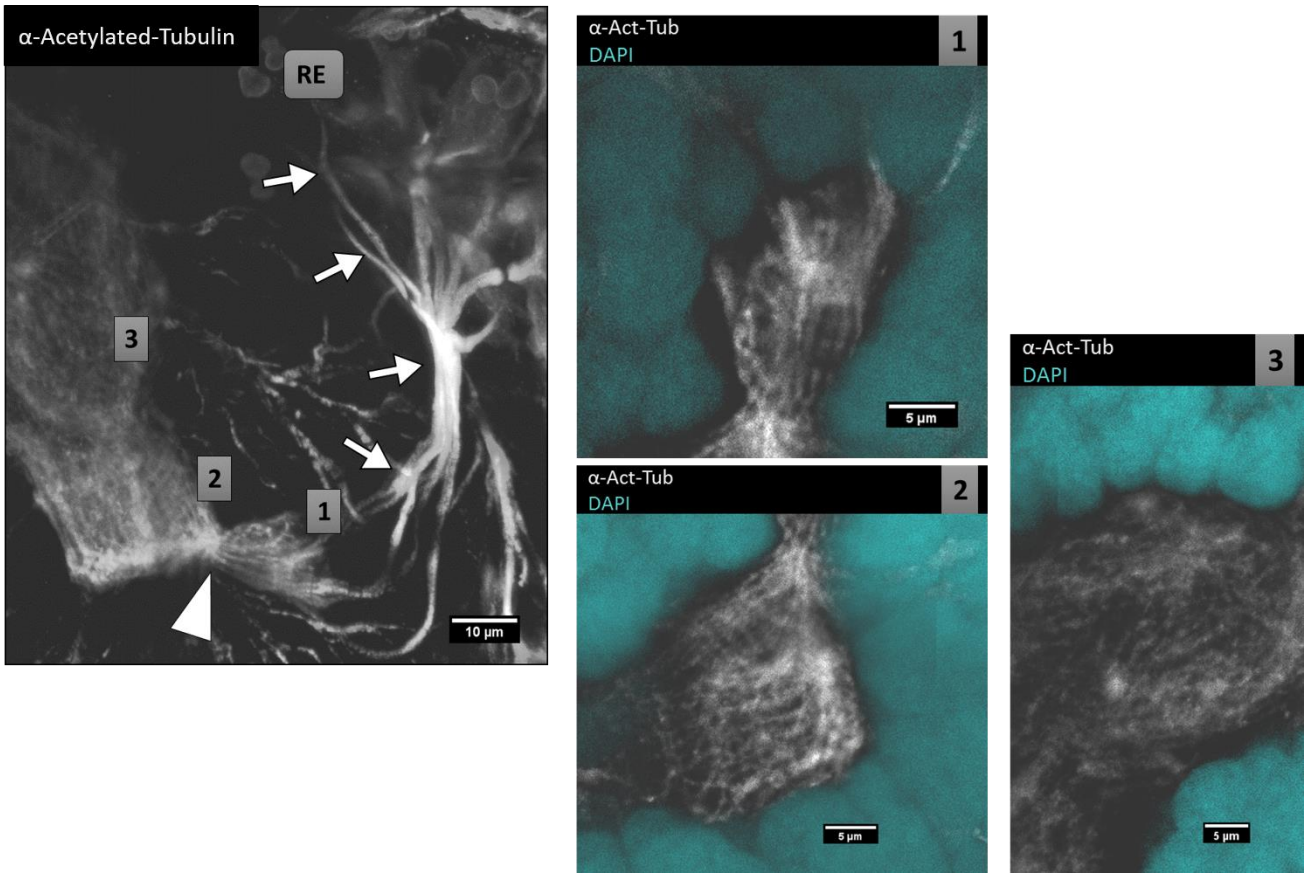

Fig. II-7 *Parhyale* embryonic eye and optic lobe – Detail from the retina **RE** and optic lobe of an embryo at S27-28, immuno stained with acetylated tubulin antibody. White arrows point to the axons sent from the retina to the 1st neuropil, the lamina **(1).** Arrowhead points to the chiasm between the 1st and 2nd neuropil **(2)**, the medulla. A second chiasm between the 2nd and 3rd neuropil **(3)** is not seen.

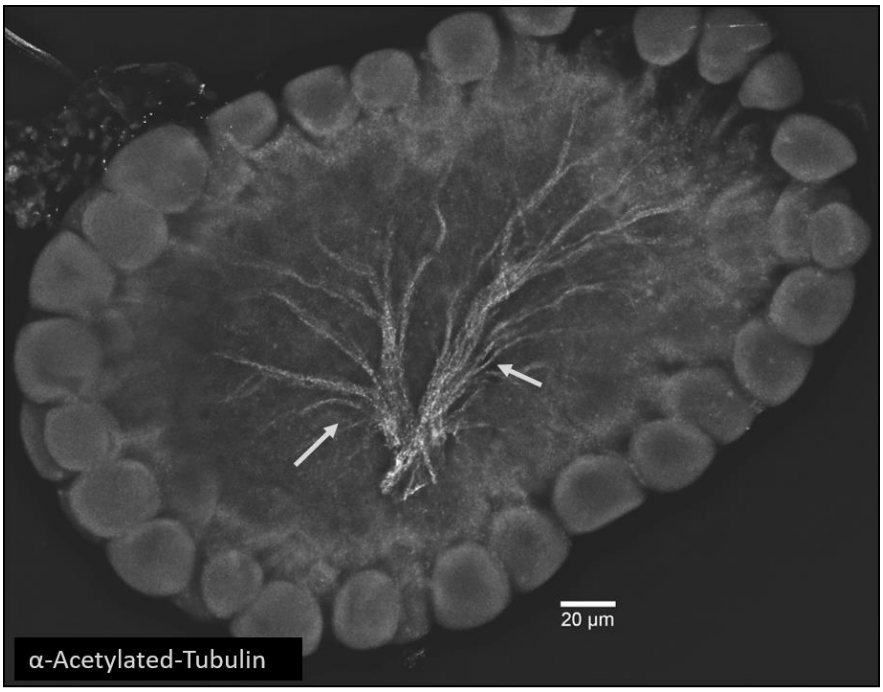

Fig. II-8 *Parhyale* adult retina – A dissected and immunostained adult *Parhyale* retina, showing the photoreceptor axons converging to the centre, forming an axon bundle

Fig. II-9 *Parhyale* adult optic lobe (next page) – A) Immuno staining with acetylated tubulin antibody of a vibratome section trough an adult *Parhyale* head, showing the structure of the optic lobe and eye. **B-C)** Zoom from the dashed box in A. (B) Two rows of nuclei (red arrows) is seen along the axon bundle coming from the retina. (C) An axonal bundle is seen from the retina to the lamina. Between the lamina and medulla we can distinguish a chiasma (arrowhead). The 3rd neuropil is possible the lobula or lobula plate, however a chiasma is not distinguishable. **D-D')** Detail from the dashed box in C, showing the axon bundle at different depths. The axons seem to cross each other (red arrows) **RE-** retina **LP-** lateral protocerebrum **LA-** lamina **ME-** medulla **LO-** lobula or lobula plate.

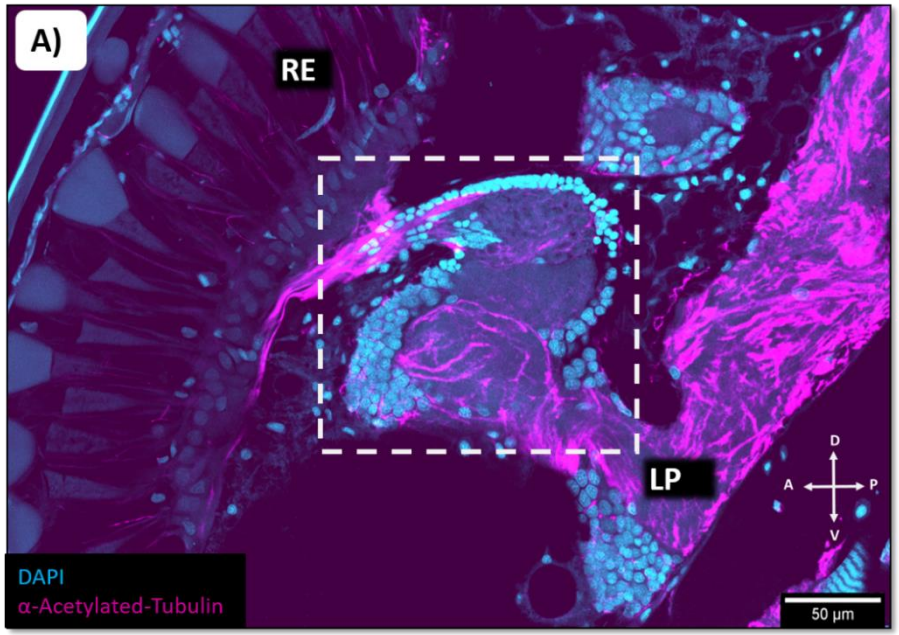
A)
RE
LP
D
A
P
V
DAPI
α-Acetylated-Tubulin
50 µm

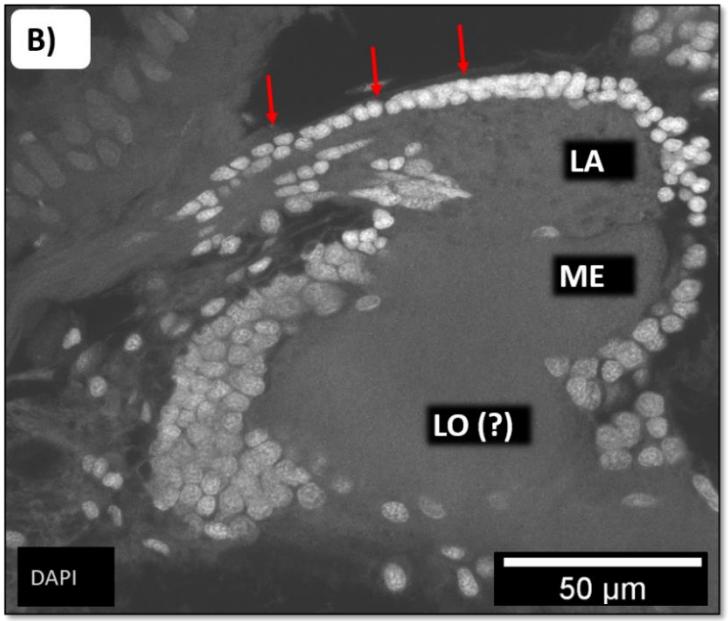
B)
LA
ME
LO (?)
DAPI
50 µm

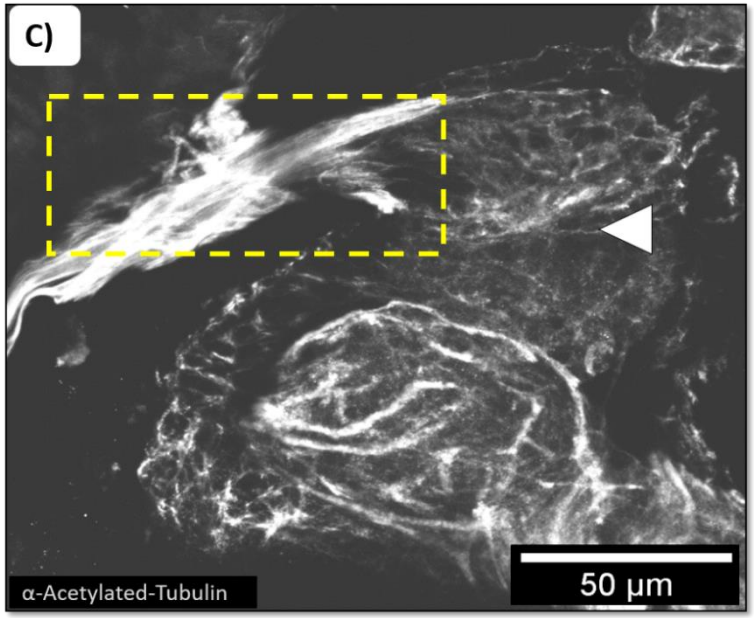
C)
α-Acetylated-Tubulin
50 µm

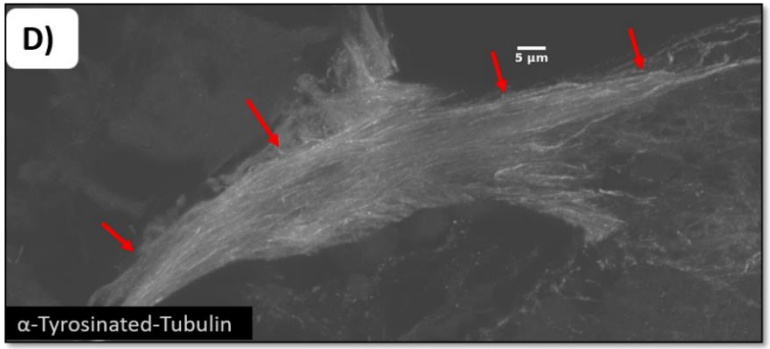
D)
5 µm
α-Tyrosinated-Tubulin

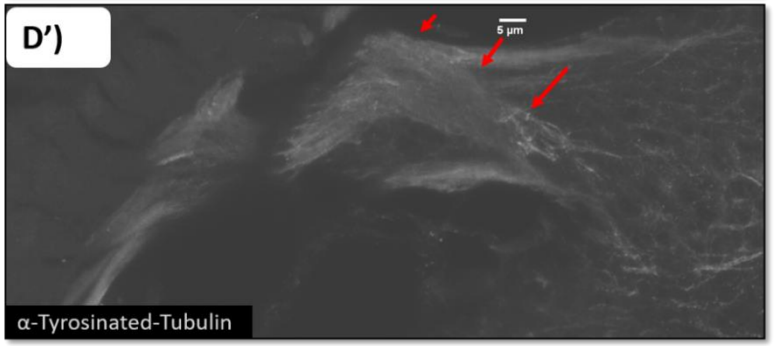
D')
5 µm
α-Tyrosinated-Tubulin

R1 to R5 project to the lamina

In malacostracan and hexapod species where photoreceptor projections have been previously studied, it was found that photoreceptors have either short fibers and connect to the lamina (R1-R6 in flies and R1-R7 in crabs), or long fibers and connect to the medulla (R7-R8 in flies and R8 in crabs).

The DC5 promoter, previously described for *Parhyale* (Konstantinides and Averof, 2014), is a central nervous system marker, driving expression of reporter proteins in the brain. I used a DC5::CFP reporter to generate G0 mosaic embryos where the DC5 signal was seen only in certain parts of the CNS, including the eyes (but not the totality of the optic lobe). Live imaging of two of these embryos, at S27-28, shows the retina and the axons that project from it, forming the optic nerve (Fig. II-10 A). Most of these axons are seen terminating in the lamina and a few are seen extending further (arrows in Fig. II-10 A).

To establish whether these projections correspond those of photoreceptors R1-R4 or R5, I imaged live embryos from the Ph-Opsin1 and Ph-Opsin2 transgenic lines, at S28. In both lines (Fig. II-10 B-C) photoreceptor axons are clearly seen emerging from the retina and forming an axon bundle, in a pattern comparable to what is seen in embryonic immunostainings for acetylated-tubulin and the live imaging of mosaic DC5::CFP embryos. The number of axons labelled in the Ph-Ops1 line is higher than those labelled in Ph-Ops2 line, corresponding to the axons projecting from R1-R4 and R5, respectively. For both lines, the axons terminate in a structure with similar position and morphology to the lamina.

To clarify whether the axons from different photoreceptor types terminate at different neuropils, I imaged live double transgenic embryos from the cross between Ph-Ops1 and Ph-Ops2 stable transgenic lines, at S29. The photoreceptor projections of both Ph-Ops1 and Ph-Ops2 are seen terminating at the same optic neuropil, the lamina, and there were no axons detected extending further from this neuropil (Fig. II-10 D). It was not yet possible to image adults from this cross (at the time of writing, they were still not fully grown).

To support these results, immunostaining of double transgenic embryos for acetylated-tubulin would have been ideal. However, staining of the whole embryonic brain is only possible if embryos are heat-fixed, which leads to denaturation of the fluorescent protein. This process results in a loss of endogenous signal and destroys the epitope recognized by antibodies.

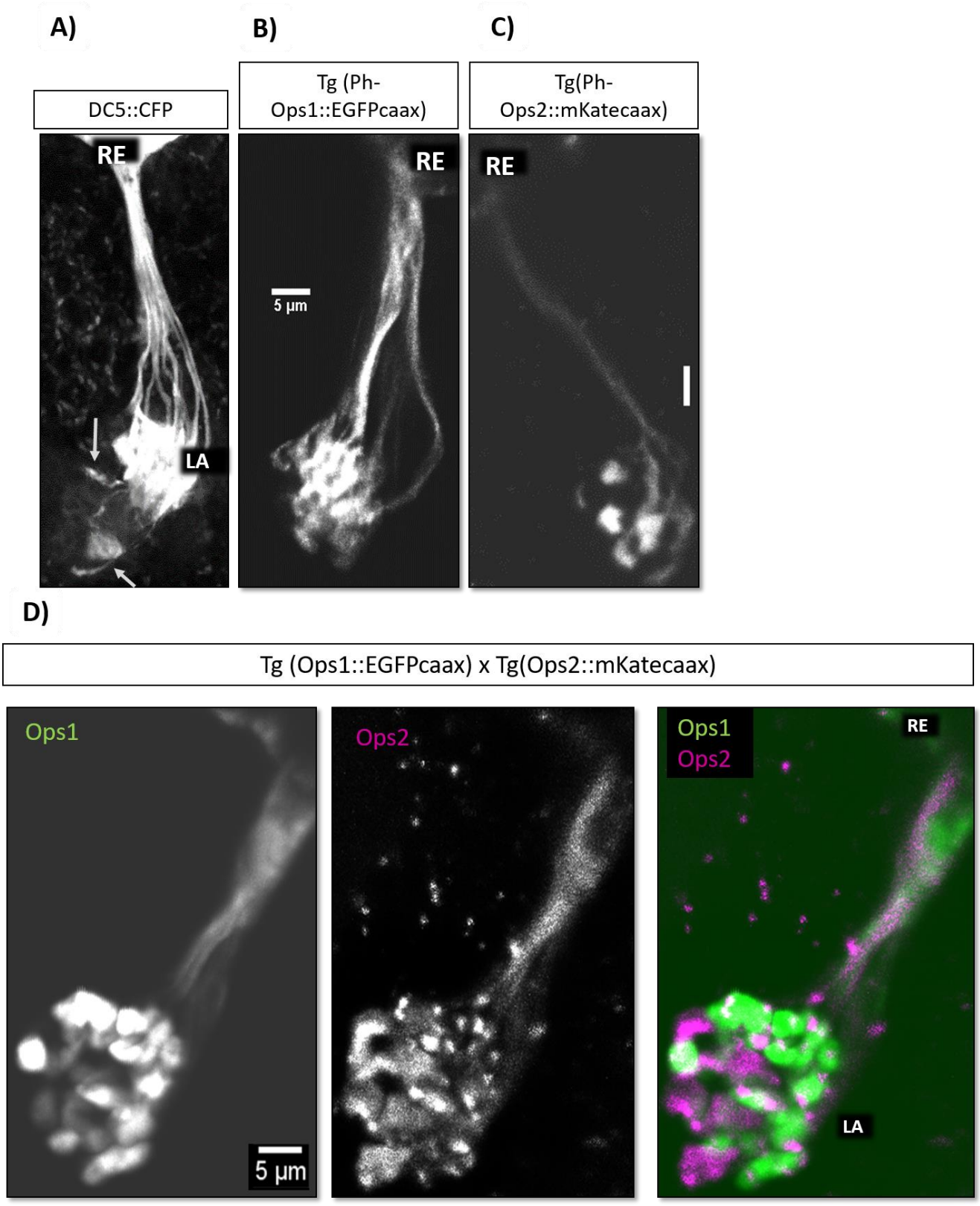

Fig. II-10 Photoreceptor projections to the optic lobe – **A)** Live imaging of a st27 embryo injected with the DC5::CFP construct. DC5 is a marker of the CNS in *Parhyale*. Most part of the axons coming from the retina end up in the lamina, and few are seen passing it. **B)** Live imaging of a S28 embryo from the Ph-ops1 and **C)** Ph-ops2 transgenic lines, showing the axonal projections from R1-R4 and R5, respectively. **D)** Double transgenic embryos. R1-4 and R5 project to the same neuropil. **RE**-retina **LA**- lamina.

III. Discussion

This thesis describes for the first time the structure of the visual system of the amphipod crustacean *Parhyale hawaiensis*.

General eye structure

Based on our observations on the structure of the eye, *Parhyale* has an apposition compound eye, with five photoreceptors per ommatidium and a fused rhabdom. This structure is in line with what has been described in other species of amphipods, including semi-terrestrial and shallow-water gammarids, and also more distant amphipods like hyperiids (Hallberg and Nilsson, 1980). The number of ommatidia per eye increases linearly with the growth of the animal throughout its lifetime, ranging from 8 ommatidia in hatchlings to ~50 in >1 year old adults.

The area of the eye also increases in part due to the addition of new ommatidia but also due to an increase in size of the facet diameter. This life time growth poses several questions regarding the visual capacities of older vs younger animals: are eyes from older animals more sensitive? If so, is there a difference in the behaviour of the animal? Post-embryonic eye growth has been previously described in other crustaceans during larval stages and in continuously growing adults(Meyer-Rochow et al., 1990). Of particular interest is a study on isopods (Keskinen et al., 2002)in which body size, facet diameter and rhabdom length increase with age. In this study the authors were able to show that indeed sensitivity in each ommatidium increases with age, making larger adults more sensitive to light. However in this study it was not shown whether there are repercussions on the behaviour of the animals.

Another question raised by these observations is where the new ommatidia are formed. In embryos new facets are seen emerging from the rim area of the entire circumference of the eye, but it is not clear if this mode of growth is maintained at post embryonic stages. It would be interesting to investigate whether there is a specific proliferation zone kept from embryos to adult stages and where this zone is located.

Visual pigments and spectral sensitivity in Parhyale

The opsin data shows that *Parhyale* may have a 2-channel colour vision, similar to what has been described in other marine crustaceans. This is mediated by expression of two opsins: Ph-opsin1, expressed in R1-R4, and Ph-opsin2 expressed in R5. In phylogenetic analysis, these opsins cluster with the crustacean LWS (from ~490 nm to ~530nm) and MWS (480nm), respectively.

It has been proposed for other shallow water crustaceans that green (LWS) absorbing photoreceptors are well adapted for enhanced photon capture at twilight,while UV/blue sensitivity is used for sun compass (light polarisation patterns, discussed in part 2) orientation(Marshall et al., 2003). This would fit well with recent *Parhyale* circadian rhythm studies showing that individuals are most active at twilight (B. Hunt and E. Rosato personal communication).

The phylogenetic data also agrees with studies in other shallow-water amphipods where, by extracellular electro-retinograms (ERGs), it was shown that ommatidia sensitivity to light peaks at around 430-450 and 520-550nm (corresponding to a MWS and LWS opsin class, respectively) (Forward et al., 2009; Gambineri and Scapini, 2008; Ugolini et al., 2010). In one of these studies, these peaks were recorded at the distal and proximal part of the ommatidium (Cohen et al., 2010). This observation lead the authors to argue that the rhabdomere of the R5 cell is positioned distally and does not extend to the full length of the rhabdom, an analogous situation to the R8 cell position in decapods. However, my data show that this is not the case in *Parhyale*, since the R5 rhabdomere, as well the rhabdomeres of R1-R4, are present from distal to proximal positions of the ommatidium.

On photoreceptor identity and homology

It is tempting to speculate that the R5 photoreceptor of *Parhyale* is homologous to the R8 of decapods, or even to the R7-R8 cells in *Drosophila,* and that *Parhyale* R1-R4 are homologous to decapod R1-R7 and *Drosophila* R1-R6. The latter have in common the fact that they are the largest photoreceptors and all express a LWS opsin. In contrast, *Parhyale* R5, decapod R8 and *Drosophila* R7-R8 have a smaller size and express a shorter wavelength opsin (either MWS or SWS). Homology could be further investigated by studying the different sets of genes responsible for photoreceptor specification and differentiation. I was unable to find such data for decapod R8, but many genes are described in *Drosophila*. Candidate genes to study could be spalt (regulate R7-R8 terminal differentiation)(Domingos et al., 2004), senseless (R8 differentiation) , Prospero (R7 differentiation), and Seven-Up, Rough and BarH1 (involved in R1-R6 differentiation) (Hayashi et al., 1998; Higashijima et al., 1992; Mlodzik et al., 1990; Tomlinson et al., 1988).

There is however one important feature that differentiates *Parhyale* R5 from R8 of decapods and R7-R8 of *Drosophila*. Using *Parhyale* opsin CREs to drive expression of reporter proteins in the photoreceptors (Ph-ops1::GFPCAAX and Ph-ops2::mKateCAAX), I showed that, at least in embryos, all labelled photoreceptor axons terminate at the lamina. I did not find labelled axons projecting further to the medulla. For technical reasons (the animals were not fully grown by the time of the writing), the data on adults is still missing. A similar situation has only been observed in the branchiopod *Daphnia*

magna, where all the projections, from the 8 photoreceptors that compose the ommatidium, terminate at the lamina (Nässel et al., 1978; Sims and Macagno, 1985)

Photoreceptor connections and colour processing

Colour vision in pancrustaceans is generally associated with the medulla, where colour opponent neurons (neurons receiving opposing excitatory and inhibitory inputs from receptors of different spectral types) are found. In *Drosophila*, L3 lamina monopolar neurons, which receive input from R1-R6, travel with R7-R8 axons from the lamina to the medulla, providing trichromatic input in the medulla (Fischbach and Dittrich, 1989; Schnaitmann et al., 2013a) , while in crayfish M1-M5 lamina neurons (similar to L3 in *Drosophila*) travel with R8, providing dichromatic input (KIRK, 1982). Despite the contribution of *Drosophila* R1-R6 in colour discrimination (Schnaitmann et al., 2013b), and the contact between R7/R8 and R6 axons in the lamina (through gap junctions)(Shaw et al., 1989; Takemura et al., 2008), there is no evidence for colour opponent coding in this neuropil (Kelber and Henze, 2013). Similarly, the lamina of dragonflies receives input from multiple spectral photoreceptor types, but colour opponent neurons (as described above) have not been found (Yang and Osorio, 1996).

These data highlight the importance of the medulla for primary processing of colour information, but is this the only way to achieve colour vision? *Daphnia magna* has tetra-chromatic vision(Young, 1974) but, as other branchiopods, it only has two optic (Nässel et al., 1978): the lamina (where all photoreceptor axons terminate) and a tectum-like neuropil (probably homologous of the lobula plate of insects (Strausfeld, 2005; Strausfeld et al., 2016). We still do not know in which neuropil colour opponent coding happens.

The expression of two different opsins in *Parhyale* indicates that the animals have dichromatic vision. However we still need to test, through behavioural experiments, whether they have colour vision, i.e., if they can indeed discriminate different wavelengths. If that is the case, it would be interesting to study where primary colour opponent coding occurs. There are two possible scenarios: 1) colour opponent coding occurs in the lamina, based on direct inputs from R1-R4 and R5; 2) colour opponent coding is carried out in the medulla exclusively through interneurons that carry the signals from R1-R4 and R5 from the lamina to the medulla.

We should also consider the possibility that I was not able to label all the photoreceptors. Data from DC5::CFP mosaic embryos shows some neurons extending beyond the lamina. These neurons might be lamina interneurons or photoreceptor projections that were not labelled by either of the Ph-Opsin reporters. This could be due to a failure or a delay in the activation of the Ph-Opsin CREs, or because there is a third, overlooked, opsin. Another possibility is that these small projections labelled by DC5 are pioneer photoreceptor neurons, coming from developing ommatidia, in which opsin expression was not yet

activated. R8 photoreceptors in *Drosophila* are the first ones to differentiate and to extend axons towards the optic lobe. These pioneer axons are crucial for lamina development and differentiation (reviewed in Hadjieconomou et al., 2011a)

Structure of the optic lobe

I was able to identify at least 3 consecutive visual neuropils, with 1st and 2nd neuropil being connected through a chiasm. These characteristics point to the presence, in the optic lobe of *Parhyale*, of a lamina, a medulla and a 3rd neuropil, which possibly corresponds to the lobula (based on the proposed nomenclature by Harzsch and Hansson, 2008; Sandeman et al., 1992), thus following the same pattern of other malacostracan crustaceans. A fourth distinct neuropil was not found, but its existence cannot be excluded, since it might be in close contact (or within) the lateral protocerebrum, and therefore hard to distinguish. These results confirm the recent findings in another amphipod, *Orchestia cavimana*, but also previous studies in gammaridea amphipods (Macpherson, 1977; Ramm and Scholtz, 2017). Through histological sections (stained with either reduced silver or toluidine blue), this studies demonstrated the presence of three optic neuropils and of one chiasm between the 1st and 2nd neuropil, but not between the 2nd and the 3rd. This leaves open the question if the third neuropil is indeed related to the lobula of insects (which receives crossed axons from the medulla), to the lobula plate (which receives uncrossed axons) or to none of these neuropils.

The photoreceptor axons from the retina of *Parhyale* connect to the lamina through an optic nerve. Unexpectedly, in *Parhyale* adults the neurons that form this nerve seem to cross over each other. The presence of the optic nerve was also described for *Orchestia cavimana*, but it is not possible to observe whether a crossing of the neurons exist. A more detailed description of single axons would be needed to confirm if this crossing represents a chiasm, with inversion of the retinotopic map, and how is it formed.

Ongoing projects

To complement the present data, a more detailed description of the connection map between neuropils would be needed to confirm the presence /absence of chiasms. This could be achieved by classic Golgi staining. The crossing over of axons could be better resolved also with the use of genetically encoded stochastic cell markers such as Brainbow (Hadjieconomou et al., 2011b; Livet et al., 2007).

Briefly, the original Brainbow cassette consists of several fluorescent proteins (usually 3) arranged in a tandem array, and separated by lox sites. Expression of a Cre recombinase results in random recombination between the lox sites and consequent “flip-out” of some of the fluorescent proteins. The final outcome depends on the fluorescent protein gene that is placed immediately downstream of the promoter, after the recombination event. If

more than one copy of the Brainbow cassette is present in the genome of the cell, multiple combinations of fluorescent proteins can be expressed, creating additional colours.

A similar technique, named Raeppli, was created for *Drosophila*, using the phiC31 integrase system as the method to achieve recombination (Fig. III-1) (Kanca et al., 2014). The phiC31 recombination system has already been used in *Parhyale* for gene trapping and trap conversion (Kontarakis et al., 2011). Therefore I started to implement this stochastic cell labelling method in *Parhyale*, by expressing the Raeppli cassette and the phiC31 integrase using either the *Parhyale* heat-shock promoter, the DC5 promoter or the Ph-Ops1 CRE (the final constructs can be found in Material and Methods). With this tool we may be able to trace single neurons, including individual photoreceptor axons from the retina to the optic lobe, and thus gain insight on the establishment of the retinotopic map in *Parhyale*, and on the presence/absence of chiasms between the retina and lamina and between the optic neuropils.

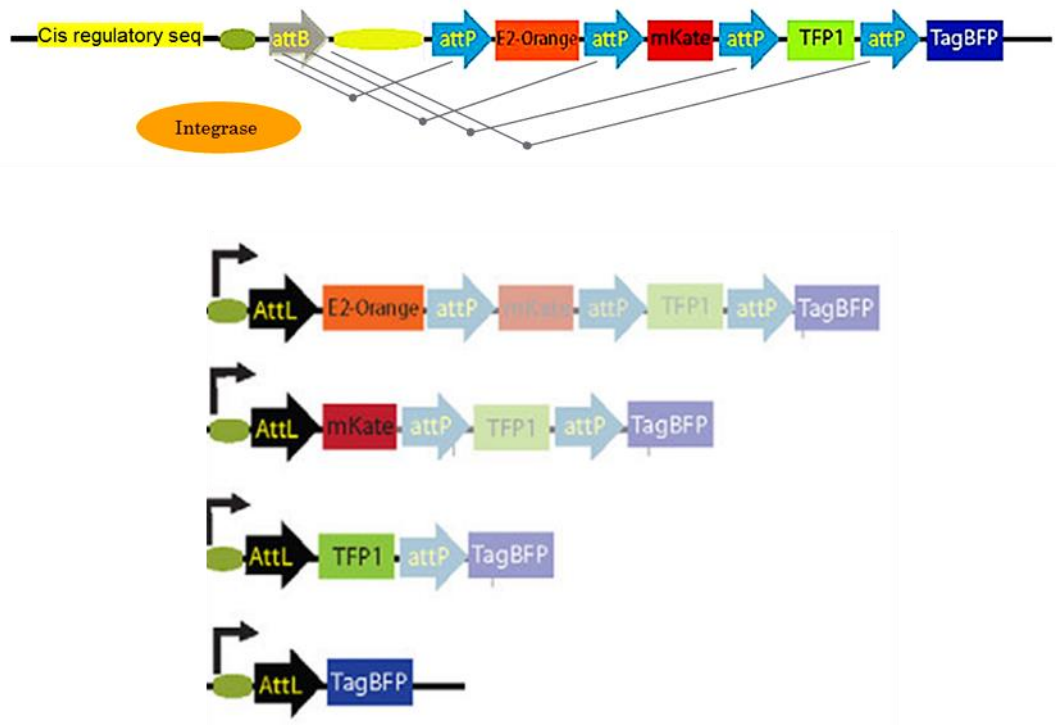

Fig. III-1 Raeppli cassette – The Raeppli cassette is composed of four fluorescent proteins. Recombination between the attB and attP sites is mediated by the phiC31 integrase. Depending on which attP site is used for recombination, the outcome can be expression of a E2-orange, mKate, Teal FP or Blue FP. *From* (Kanca et al 2014)

PART 2

EYE ADAPTATIONS TO THE ENVIRONMENT IN *PARHYALE*

I. Introduction

Arthropod visual systems constitute a spectacular example of how sensory systems adapt to the environment, so that the animal can profit from all the information given by its surroundings. These adaptations are crucial for fitness and have made it possible for arthropods to colonize almost all habitats on earth, in all possible light conditions.

Examples of these adaptations include the use of light polarisation and adjustments of the eye to temporary changes in light intensity.

I.1 - Light intensity adaptations – pigment cells and the arthropod pupil

When we look towards a bright beam of light, the pupil in our eyes closes in order to limit the amount of light hitting the photoreceptors. In conditions of low light, the opposite happens.

Compound eyes are also able to adjust the amount of light that reaches the rhabdoms. This adaptation to light intensity can be achieved by several mechanisms: an adjustable pupil/iris that regulates the amount of incoming light, mediated by the repositioning of pigment granules inside photoreceptor cells and/or at the pigment cells surrounding the photoreceptors and crystalline cone; changes in rhabdom dimensions; or rhabdom movements towards or away from the lenses (reviewed in Fleissner and Fleissner, 2006; Hoglund et al., 1969; Narendra et al., 2013; Ro and Nilsson, 1995).

These mechanisms can be triggered directly by light itself, or indirectly based on circadian rhythms and controlled by efferent signals from the brain (Reisenman et al., 2002). This adaptation is crucial for animals living in dim light conditions, where extra efforts must be made to collect every photon available. This is why in most nocturnal animals these changes happen according to the time of the day, in a very predictable pattern. For example, the beetle *Pachyomorpha sexguttata* (Dube and Fleissner, 1986) has superposition compound eyes during the night, with screening pigment completely retracted from the cone cells and clear zone. As the day approaches, the pigment moves distally into the clear zone, transforming the eye into an apposition-type compound eye. These major structural changes are initiated by circadian rhythms, and fine-tuned by light intensity.

I.2 - Polarisation vision

Light can be described as an electromagnetic wave, with electric and magnetic fields that oscillate perpendicular to each other, at the same frequency. The plane of oscillation of the electric field waves (the e-vector) determines whether a beam of light is linearly, elliptically or circularly polarised (Fig. I-1).

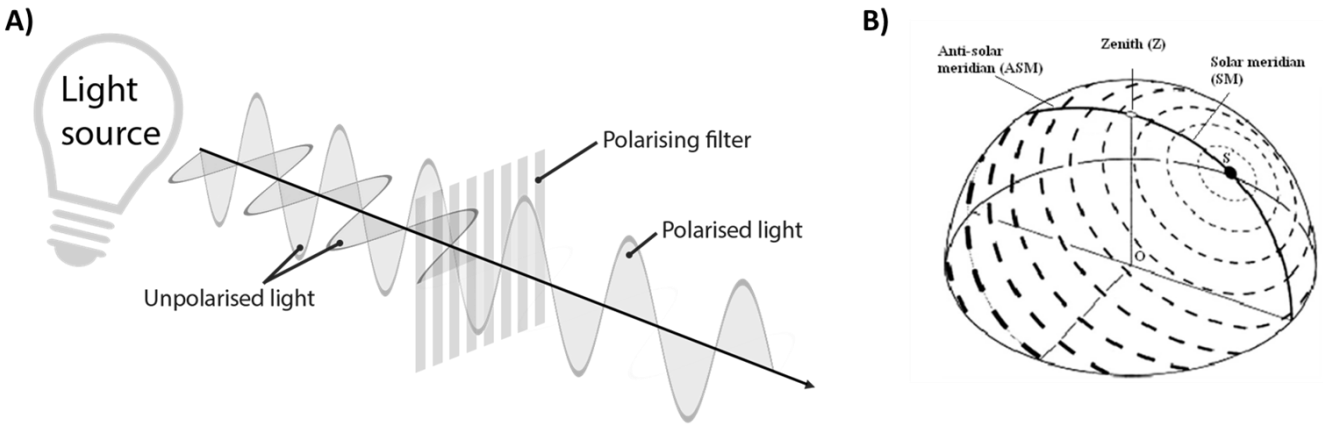

Fig. I-1 Light polarisation – A) Light coming from a light source is generally said to be unpolarised since it contains photons oscillating in different directions (the e-vector of two photons is represented here by the two waves). A polarising filter blocks the progression of photons which oscillate in certain directions, producing a beam of linear polarised light. **B)** 3D representation of the pattern of polarisation in the sky (sun position marked in **S**). *From* (Karman et al., 2012)

Natural light is composed of a collection of beams with different wavelengths and directions of polarisation. Light can become linearly polarised either through scattering of the sunlight by particles in the atmosphere, or through reflection by a non-metallic shiny surface and dielectric (non-conducting) surfaces, like water, soil, vegetation or even particular body surfaces (fish scales and arthropod cuticle) (reviewed in Wehner, 2001). Linear polarised light will then have 3 characteristics: an angle (preferential orientation of the e-vector), a degree of polarisation (what proportion of photons share that e-vector) and intensity (rate of photon flux).

In the atmosphere, scattering of light generates partly linear polarised light with e-vectors arranged in concentric rings around the sun (Fig. I-1). These patterns are often used by animals as a navigation aid. In the same way, polarised light originating from reflections on water is often used by animals seeking water.

Visual pigments are more likely to absorb a photon whose e-vector is parallel to the chromophore long axis. Due to the fact that these are transmembrane proteins, the

chromophore is nearly parallel to the plane of the membrane. Therefore the probability of photon absorption will depend on the angle with which the light strikes the membrane. In sum, light polarisation detection will depend on the geometry of the photoreceptor cell membranes, where the visual pigments reside.

In rhabdomeric photoreceptors, the microvilli of each cell are stacked in parallel arrays. The concentration of visual pigments will, therefore, be higher along the parallel axis of the microvilli, leading to a preferential sensitivity of the cell to photos with e-vectors in the same plane. This physical property makes rhabdomeric photoreceptors intrinsically sensitive to linearly polarised light. Further, photoreceptors within an ommatidium are disposed in a circular fashion, such that microvilli from different photoreceptors often display orthogonal alignments when compared to each other. Thus, the ommatidium, as a whole, is sensitive to various angles of light polarisation.

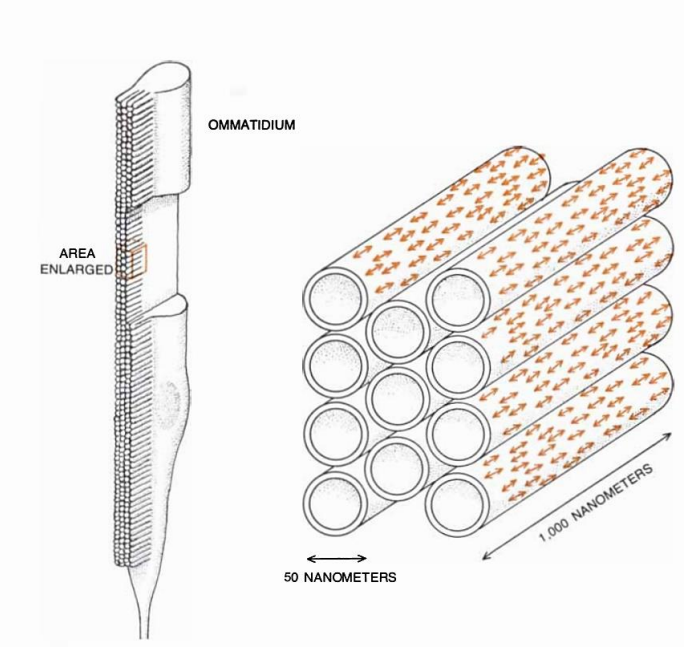

Fig. I-2 Rhabdomeric photoreceptor – Visual pigments (in orange) are oriented parallel to the long axis of the microvilli. *From* (Wehner, 1976).

Since light polarisation originates from reflection of sun light on many surfaces, habitats with a rich visual scene carry much information in the form of polarised light but also colour. To be able to fully exploit both types of information animals can separate the colour and polarisation information paths. Insects, for example, achieve this by employing different ommatidia to detect polarisation and colour.

Most of insect ommatidia are polarisation-insensitive by having their rhabdoms twisted along the direction of the incoming light, thus normalising their sensitivity with respect to different directions of polarisation. Polarisation sensitive ommatidia (whose rhabdoms do not rotate) are then grouped in specific areas of the retina – the Dorsal Rim Area (DRA) and the ventral eye – to detect polarisation patterns in the sky and polarisation cues coming from surfaces in the ground (like water ponds), respectively. In *Drosophila*, for example, photoreceptors at the DRA show several adaptations that optimize sensitivity to the sky's polarised light: rhabdomeres of R7 and R8 are not twisted, they are enlarged, orthogonal to each other and they express the same UV opsin (Rh3), a wavelength where scattering of light is stronger. These characteristics make R7 and R8, from the DRA, both necessary and sufficient for polarisation–related behaviours (Wehner et al., 1975; Wernet et al., 2012).

In malacostracan crustaceans, the solution is different. The R8 photoreceptor has orthogonal microvilli, making it insensitive to light polarisation. In contrast, the rest of the rhabdom (composed by R1-R7) is built in a way that maximizes polarisation sensitivity: the rhabdom does not rotate and the microvilli of the fused rhabdom are stacked in interdigitating layers. With this geometry, the whole stack of rhabdomeres is able to retain excellent polarisation sensitivity (Waterman, 1981).

While we have much information on how colour and motion are primarily processed, little is known about the neuronal circuits involved in the processing of polarisation signals. In the locust *Schistocerca gregaria*, one of the best studied systems, polarisation coding neurons are found at the lobula, which connect to the central brain, where the e-vector pattern is analysed (Heinze and Homberg, 2007; Omoto et al., 2017; Vitzthum et al., 2002).

I.3 - Polarisation–related behaviours

Scattering of light in the atmosphere or reflection by water surfaces creates extended sources of light polarisation used by animals for navigation.

The bug *Notonecta glauca* was the first species where a specific behaviour related to water reflection was discovered. When flying over water surfaces, this bug senses horizontally polarised light using a specialized region on the ventral surface of the retina.

When presented with horizontally polarised light this bug initiates a characteristic plunge reaction (Schwind, 1984). Similar behaviours are seen in other insect species (mayflies, dragonflies etc.) that are attracted by ponds, lakes or rivers for feeding, mating and egg laying (reviewed in (Cronin et al., 2014)).

The sky's polarisation pattern is probably the most widely used source of light polarisation. Even when the sun is not visible (due to partial cover), this pattern can provide animals with a very reliable source of information, used for orientation while walking or flying. Dung beetles use these e-vector patterns to navigate in straight lines and avoid contact with other beetles (Dacke et al., 2013). *Drosophila* also shows similar behaviours, by spontaneously aligning their body axis parallel to the e-vector of linear polarised light (polarotaxis) (Velez et al., 2014).

In addition to scattering in the sky or reflection on water, light also becomes polarised when it is reflected by objects, plants or animals. This feature is especially useful underwater, since it can be used as a source of contrast (which is generally reduced in the aqueous environment). In marine environments there is a general background of horizontally polarised light. An animal swimming within this background, even if not easily distinguishable by colour, will create a contrast of light polarisation. It is not surprising then that many predators use this contrast to detect preys, even partially transparent ones (reviewed in (Cronin et al., 2014)).

An extreme example of the use of polarisation vision is its use for intra-species signalling by stomatopod crustaceans. The eyes of the mantis shrimp are packed with polarisation sensitive photoreceptors and some species have cuticles that generate patterns of linear and/or circular polarisation. These patterns are used for mating but also for fighting conspecifics (Chiou et al., 2008).

I.4 - Purposes of Part 2

This part of my project is dedicated to understanding if *Parhyale* eyes adapt to and use the different light conditions (intensity and polarisation) in their environment; namely how the eyes adapt to different light intensities and whether the eyes of *Parhyale* are sensitive to light polarisation.

II. Results

II.1 - Pupil adaptation in Parhyale

Parhyale eyes adapt to light intensity independently of the circadian rhythm

Adaptation to light intensity in arthropods is mediated by several mechanisms, including the movement of pigment granules within the ommatidia. We have seen in the previous chapter that in *Parhyale* the dark shielding pigment is enclosed in the photoreceptor cells and that the reflective pigment surrounds the ommatidia, possibly within reflective pigment cells (see part 1 Fig. II-1). To investigate if *Parhyale* eyes would adapt to differences in light intensity, I imaged the effects in the eye when transferring the animals from dark to bright environments. For this, animals were initially kept in the dark for 20 min, so that they would become dark adapted. Then the eyes were imaged every 30sec from the moment lights were turned on, as the eyes became light adapted.

Dark adapted eyes (as imaged at 0sec after illumination) showed a white reflection throughout the eye (white arrow in (Fig. II-1 A)). This reflection quickly disappeared after illumination: within 1 min a clear reduction is seen in brightness intensity, and after 2-3 min the eye becomes dark. This experiment was repeated during the day (with 6 different animals) and night (with 2 animals). In both cases there were no visible changes in the capacity and timing of adaptation to bright light. The reverse experiment, adaptation from bright to dark environments, was not performed.

Next I set out to investigate in more detail which changes occur within the ommatidia when animals were light or dark adapted. For this, animals kept in dark conditions for 30 min, were fixed and prepared for TEM. EPON-embedded samples were then sectioned in semi-thin (2μm) or ultra-thin (50nm) sections, and imaged with a light or electron microscope, respectively (3 animals were imaged with light microscopy and 1 animal with electron microscope). TEM images obtained from these dark adapted animals were compared with the TEM images taken from animals adapted to bright conditions (see Part 1).

In serial semi-thin sections of light adapted animals, the shielding pigment vesicles are seen concentrated in high numbers and in proximity to the rhabdom (highlighted in red in Fig. II-1 B), creating a dense dark shield. In contrast, in dark adapted animals, dark pigment vesicles are seen spread through the eye, in what seem to be lower numbers. Only a small number of dark vesicles are seen around the rhabdoms. I did not observe obvious changes in rhabdom morphology; the most distal tip of the rhabdom is kept in close contact with the lenses in both conditions.

TEM sections gave us a more detailed view of the changes within photoreceptor cells. In light adapted animals we can clearly see a high number of dark pigment vesicles, within the photoreceptor cell, in close contact with the rhabdom. For dark adapted animals, the number of dark vesicles is considerably reduced. Most part of the rhabdom is not covered with these vesicles and the basal side of the photoreceptor cell membrane is seen very close to it (red arrows in Fig. II-2). As a result the reflective pigment, surrounding the photoreceptor cell, is very close to the rhabdom. The reflective pigment in dark adapted eyes seems to have a different TEM contrast when compared to TEM imags of light adapted eyes. This may be an artefact due to the fixation, since usually reflective pigment cells do not fix well.

It was not possible to determine the direction of movement of the pigment vesicles from dark to light adapted stages, since there is no obvious accumulation of pigment vesicles at proximal positions of the eye (which would indicate a distal-proximal movement), neither at the basal side of the photoreceptor cell (which would indicate an apical-basal movement), as seen in *Drosophila* for example (Satoh et al., 2008).

We can therefore conclude that light adaptation in the eyes of *Parhyale* is mediated by changes in the position of the shielding and reflective pigment granules, without changes in the rhabdom structure. The movement of the pigment granules may be a cause or consequence of the changes seen on the membrane at the basal side of the photoreceptor cell.

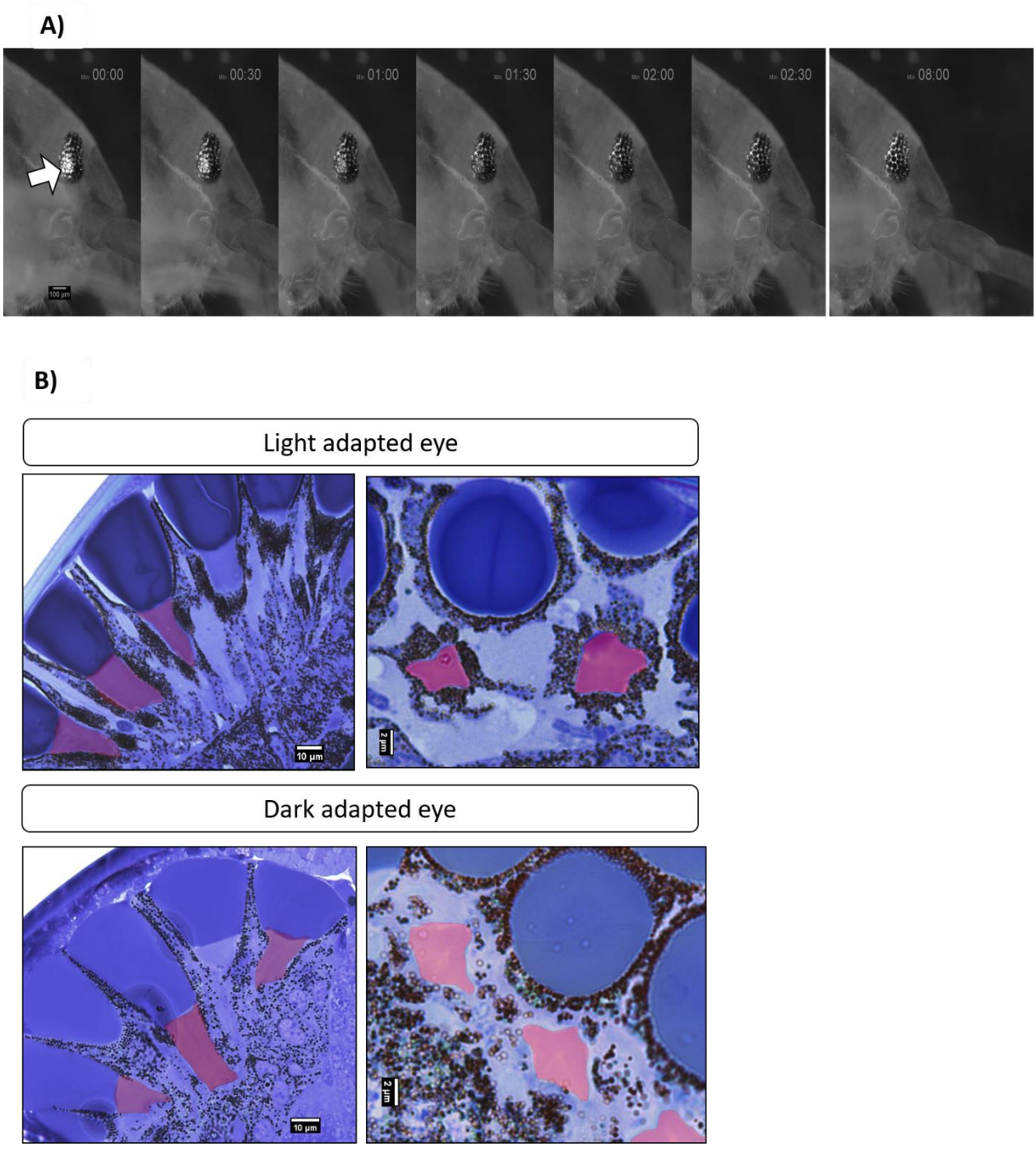

Fig. II-1 Pupil adaptation in *Parhyale* – A) Live imaging of an adult *Parhyale* showing pupil adaptation to light. After spending 20 min in the dark, a white reflection can be seen in the eye (arrow at time 00:00). After few minutes of light adaptation, this reflection disappears. **B)** Semi-thin sections of light and dark adapted eyes, stained with toluidine blue. The dark pigment granules are seen surrounding the rhabdoms (highlighted in red) in light adapted animals. In dark adapted eyes the pigment granules move away from the rhabdoms.

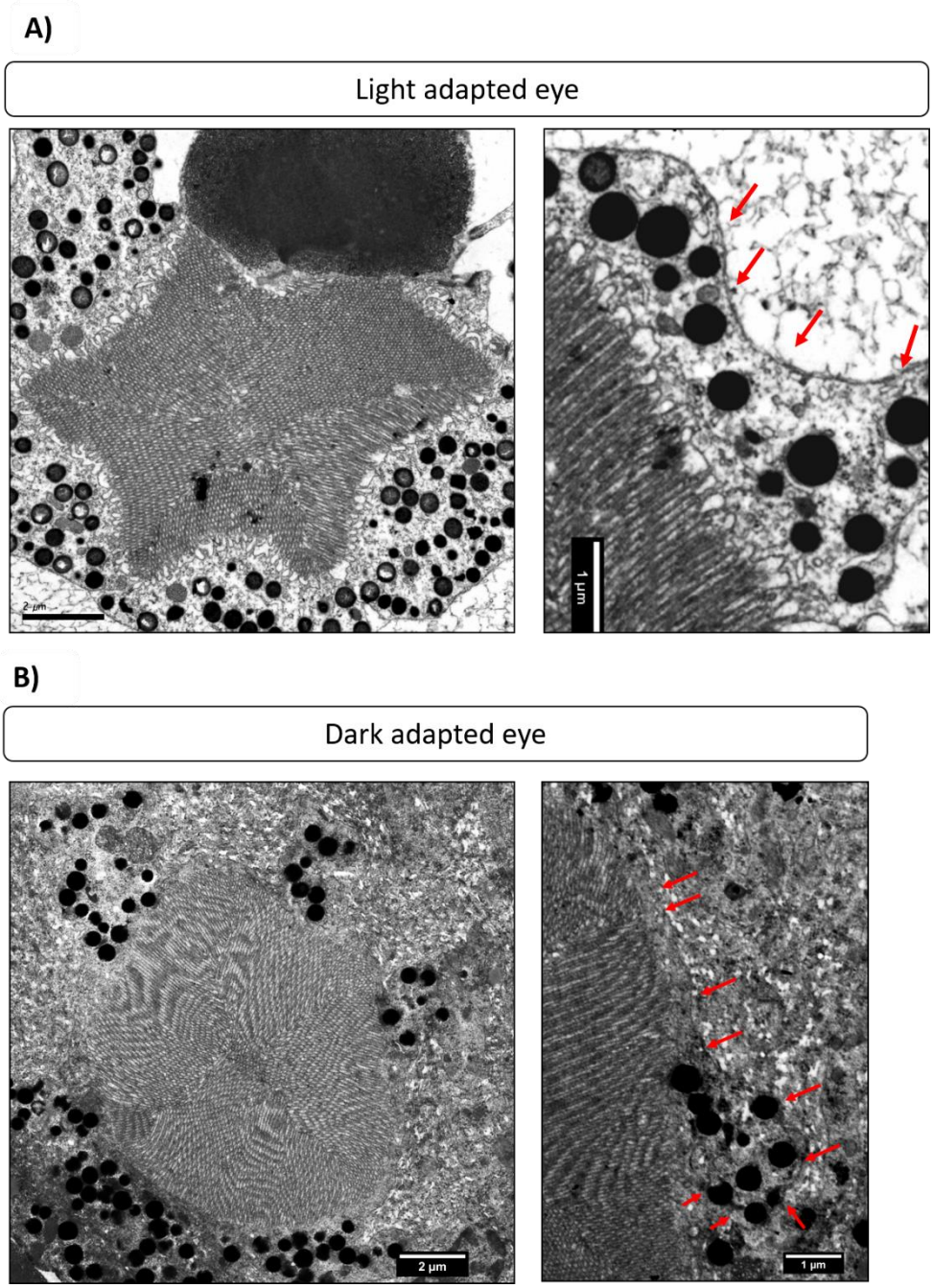

Fig. II-2 TEM in dark and light adapted rhabdoms – A) In light adapted eyes, the shielding pigment granules surround the rhabdoms and are positioned between the rhabdomere and the photoreceptor cell membrane at the basal side of the cell (red arrows) **B)** In dark adapted animals, the basal membrane of the photoreceptor cell is very close to the rhabdomere. Only few parts of the rhabdom are in contact with shielding pigment granules

II.2 - Polarisation sensitivity in Parhyale

Parhyale photoreceptors are structurally adapted to perceive light polarisation

Compound eyes are intrinsically sensitive to light polarisation due to the microvilli arrangement in parallel arrays, but in some animals this intrinsic property attenuated by rotation of the rhabdom.

In transversal TEM sections of *Parhyale* eyes (described in part 1), we can see that the microvilli of R1 and R3 are orthogonally aligned with those of R2 and R4 (Fig. II-3 A). In addition, in longitudinal sections through the rhabdoms, we can see two sets of microvilli (belonging to two adjacent photoreceptor cells) that keep their orthogonal alignment from the distal to the proximal part of the rhabdom (Fig. II-3 B). This indicates that the rhabdom does not rotate (seen in 4 ommatidia, from serial sections trough one eye) (Fig. II-3 B).

To confirm what was seen with TEM longitudinal sections, I analysed thick vibratome sections (300µm) from an adult retina of the Ph-Ops2 transgenic line. In single ommatidia the signal from the R5 cell (in magenta Fig. II-3 C-D) is seen in the same side of the rhabdom, from the distal to the proximal part, without obvious rotation. This pattern is kept through the whole retina.

These features indicate that *Parhyale* ommatidia are intrinsically sensitive to light polarisation, with R1+R3 being most sensitive to one e-vector and R2+R4 being most sensitive to the orthogonal e-vector.

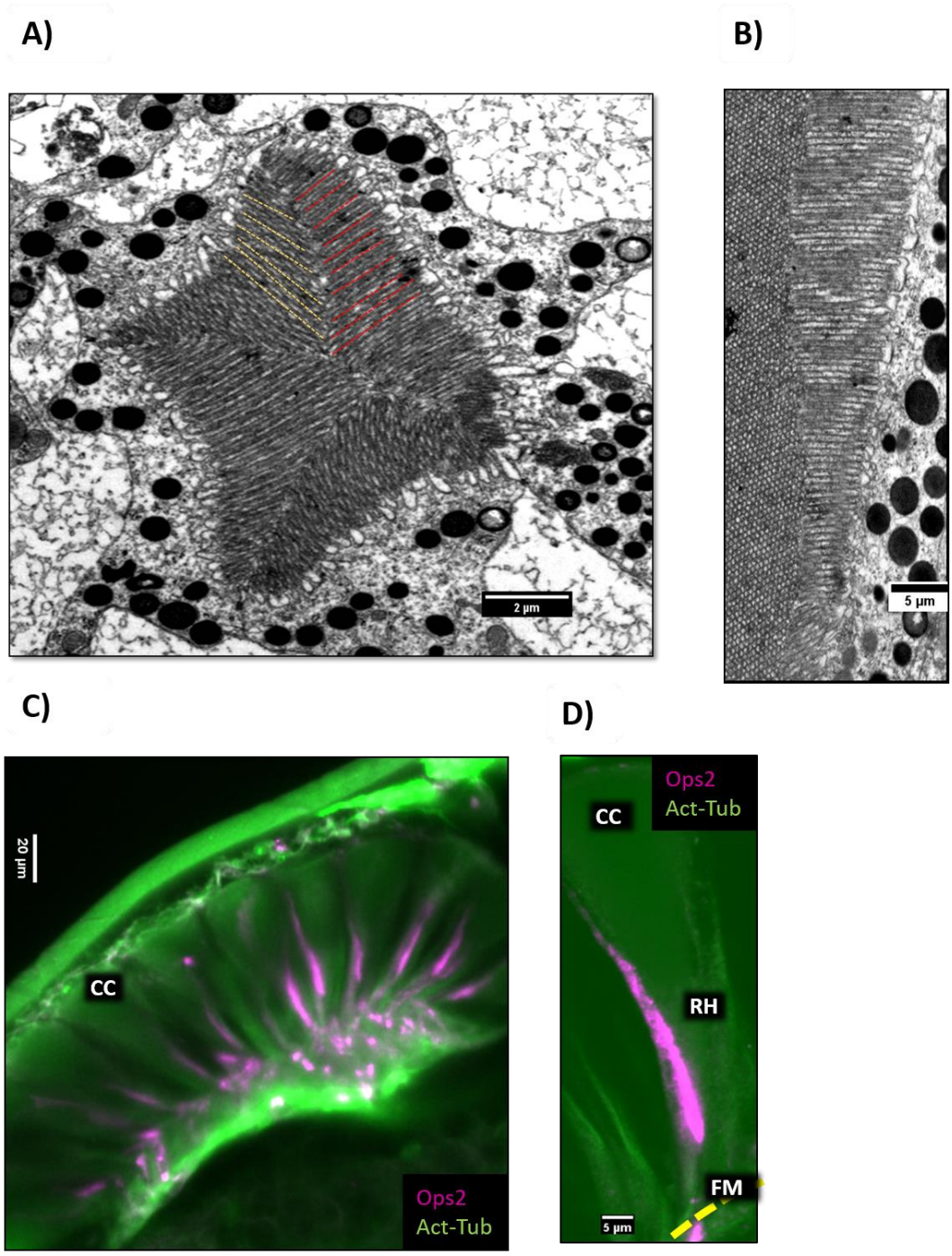

Fig. II-3 Microvilli alignment in *Parhyale* photoreceptors – **A)** transversal TEM section through the rhabdom showing the microvilli of each photoreceptor orthogonally aligned to the adjacent photoreceptor. **B)** Longitudinal section of a rhabdom. We can see 2 sets of orthogonally aligned microvilli, showing that the rhabdom does not rotate in the distal (up) to proximal axis. **C-D)** Vibratome longitudinal section of an adult eye from the Ph-Ops2 transgenic line. The rhabdomere of R5 keeps in the same side along the rhabdom in the distal-proximal axis, indicating that the rhabdom does not rotate.

Parhyale are positively phototactic for low light intensity but do not show polarotaxis

The fact that *Parhyale* photoreceptors are sensitive to light polarisation does not necessarily mean that this sensitivity is reflected in different behaviours, guided by light polarisation information. To explore if *Parhyale* behave differently under different light conditions, I set up a simple behavioural assay consisting of a two-choice tube maze, or T-maze, placed in a tank with enough water to cover the bottom of the maze with ~3cm of water (Fig. II-4 A). In this assay, animals are given distinct light conditions at each extremity of the maze and, after being placed in the middle of the maze, animals can choose to swim to either of the extremities. For all the behavioural assays, groups of 10 animals (males and females) were placed at the centre of the maze. After 5 min the number of animals present at the extremities of the maze, or in the middle, was counted.

I first set out to test if animals show a preference for light or dark environments (Fig. II-4 A-B). For this, animals were given the choice between diffused light and a dark environment. On a first experiment, under low light intensity (<400lux), a total of 330 animals were tested. In these conditions, 182 animals (55%) swam towards the light, while only 89 (27%) swam towards the dark extremity. In a second experiment with 100 animals, when light intensity was stronger (700lux), the number of animals preferring light decreased to 31 (31%), while those preferring the dark extremity accounted for 46 (46%). These experiments show that *Parhyale* are positively phototactic at low light intensity but not at high light intensity.

To test weather animals are also polarotactic I tested animal choice between unpolarised light vs polarised light, by placing a polarising filter at one of the extremities of the maze (Fig. II-4 C-D). A total of 110 and 50 animals were tested for a choice between unpolarised and vertically or horizontally polarised light. For all light conditions, light intensity was kept at 400lux.

For unpolarised vs vertically polarised light 51 animals (46%) showed a preference for unpolarised light and 43 (39%) for vertically polarised light. For unpolarised vs horizontally polarised light the result was of 19 animals (38%) vs 23 (46%). These results indicate that *Parhyale* do not show a preference for polarised light under these conditions.

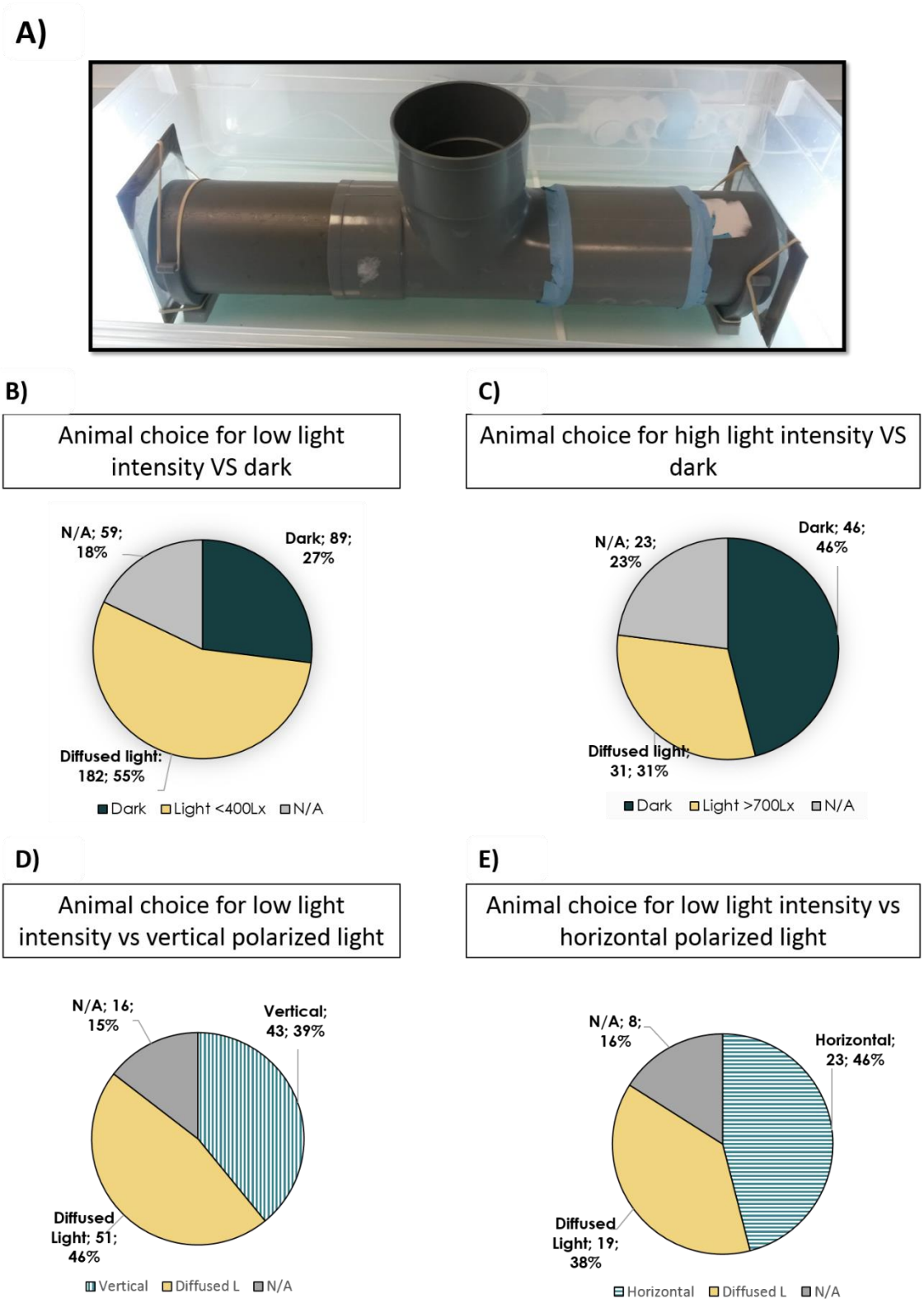

Fig. II-4 Phototactic and polarotactic behaviour in *Parhyale* – A) T-maze set up for the light choice behaviour experiments **B-E)** graphs showing the absolute number of animals choosing between: **B)** low light intensity (400 Lux) vs dark; **C)** high light intensity (700 Lux) vs dark; **D)** Diffused light vs vertically polarized light (both 400 Lux); **E)** Diffused light vs horizontally polarized light (both 400 Lux). N/A represents the number of animals that remained in the middle of the T-maze.

Parhyale escape pattern doesn't vary upon light polarisation

Although *Parhyale* did not seem to show a preference for polarised light (under the conditions of my experiment) we still wondered whether the animals might show sensitivity to polarised light in other assays. For this purpose I studied their escape response, i.e. the escape motion by an animal provoked by unpleasant or dangerous situations. When placed in open spaces, *Parhyale* have a tendency to escape towards the extremities of the container and swim around it, stopping only when a resting spot (usually a stone) has been found. To see whether direction of escape is influenced by the light polarisation pattern, I built a set up consisting of a square arena with dark walls and a transparent bottom. This arena was illuminated from above, either with unpolarised or polarised light, at the same intensity (<400lux) (Fig. II-5 A). Animals were placed in the middle of the arena through a little hole in the filter and the swim pattern was recorded from bellow, until one of the walls was reached. Three light conditions were used: diffused light, and polarised light in two orthogonal directions. Approximately 35 animals were used per condition. Their trajectory and final destination was followed and plotted (Fig. II-5 B).

In all conditions, the animals quickly swam from the centre to the periphery of the arena. This escape movement was immediate, except for few animals which took a few turns before reaching the periphery (this was more frequent in the second condition, with horizontally polarised light). However, the direction of the trajectory and the final destination of the animals seemed to vary independently of the light conditions presented. The velocity of the escape response was not measured.

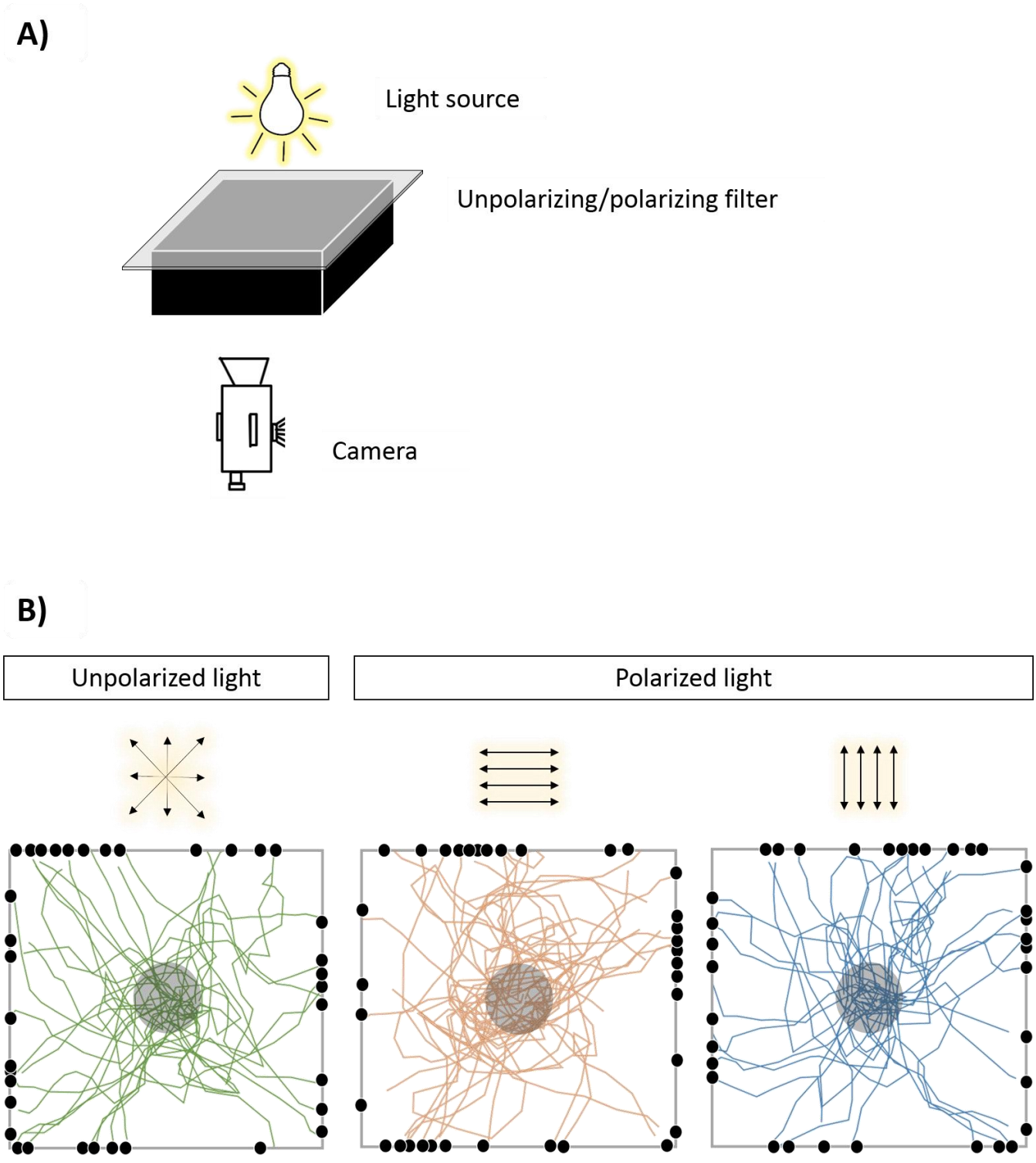

Fig. II-5 Escape trajectories in *Parhyale* – A) Set up for the escape behaviour experiments. **B)** Tracks of individual animals from the centre to the periphery under different light conditions. Dark circles represent the final position of the animal. The grey area depicts the site were animals were placed at the start of the experiment.

III. Discussion

Pupil adaptions

I have shown that *Parhyale* eyes can rapidly adapt from dark to light conditions. When animals are adapted to dark environment, the surface of their eyes shows a bright white reflection, which derives from the movement of shielding pigment granules away from the rhabdom and the approximation of the reflecting pigment. The basal membrane of the photoreceptor cells appear to move closer to the rhabdom. Once the eyes are subjected to light conditions, the white reflection quickly disappears due to the return of the shielding pigment to the surroundings of the ommatidia.

I was not able to access clearly the direction of pigment movement. In *Drosophila* compound eyes (see Fig. III-1 (Satoh et al., 2008)) the pigment granules are clearly seen displaced from the basal side of the cell in dark conditions, towards the apical side (next to the rhabdomeres) after light adaptation. In *Parhyale* the pigment granules do not seem to move on the apical-basal axis, however it was also not clear, even in serial sections, whether there was any shielding pigment accumulation at the proximal or the distal part of the eye in dark adapted animals.

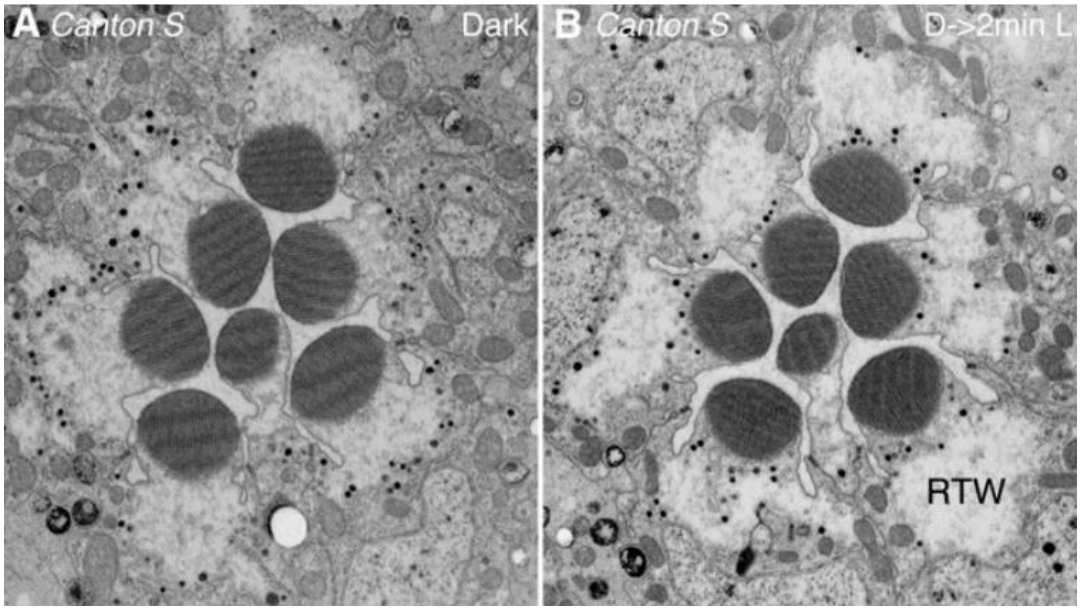

Fig. III-1 The *Drosophila* pupil – In *Drosophila* shielding pigment granules move from the basal to the apical side of the photoreceptor cell as the eye becomes light adapted. *From* (Satoh et al. 2008)

There are many studies describing pupil movements in insects and crustacean eyes (especially from nocturnal species) however, except for *Drosophila*, little is known about the cellular components involved. As I have described for *Parhyale*, and as it is seen in other pancrustaceans, pupil adaptation involves the movement of numerous vesicles along the cells and the re-shaping of the photoreceptor and pigment cell morphologies, which happens in a short period of time. Deciphering intracellular mechanisms and cell mechanics involved in this process would be of great interest.

Light polarisation sensitivity in Parhyale

Arthropod rhabdomeric photoreceptors have an intrinsic capability to detect light polarisation. Arthropods evolved to explore this characteristic in order to collect the maximum information possible from their surrounding environment. *Parhyale* R1+ R3 and R2+R4 rhabdomeres are orthogonally aligned and the rhabdoms do not rotate. These two simple characteristics make the eye well adapted to perceive light polarisation.

Behavioural studies in shallow-water and semi-terrestrial amphipods have already shown that these animals use the sun as a compass to direct movements towards preferred locations. Orientation in these species is dependent on specific wavelengths: short-wavelength blue light (~430-480 nm) is required for directional movement in response to polarised light, while green wavelengths (~520nm) are needed for endogenous circadian activity rhythm (Cohen and Putts, 2013; Forward, et al., 2009; Forward et al., 2009; Ugolini et al., 2010). In particular, when placed in an arena covered with a polarising filter, animals move in a direction parallel to that of the e-vector, if the incident light has a short wavelength. If the wavelength is longer (around 520 nm) their alignment with the e-vector is less strong.

The behavioural experiments that I performed show that *Parhyale* is positively phototactic, but I have failed to show that the animals react to or have a preference towards polarised light. The fact that polarised related behaviours have been shown in other amphipods with similar life styles suggests that *Parhyale* might show similar behaviours under different experimental conditions from the ones I set up.

Short wavelengths seem to be a requirement for directional movement according to the e-vector of light. This poses two main constraints on the behaviour experiments: 1) the polarising filter needs to not block short-wavelengths; 2) the light source must contain those wavelengths. The behaviour set-ups described above for other amphipod species, used the sun as a light source to test light polarisation sensitivity and bandpass filters to select the specific wavelengths. For *Parhyale* I used a white LED as light source, with a colour temperature that mimics natural sun light, expected to have a peak of intensity between 450 and 500nm (Fig. III-2), and a polarising filter that does not block short-wavelengths. It is possible that the light intensity at short-wavelengths coming from the

LED lamp was not sufficient to induce polarised light guided behaviour. Therefore the behaviour experiments should be repeated using either direct sunlight or LED lights of more specific wavelengths.

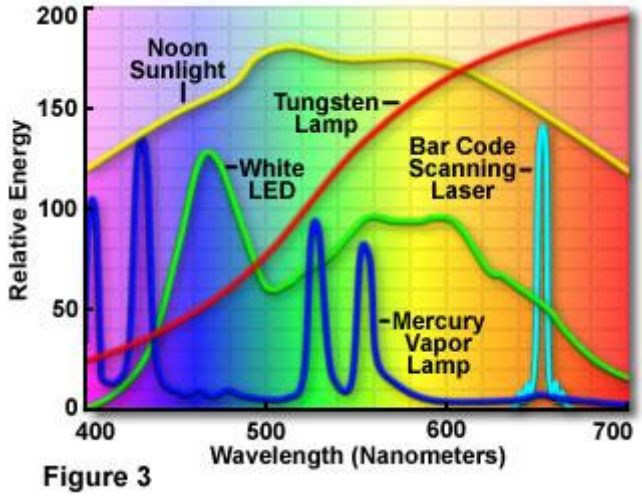

Fig. III-2 Spectra from common light sources

It is intriguing that the wavelengths needed for induction of light polarisation guided behaviour in other amphipods (short wavelengths) are not the ones maximally absorbed by the orthogonally aligned photoreceptors R1-R4 (long wavelengths).

In beach amphipods, that belong to the same family as *Parhyale* (talitrid amphipods), were λmax was measured in the eyes, a major peak was found at ~520nm accompanied by a smaller peak bellow 400nm (Fig. III-3). We can therefore speculate that this small peak is sufficient to activate R1-R4 photoreceptors thus delivering light polarisation information.

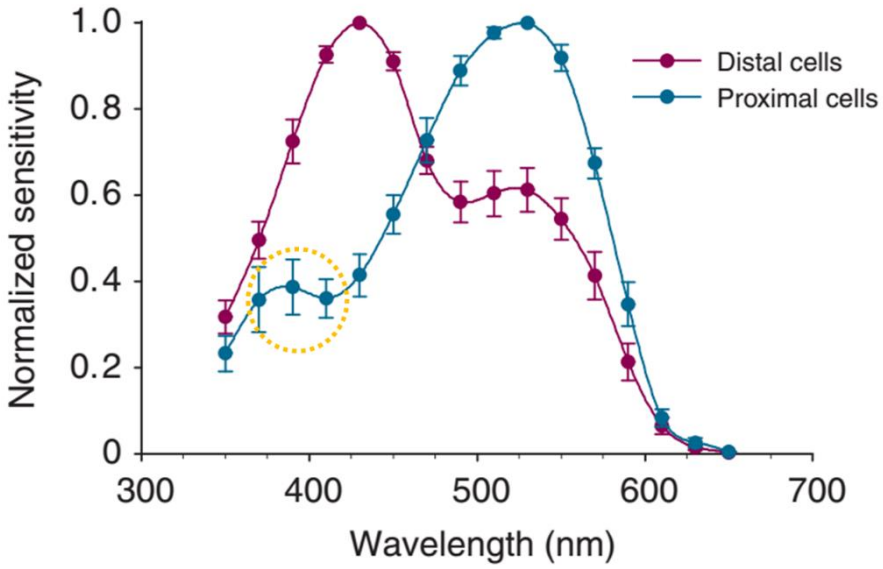

Fig. III-3 Electro-retinograms in *Talorchestia longicornis* – Spectral sensitivity curves of dark-adapted *T. longicornis* eyes at proximal and distal parts of the ommatidium. When a peak of sensitivity is recorded at 520nm (at the proximal part of the ommatidium), it is followed by a small peak at ~400nm (yellow dashed lines). *From* (Cohen et al. 2010)

This hypothesis could be explored by measuring activity of single photoreceptors in the presence of light of different wavelengths and e-vectors. This could be achieved by intracellular recordings or by using calcium indicators (GCamp for example (Chen et al., 2013; Miyawaki et al., 1997).

Fluorescent calcium indicators (either injected or genetically encoded) have been used for a long time to detect, in real time, calcium changes from which neuronal activity can be extrapolated: a fluorescent signal is detected in the presence of free calcium in the cytoplasm, which disappears once calcium levels drop. The transient signal must therefore be detected through live imaging of the tissue. For studies in visual system neurons this poses several problems, as the light source used to stimulate the photoreceptors and to image the calcium sensor must be separated. Another potential difficulty is the need to image live animals in, sometimes, deep layers of tissue. A possible solution for these problems is the use of permanent markers of calcium changes.

Ongoing projects

A recent paper has described the use of CaMPARI, a modified GCaMP calcium indicator that undergoes an irreversible green-to-red conversion when elevated intracellular calcium and UV illumination coincide in the same cell (Fosque et al., 2015). This means that a "snapshot" can be taken at the moment when the neuron is active. This snapshot can be imaged later, either in live animals or in fixed tissue.

I have started to apply this technique in *Parhyale* by creating transgenic lines expressing CaMPARI under the control of the DC5 promoter or the Ph-Ops1 CRE (the final constructs can be found in Material and Methods). This tool will allows us to understand: 1) which photoreceptors are active upon illumination with polarised light; 2) which wavelengths are they sensitive to and 3) which neuropils are involved in the processing of light polarisation information.

Conclusions and future perspectives

Parhyale is emerging as a powerful model system for studying diverse questions regarding evolution, development and regeneration. This success is mainly due to the ability to apply diverse molecular and genetic tools in this organism, and the impressive amenability of this animal for live imaging, both in embryonic and adult stages. At a time when most of cell biology, neurobiology and developmental biology studies in arthropods come from a single organism, *Drosophila*, studies in *Parhyale* bring new perspectives and open the door for comparative work. Such comparative work is essential for a better understanding of how sensory systems evolve.

The work presented in this thesis differs from other studies on crustacean visual systems by the implementation of modern genetic tools, namely the development of stable transgenic lines that label the photoreceptors and the ongoing work to apply clonal analysis/marking tools (RAEPPLI) and genetically encoded calcium indicators (CaMPARI) in *Parhyale*. These tools will help to address some of the questions that were left open by this work, namely: 1) how the visual space maps in the optic neuropils; 2) how the addition of new photoreceptors during development/growth is accommodated both in the retina and in the retinotopic map of the visual neuropils; 3) whether photoreceptors are sensitive to different directions of polarised light and in which neuropils this information is primarily processed. The identification of cis-regulatory elements that drive expression in specific photoreceptor cell types, presented in this work, also provides opportunities to manipulate development, connectivity and neuronal activity of those cells in the future.

An exciting discovery is the possible lack of long photoreceptor fibers connecting directly to the medulla in the *Parhyale* visual system. Considering the importance of these long fibers for colour information processing in hexapods, it would be interesting to study if and how/where colour information is processed in *Parhyale*. This also raises interesting questions for the evolution of colour processing.

The description of the *Parhyale* visual system sets the foundations from which more detailed work can be performed. The small number of ommatidia in the eye of *Parhyale* (50 as opposed to nearly 800 in *Drosophila*), makes their visual system a “simpler” case to study, which can be an advantage when describing developmental and neurobiology processes, especially if allied to live imaging. The phylogenetic position of *Parhyale*, as a member of the Pancrustacea which include the hexapods, will bring new insights on the evolution of visual systems within this vast and very diverse clade of animals.

Materials and Methods

Animals

Animals were kept in plastic boxes with artificial sea water (ASW) at room temperature.

When anaesthesia was needed (before fixation, mounting for live imaging or embryo collection), animals were kept in a clove oil solution (1:2500 in ASW) for up to 20 min, until they were immobile.

For embryo collection, pregnant females were anaesthetised and embryos were removed from the brood pouch with fine forceps, in coated Nunclon Petri dishes (Thermo Fisher Scientific) with Filtered ASW (as described in Rehm et al., 2009). Embryos were then kept in an incubator at 26ºC in FASW.

Embryo staging was made according to (Browne et al., 2005)

Fixation

For in situ hybridization and immunostainings, embryos were heat-fixed. Heat-fixation promotes the detachment of the cuticle from the tissue, which improved probe and antibody penetration in late embryos. Embryos were first dissected from the eggshell in FASW using fine forceps and submerged in a boiling heat-fixation buffer for 2 sec (0.4% NaC1 and 0.3% Triton). The buffer was immediately cooled down by pouring ice cold buffer. The embryos were then left on ice (inside the buffer) to completely cool down.

For in situ of adult heads, adult animals were anaesthetized and heat-fixed (same procedure from above). This procedure allowed to remove the head cuticle. For this the head was separated from the thorax and the cuticle was carefully opened from the dorsal part of the head, using very fine forceps, on a petri dish coated with Sylgard (Dow Corning).

After heat fixation, embryos and adult heads were quickly washed in PBS (2x 1min) before any other procedure.

Eye pigmentation removal

To remove dark eye pigmentation, fixed and dissected adult heads were submerged in a solution of 3% H_2O_2 and 0.5% w/w (Thisse and Thisse, 2008) KOH in water until the eye became light red (usually 10 to 20 min). A quick wash is PBS (3x5 min) was performed before any other procedure.

DNA / RNA extraction

Total mRNA or genomic DNA from *Parhyale* were used for gene and intergenic regions amplification.

Total RNA extraction

Total RNA was extracted from a mix of 5 embryos plus 5 adult heads (dissected from anesthetised adults with fine forceps in FASW, around the level of the first thoracic segment). The tissue was first homogenized in 300 µl of TRIzol™ (Thermo Fisher Scientific) with a plastic pestle within a 1.5mL Eppendorf® tube. Then an extra 700 µl of TRIzol™ were added to the tube. RNA extraction was then performed using the Direct-zol™ RNA MiniPrep Kit (Zymo Research), according to the manufacturer's instructions.

Genomic DNA extraction

Genomic DNA was extracted from 1 adult male. The tissue was first homogenised in 250ul of grinding buffer (Tris HCI 0.1 M (pH 9.0); EDTA 0.1 M; SDS 1%). The following protocol was then followed:

1. Add equal volume of phenol-chloroform, vortex
2. Spin 13.000rpm at 4ºC for 5min, take upper phase to new tube
3. Repeat step 1-2
4. Add 1 vol Chloroform
5. Spin 13.000rpm at 4ºC for 5min, take upper phase
6. Repeat step 4-5
7. Add 1/10 vol of 3M Sodium Acetate plus 1 vol of Isopropanol
8. Keep in freezer for more than 30 min
9. Spin 13.000rpm at 4ºC, for more than 30 min
10. Wash pellet in 500ul EtOh 70%
11. Spin 13.000rpm at 4ºC, 5 min
12. Dilute pellet in 50ul of water

Opsin identification in *Parhyale* (results Part 1)

To identify opsin homologues in *Parhyale*, the *Drosophila* RH1 protein sequence was used as a query in BLAST searches of embryonic (Zeng et al., 2011) and head transcriptomes (courtesy of B. Hunt and E. Rosato). Sequences showing a high degree of identity to the input query were retrieved and reverse-BLASTed against the arthropod sequences of the NCBI Genbank database. Further confirmation was performed by analysing the predicted transmembrane structure (using the web tool PRALINE (Pirovano et al., 2008)) to identify the 7 transmembrane helices, characteristic of opsin proteins.

Opsins phylogenetic reconstruction

For reconstruction of the opsins phylogenetic tree a dataset of arthropod opsins was used, based on a previous study (Porter et al., 2007). Protein sequence data was retrieved from NCBI (see Table 1 for a complete list of the species and accession number of the opsin sequences used).

Table 1 Species name, accession number and λmax of the opsins used for the phylogenetic reconstruction

Group	*Species*	Acession #	λmax	λmax Ref
Cephalopoda	*Loligo forbesi*	X56788	494	(Morris et al., 1993)
	Loligo pealii	AY450853	493	(BROWN and BROWN, 1958)
	Loligo subulata	Z49108	499	(Morris et al., 1993)
	Sepia officinalis	AF000947	492	(BROWN and BROWN, 1958)
	Todarodes pacificus	X70498	480	(Naito et al., 1981)
	Enteroctopus dofleini	X07797	475	(Koutalos et al., 1989)
Chelicerata LWS	*Limulus polyphemus* (lateral eye)	L03781	520	(HUBBARD and WALD, 1960)
	L. Polyphemus (ocelli)	L03782	530	(Nolte, 1972)
Crustacea LWS	*Euphausia superba*	DQ852576	487	(Frank and Widder, 1999)
	Homarus gammarus	DQ852587	515	(Kent 1997, phD thesis)
	Cambarellus shufeldtii	AF003544	526	(Crandall and Cronin, 1997)
	Cambarus ludovicianus	AF003543	529	
	Orconectes virilis	AF003545	530	(Goldsmith, 1978)
	Procambarus milleri	AF003546	522	(Crandall and Cronin, 1997; Cronin, 1982)
	Procambarus clarkii	S53494	533	(Zeiger and Goldsmith, 1994)
	Archaeomysis grebnitzkii	DQ852573	496	(Porter et al., 2007)
	Holmesimysis costata	DQ852581	512	
	Mysis diluviana	DQ852591	501	
	Neomysis americana	DQ852592	520	
	Neogonodactylus oerstedii Rh1	DQ646869	489	(Cronin and Marshall, 1989a)
	N. oerstedii Rh2	DQ646870	528	
	N. oerstedii Rh3	DQ646871	522	
Insecta LWS	*Manduca sexta*	L78080	520	(White et al., 1983)
	Spodoptera exigua	AF385331	515	(Langer et al., 1979)
	Galleria mellonella	AF385330	510	(Goldman, 1975)
	Papilio Xuthus Rh1	AB007423	520	(Arikawa et al., 1987, 1999)
	P. xuthus Rh2	AB007424	520	
	P. xuthus Rh3	AB007425	575	
	Pieris rapae	AB177984	540	(Ichikawa and Tateda, 1982)
	Vanessa cardui	AF385333	530	(Briscoe et al., 2003)
	Junonia coenia	AF385332	510	(Briscoe, 2001)
	Heliconius erato	AF126750	570	(Struwe, 1972)
	Heliconius sara	AF126753	550	
	Bicyclus anynana	AF484249	560	(Vanhoutte et al., 2002)
	Camponotus abdominalis	U32502	510	(Popp et al., 1996)
	Cataglyphis bombycinus	U32501	510	
	Apis mellifera	U26026	529 m, 540 f	(Peitsch et al., 1992)
	Bombus terrestris	AY485301	529	
	Osmia rufa	AY572828	553	
	Schistocerca gregaria	X80071	520	(Gärtner and Towner, 1995)
	Sphodromantissp.	X71665	515	(Rossel, 1979)

Group	*Species*	Acession #	λmax	λmax Ref
Crustacea MWS	*Hemigrapsus sanguineus*	D50583	480	(Sakamoto et al., 1996)
Insecta MWS	*Drosophila melanogaster* Rh6	Z86118	508	(Salcedo et al., 1999)
	D. melanogaster Rh1	AH001026	478	(Feiler et al., 1988)
	Calliphora erythrocephala Rh1	M58334	490	(Paul et al., 1986)
	D. melanogaster Rh2	M12896	420	(Feiler et al., 1988)
Insecta blue	*S. gregaria*	X80072	430	(Gärtner and Towner, 1995)
	M. sexta	AD001674	450	(White et al., 1983)
	P. xuthus Rh4	AB028217	460	(Eguchi et al., 1982)
	A. mellifera	AF004168	439	(Townson et al., 1998)
	D. melanogaster Rh5	U67905	437	(Salcedo et al., 1999)
Insecta UV	*A. mellifera*	AF004169	353	(Townson et al., 1998)
	C. abdominalis	AF042788	360	(Smith et al., 1997)
	C. bombycinus	AF042787	360	
	M. sexta	L78081	357	(White et al., 1983)
	P. xuthus Rh5	AB028218		
	D. melanogaster Rh4	AH001040	375	(Feiler et al., 1992)
	D. melanogaster Rh3	M17718	345	
	Hyalella azteca	XP_018018325		
	Daphnia magna LWS	KZS05019.1		
	Daphnia magna UV	KZS12137.1		
	Daphnia magna blue	KZS21495.1		
	Procambarus clarkii LWS	ALJ26467.1		
	Procambarus clarkii SWS	ALJ26468.1		
Outgroups	*Bos taurus* rhodopsin	AH001149		
	Gallus gallus pineal opsin	U15762		
	Anolis carolinensis pineal opsin	AH007737		
	Homo sapiens GPR52	NM_005684		
	H. sapiens melatonin receptor 1A	NM_005958		

Protein sequences were aligned using the online tool MAFFT (Katoh et al., 2017), using default parameters (scoring matrix: BLOSUM62; gap opening penalty 1.53; strategy=L-ins-i). The alignment was then trimmed with TRIMAL (Capella-Gutiérrez et al., 2009) and AliView (Larsson, 2014) to remove columns with less than 8 positions and unaligned variable ends. The final alignment to reconstruct the phylogenetic tree had a total of 450 a.a. sequences.

The final Maximum Likelihood tree was obtained using the webserver IQTREE (Trifinopoulos et al., 2016). The best substitution model was chosen automatically by the program. Branch support values were estimated from 1000 bootstrap replicates.

In Situ Hybridization of Ph-Opsin 1 and Ph-Opsin2 (results Part 1)

Opsin probe synthesis

cDNA synthesis

~ 700 ng of the total RNA (extracted from a mix of 5 embryos and 5 adult heads) was Reverse transcribed into cDNA with SuperScript III and oligo(dT) primers (Invitrogen's SuperScript III First-Strand Synthesis SuperMix) according to manufacturer's instructions.

Opsin mRNA amplification

A region of 1.4kb of the Ph-Opsin1 transcript and a region of 600 bp of the Ph-Opsin2 transcript were amplified from ~150 ng of cDNA. Detailed conditions and primers used are depicted in Table 2.

Table 2 PCR conditions for Ph-Opsin1 and Ph-Opsin 2 probe amplification

		annealing Temp (X)
Ph-Opsin1	GATTGGTTCTGCACGTGGC	55ºC
	TTGAGTGACAACGTTTGTTGTCGG	
Ph-Opsin2	ATGTCCCACAGCCACAGCCCAT	62ºC
	TCCGGAATGTAGCGGCCCCAGC	

PCR		
95 ºC	2 min	
95 ºC	1 min	
X ºC	30 sec	x 35 cycles
72 ºC	1-2 min	
72 ºC	5 min	

Amplified transcripts were ligated to pGem®Teasy, which contains the SP6 and T7 RNA promoters, using a T4 DNA ligase (Promega). Success of ligation was accessed by colony PCR, and the insert sequence was confirmed by sequencing.

Probe Synthesis

For probe synthesis, the final pGemT-Ph-opsin1/2 plasmid was linearized with NcoI and the probe synthesized using a Sp6 Polymerase (Promega) and the DIG RNA Labelling Mix (Roche), according to manufacturer's instructions. A total of 1ug of linearized plasmid was used for the reaction. The probe was then stored at 100ng/ul in Hybridization buffer and used for *in situs* at 3ng/ul.

In Situ Protocol

For *in situ* hybridization, embryos from S26 to S28 were heat-fixed and re-fixed overnight (ON) at 4ºC in 4% formaldehyde (Polysciences) solution in PBS (PFA). Adult heads (after heat fixation and cuticle removal) were also re-fixed in 4% PFA ON at 4ºC.

The in situ protocol (based on Pavlopoulos et al., 2009; Rehm et al., 2009b) is summarized in Table 3. Samples were then mounted in 70% Glycerol, between a microscope slide and a coverslip, using clay as a spacer to avoid crushing of the samples. The embryos were cut along the anterior posterior axis using a fine razor blade and opened.

Table 3 In situ Hybridization protocol

Temp	Time	Procedure	Notes
RT	3x 10 min	PTw	PTw: 1x PBS, 0.1% Tween-20
RT	5 min	25% Methanol in PTW	
RT	5 min	50% Methanol in + PTW	
RT	5 min	75% Methanol in + PTW	
RT	5min	100% Methanol	
RT	5min	100% Methanol	
-20˚C		100% Methanol	
RT	5 min	75% Methanol in PTW	
RT	5 min	50% Methanol in PTW	
RT	5 min	25% Methanol in PTW	
RT	30 min	4% PFA	
RT	1X 5Min	PTW	
RT	3X 10 Min	PTW	
RT	30 Min	Detergent Solution	50mM Tris-HCl pH 7.5; 1mM EDTA pH 8.0; 150 mM NaCl; 1% SDS; 0.5% Tween-20
RT	1X 5Min	PTW	
RT	3x 10 min	PTW	
RT	10 min	50% Hyb/ 50% PTw	Hyb: 50% Formamide; 5xSSC; 50µg/ml heparin; 0.25%Tween-20; 1% SDS; 100µg/ml SS DNA
RT	10 min	Hyb mix	
65˚C	>3hr	Hyb-Mix	
40˚C	10 min	Unfreeze Probe stock	
		Dilute probe 1ng/ul	10 to 0.05ng
85˚C	5 min	Denature probe	
65˚C	35 hours	Add Probe	
65˚C	5x 20min	Hyb-mix (pre-heated to 65ºC)	
RT	45 min	Hyb-mix (pre-heated to 65ºC)	
RT	3x 10 min	TBST (replace half volume)	TBST : 150 mM NaCl; 10 mM KCl ; 50mM Tris pH 7.5
RT	2x10 min	TBST	
4˚C	1h	TBST + 1% BSA	
RT/4˚C	3h / ON	Dig AB	1:3000 anti-DIG Fab (Roche) in TBST+1% BSA
RT	4x 20 min	TBST	
RT	3x 5 min	AP buffer (fresh)	50 mM MgCl2; 100 mM NaCl; 100 mM Tris pH 9.5; 0.1% Tween-20
RT	Until developed	BCIP/NBT solution	1ml AP reaction buffer; 5µl NBT; 3.75µl BCIP
RT	10 min x4	TBST	
4˚C	ON	50% Glycerol in PBS	
RT	2h	70% Glycerol in PBS	

Immunocytochemistry and vibratome sectioning (results Part 1)

Antibody stainings were performed on whole mount embryos and vibratome sections. Embryos were dissected from the eggshell and heat-fixed as described above.

For vibratome sections, entire adults were fixed in Bouin solution (Sigma) for 24h and washed several times in PBS with 1% Triton (X-100) until the yellow colour disappeared. The animals were then mounted by submerging them in a petri dish filled with melted 3% agarose (in PBS), with the anterior part facing up. Once cooled down, a block of agarose (containing the sample) was cut and glued to the vibratome stage in order to section it. Sectioning was performed inside a bath of PBS. Sections of 150 to 300 µm thickness were taken and kept in PBS until staining. Sections were then treated with 3% H_2O_2 and 0.5% w/w KOH to remove pigmentation.

After fixation, embryos or floating vibratome sections were washed in PBS Triton 1% (4x 20min) and incubated in blocking solution (1%BSA in PBS 1% Triton) for 1h at room temperature (RT) for blocking. The primary antibody was diluted in blocking solution (in a total of 200ul) and incubated for 4 to 5 days at 4ºC. Samples were then washed in PBS 1% Triton (4x 30min). The secondary antibody was diluted in blocking solution (in a total of 200ul) and incubated for 3 days at 4ºC. Nuclei were counterstained with DAPI (4', 6-diamidino-2-phenylindole) at a concentration of 1:10000, alongside with secondary antibody incubation. Samples were then washed in PBS 0.1% Triton (4x 20min), incubated overnight in 50% glycerol and mounted in Vectashield® antifade mounting medium, between a microscope slide and a coverslip, using clay as a spacer to avoid crushing of the samples.

Primary antibodies used: mouse monoclonal 6-11B-1 for acetylated tubulin (1:1000) (Sigma) and rat monoclonal YL1-2 for tyrosinated tubulin (1:100). Secondary antibodies: goat anti-mouse Alexa 647 (Invitrogen) (1:2000); goat anti-rat Alexa 654 (Invitrogen) (1:2000).

Semi-thin sections, Ultra-thin sections and Transmitted electron microscopy (Results part 1 and part 2)

Transmitted electron microscopy was performed at Lund University, in collaboration with Dan-Eric Nilsson team. Ola Gustafsson from the TEM facility performed most of the manipulation to prepare the samples for TEM.

For fixation adult animals were cut in half to improve fixative penetration. The following protocol was used for fixation and embedding of adult *Parhyale.*

1. Pre fixation (2.5% Glutaraldehyde - 2% PFA -2% sucrose in phosphate buffer (PB) overnight (ON) +4°C
2. 5 or 6 rinses in PB, 1 hour at room temperature (RT)
3. Post fixation in 1% OsO_4 (in PB), 2 hours at RT
4. Several washes in PB
5. Dehydration at RT
    a. EtOH 70%, 2 x 10 min
    b. EtOH 96%, 2 x 10 min
    c. EtOH 100%, 2 x 10 min
6. Acetone, 2 x 20 min
7. Acetone/Epon 2:1, 30 min
8. Acetone/Epon 1:1, ON at RT
9. Epon 6-8 hours, RT
10. Embedding in fresh Epon and polymerization for 48 hours at 60°C

Solutions:
Phosphate Buffer PH 7.4 -0.1M
Solution A : Na_2HPO_4, $2H_2O$ 35.61g, in milliQ water
Solution B : NaH_2PO_4, $2H_2O$ 31.21g, in milliQ water
40.5 ml solution A + 9.5 ml solution B, fill up to 100 ml with milliQ water (osmolarity should be 226mOsm)
OsO_4 : = 2ml bulb of 4% OSO_4 from Electron Microscopy Sciences (EMS # 19150)
Epon: Kit EMbed_812 (EMS # 14120) OR epoxy resin (Agar 100; Agar Scientific)
Glutaraldehyde (EMS #16300)

For semi-thin sections, after embedding samples were sectioned with a glass blade at a thickness of 2-5um and stained with toluidine blue. Post fixation and sectioning were performed by Nicolas Labert.
Ultra-thin sections (50 nm) were made using a Leica EM UC7 ultratome with a diamond knife. The sections were mounted on copper grids, stained with uranyl acetate (2%, 30 min) and lead citrate (4 min), and examined using a JEOL JEM 1400 Plus transmission electron microscope.

Generation of Ph-Opsin transgenic animals (results Part 1)

In total, 6 constructs were used for generation of transgenic embryos using the Ph-Opsins genomic regions:

- Minos 3xP3::GFP, Ph-Ops1::GFP T2AmKateCAAX
- Minos 3xP3::GFP, Ph-Ops2test (1.5/ 2.5/ 5 kb) ::GFP T2AmKateCAAX
- Minos, Ph-Ops1::EGFPCAAX
- Minos 3xp3::DsRed, Ph-Ops2::mKateCAAX

Plasmids construction

Most plasmids were constructed using the MultiSite Gateway ®(GW) Pro recombination kit (Invitrogen), except for Minos 3xp3::DsRed, Ph-Ops2::mKateCAAX which was constructed using the Gibson® Assembly Kit (NEB).

An overview the GW cloning system can be seen in Figure 1. The original GW Tol2Kit plasmid library (Kwan et al., 2007) was a kind gift from the C. Norden lab (MPI-CBG). I then constructed several plasmids to adapt the library (originally with a Tol2 transposon vector) for Minos transposon-mediated transgenesis.

The final and intermediate plasmids, as well the cloning steps, including primers, are summarized in Table 4 and Table 5.

For all the PCRs a Phusion Polymerase (NEB) was used with the program: 98ºC for 30 s, 35x [98ºC for 15s X ºC for 45 s, and 72ºC for 1 to 2 min] followed by chain extension at 72 ºC for 15 min. The DNA template was used at a concentration of 100 ng/ul.

For the BP recombination (for construction of the entry clones) the following reaction was set up: 1 µL PCR product (50fmol); 1 µL pDONR (50fmol); 1 µL BP clonase 5x mix (Invitrogen); 2 µL TE Buffer. For the LR recombination (construction of the final plasmids), the final solution had: 1 µL pDest (20 fmol); 1 µL p3ENT (10fmol); 1 µL pME (10fmol); 1 µL p5ENTR (10fmol); 1 µL LR Clonase plus 5x mix (Invitrogen).

PDONR and pDest plasmids were amplified using CCDB Survival™ competent cells (Invitrogen) and PENTR plasmids amplified using TOP10 competent cells (Termo fisher Scientific), in agar plates supplemented with the suitable antibiotic (see Figure 1)

For the Gibson cloning, PCR products and linearized plasmid (Table 6) were assembled with the Gibson master mix, according to manufacturer's instructions.

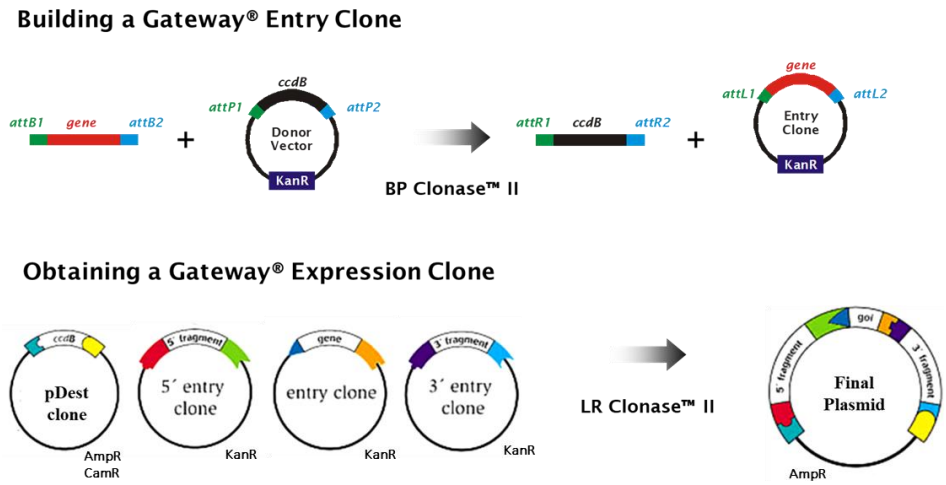

Figure 1 Overview of the GW cloning system - The Gateway® in vitro recombination system relies on 4 artificial, orthogonal att sequences. That is 4 of each attP, B, L, and R sequences that work in parallel. The cloning process involves two steps: 1) the generation of entry clones 2) recombination of entry clones to obtain a final plasmid. Entry Clones can be obtained through a BP clonase reaction. The final plasmid is obtained by a LR clonase reaction. Adapted from Invitrogen

MicroInjections

1-cell stage embryos were removed from anaesthetized wild-type females and aligned on a 3% agar step (in FASW) for injection, as described in (Kontarakis and Pavlopoulos, 2014). Injections were carried out on a stereoscope using quartz needles with a filament (Sutter Instruments #Qf100-50-10). For integration of the DNA constructs into the *Parhyale* genome, the plasmids were injected together with the Minos transposase mRNA. The final injection solution consisted of the plasmid at 100-150ng/µl and the Minos transposase mRNA at 100 ng/ul.

Injected embryos were kept in Nunc petri dishes with FASW supplemented with a mix of antibiotics and antifungal agents (Penicillin/Streptomycin/ Amphotericin B; PAN Biotech). Fluorescent signal was assessed from S26 to the end of embryogenesis using a Leica MZ 16F epifluorescence stereoscope. Positive G0s where either imaged or kept and crossed with wild-type animals once sexual maturation was reached to produce G1s. Positive G1s were then kept to establish the transgenic line.

Table 4 Entry plasmids for GW cloning

Final Plasmid	Fragment 1	Tm anneal	Vector	Cloning method
pDest minos 3xP3::dsRed R4R3 pDest minos 3xP3::GFP R4R3 pDest minos R4R3	**PCR from pTol2PA (Norden Lab)** TAAGCAGGCGCGCCCCATGATTACGCCAAGCTAT TAAGCAGGCGCGCCCGACGGCCAGTGAATTAT Digested: Asc1	56º	**Minos 3xP3 dsRed/GFP or Minos (only)** Digested: Asc1	Ligation (T4 Ligase Promega) ON 16ºC
P5ENTR Psl Polylinker	**PCR from pSLfa1180fa** GGGGACAACTTTGTATAGAAAAGTTGCGGGCGCGCCGGACGTCGACCTGAGGTAAT GGGGACTGCTTTTTTGTACAAACTTGCCCGGCCTAGGCGCG	58º	**pDONR P4P1R**	Recombination - BP reaction; 2h RT
PMENTR Psl Polylinker	GGGGACAAGTTTGTACAAAAAAGCAGGCTGGCGCGCCGGACGTCGACCTGAGGTAA GGGGACCACTTTGTACAAGAAAGCTGGGTCCCGGCCTAGGCGCG	60º		
P3ENTR Psl Polylinker	GGGGACAGCTTTCTTGTACAAAGTGGCTGGCGCGCCGGACGTCGACCTGAGGTAA GGGGACAACTTTGTATAATAAAGTTGCCCGGCCTAGGCGCG	60º		
P5ENTR Ph-Ops1	**PCR from *Parhyale* gDNA** TAAGCAGGATCCAAGGAATACAGAATATCTCTGAGATTA TAAGCACTCGAGATTACTCACTGTTCTCGAAGATTT Digested: BamH1 and Xho1	55º	**P5ENTR Psl Polylinker** Digested: BamH1 and Xho1	Ligation (T4 Ligase Promega) ON 16ºC
P5ENTR Ph-Ops2test 1.5kb	TAAGCAGGATCCATTGTCAGAGATTTGTTAAGACGAGGCCA TAAGCAGGATCCGGAATCTGTGGTGCCCCCC Digested: BamH1 and Xho1	66º		
P5ENTR Ph-Ops2test 2.2kb	TAAGCACTCGAGCTTTGTTGTAGTAAATCGGGCAACGC TAAGCAGGATCCGGAATCTGTGGTGCCCCCC Digested: BamH1 and Xho1	66º		
P5ENTR Ph-Ops2test 5kb	TAAGCAGGATCCGGAATCTGTGGTGCCCCCC TAAGCAGGATCCGGAATCTGTGGTGCCCCCC Digested: BamH1 and Xho1	66º		

Table 5 Gw reactions for final plasmids

Final Plasmid	middle plasmids	Cloning
Minos 3xP3::GFP, Ph-Ops1::GFP T2AmKateCAAX	pDest minos 3xP3::GFP R4R3 P5ENTR Ph-Ops1 pMENTR EGFP (no stop) (Norden Lab) P3ENTR T2A_mKate2CAAX (Norden Lab)	Recombination - LR reaction; ON RT
Minos 3xP3::GFP, Ph-Ops2test(1.5/2.5/5 kb)::GFP T2AmKateCAAX	pDest minos 3xP3::GFP R4R3 P5ENTR Ph-Ops2test 1.5kb /P5ENTR Ph-Ops2test 2.2kb /P5ENTR Ph-Ops2test 5kb pME EGFP (no stop) P3ENTR T2A_mKate2CAAX	Recombination - LR reaction; ON RT
Minos Ph-Ops1::EGFPCAAX	pDest minos R4R3 P5ENTR Ph-Ops1 pMENTR EGFP (Norden Lab) P3ENTR polyA (Norden Lab)	Recombination - LR reaction; ON RT

Table 6 Gibson Reaction set up

Final Plasmid	Fragment 1	Tm anneal	Fragment 2	Tm anneal	Fragment 3	Cloning
Minos 3xp3::dsRed, Ph-Ops2::mKateCAAX	**PCR from *Parhyale* gDNA** ATCGATACGCGTACGGCGCGACGGAACATTCTGCATCTTAGCTTGTGC CCTCTGCCCTCTCCACTGCCCATCCTGAGCCTCTTCACCTTGAGG	63º	**PCR from P3ENTR T2A_mKate2CAAX** AGGTGAAGAGGCTCAGGATGGGCAGTGGAGAGGGCAGAGG TGGATCCCCCCCTAGGCGCGTCAGGAGAGCACACACTTGCAGC	63º	**minos 3xp3dsRed** Digested: Asc1	Gibson assembly 1h 50ºC

Imaging

For live imaging of the transgenic lines (results in part 1), embryos were mounted in a drop of 1% low melting agarose in FASW on the surface a 30 mm glass bottom dish, with the eye facing the glass surface of the dish. For this the embryos were place in the dish and all the FASW was removed. The agarose was then carefully poured with a Pasteur pipette, forming a drop on the surface of the dish. Embryos were aligned using a thin brush.

Confocal images were obtained using a Zeiss LSM 780 single point scanning confocal microscope and a Zeiss C-Apochromat 40x NA 1.2 water immersion objective.

Fixed and immunostained embryos and vibratome sections (results in part 1 and 2) were mounted in Vectashield® antifade mounting medium, between a slide and a coverslip, using clay as a spacer to avoid crushing of the samples. Confocal images were obtained with a Zeiss Plan-Apochromat 40x NA 1.3 oil and a Plan-Apochromat 63x NA 1.4 oil objectives.

To study pupil adaptation, live adults (results in part 2) were mounted in a petri dish by gluing the head with surgical glue (Dermabond) and imaged using a Leica M205 stereoscope. After dark adaptation of the eyes, a single image was taken every 30 sec once the lights were turned on.

Image analysis

Images were treated using FIJI (Schindelin et al., 2012, 2015). Confocal images from Fig. II-6 F, Fig. II-7, Fig. II-8, Fig. II-9, Fig. II-10 were deconvolved using the FIJI plugin Deconvolution Lab2 (Sage et al., 2017). Pont spread function was calculated theoretically by the PSF generator plugin (Kirshner et al., 2013).

Behaviour experiments

For all behaviour experiments, a mix of wild-type males and females was used.

T-maze

A two-choice tube maze, or T-maze, was used to access *Parhyale* light preferences. The T-maze was built using dark PVC tubes whose walls were entirely covered with a white felt fabric, to avoid scattering/reflection of light. The maze was placed in a tank with enough water to cover the bottom with ~3cm of water.

Optical filters were built using 1 layer of polarising filter (ROSCO 7300 neutral grey linear polarizing film) and 2 sheets of tissue/crepe paper to diffuse the light, sandwiched in between two pieces of glass.

The same filters were used either with the polarising film facing the interior of the T-maze (for polarised light) or with the diffuser sheets facing the interior of the T-maze (for unpolarised light). This way it was guaranteed that the amount of light entering the T-maze did not vary in polarised and unpolarised light conditions. A piece of black felt fabric was used as dark filter.

Light intensity was measured using a LuxMeter (Sinometer LX1010B, JZK) place just after the filter. To vary light intensity, the light source (an LED bulb, 650 lm, 6500K; LemonBest) was placed at different distances from the extremities of the maze.

For each experiment, groups of 10 animals were placed in the centre of the maze. The centre was then covered to avoid entrance of light. The number of animals on either side of the maze (or in the middle) was counted after 5 min.

The experiments were performed at several times of the day (between 9h and 19h).

Arena

For studying the escape behaviour, a glass aquarium (50x50cm) was used as an arena. The sides of the arena were covered with black felt fabric to block light. The light filter was built with 1 layer of polarising filter and 2 layers of tissue/crepe paper. The same filter was used to polarise or unpolarise the light (as described above). The light source (an LED, 700Lux, 6500K) was placed above the arena at the necessary distance to illuminate it homogeneously (~50cm), keeping the light intensity below 400 Lux (measured with a Lux Meter).

Animals were placed in the centre of the arena through a little whole cut in the filter. Escape trajectories were recorded from bellow, using a digital camera. Individual tracks were then manually plotted using the ICY bioimage analyser and the ROI function.

Ongoing Projects

Stochastic cell labelling - RAEPPLI

For stochastic cell labelling using Raeppli (Kanca et al., 2014) there are currently 4 transgenic lines being prepared, using 2 strategies:

1. A heat inducible recombination using 2 separate transgenic lines. In animals carrying the two constructs, the recombination and fluorescent protein expression occurs after heat-shock. The nuclear marker H2B RFP is use to label cells were recombination does not occur.
   - Minos 3xP3::GFP, Ph-HS::Integrase
   - Minos 3xP3::dsRed, Ph-HS ATTB H2BRFP, RAEPPLI

2. Two transgenic lines carrying a Raeppli construct that includes an excisable integrase. Recombination and fluorescent protein expression occurs as soon the promoter is active. Recombination leads to stochastic labelling, concomitantly with excision of the integrase.
    - Minos DC5 ATTB:: Integrase, RAEPPLI
    - Minos Ph-Ops1 ATTB:: Integrase, RAEPPLI

All the plasmids were constructed using the GW recombination kit. The list of intermediate and final plasmids is depicted in Table 7.

Labelling of active neurons: CaMPARI

For expression of the calcium marker CaMPARI (Fosque et al., 2015), there are currently 2 transgenic lines being prepared, which express this fluorescent protein in photoreceptors and central nervous system:

- Minos 3xP3::GFP,Ph-Ops1::Campari
- Minos 3xP3::GFP,Ph-DC5::Campari

Table 7 Entry plasmids for GW reactions for the plasmids of ongoing projects

Final Plasmid	Fragment 1	Tm anneal	Vector	Cloning method
P5ENTR Ph-HS	**pMinos HS GFP** Digested BstXI; SalI		**P5ENTR PsI Polylinker** Digested: BstXI; SalI	Ligation (T4 Ligase Promega) ON 16ºC
P5ENTR Ph-HS ATTB	**PCR from Raeppli_V2_Ras (Kanca 2014)** taagcaggatccTCTccgcggtgcgggtg taagcaggatcccCGgtggagtacgcgcccgg Digested: BamH1	65º	**P5ENTR Ph-HS** Digested: BamH1	Ligation (T4 Ligase Promega) ON 16ºC
P5ENTR DC5 ATTB	**P5ENTR Ph-HS ATTB** Digested NarI; AscI		**PsI DC5 dsRed** Digested NarI; AscI	Ligation (T4 Ligase Promega) ON 16ºC
P5ENTR Ph-Ops1 ATTB	**PCR from Raeppli_V2_Ras (Kanca 2014)** taagcaggatccTCTccgcggtgcgggtg taagcaggatcccCGgtggagtacgcgcccgg	65º	**P5ENTR Ph-Ops1** Digested: ScaI	Ligation (T4 Ligase Promega) ON 16ºC
P3ENTR RAEPPLI	**pSL Raeppli_V2_Ras** Digested: SpeI; XbaI		**P3ENTR PsI Polylinker** Digested: SpeI; XbaI	Ligation (T4 Ligase Promega) ON 16ºC
PMENTR IntegraseNLS	**PCR from Raeppli_V2_Ras (Kanca 2014)** GGGACAAGTTTGTACAAAAAAGCAGGCTGGATGGACACGTACGCGGGTG GGGGACCACTTTGTACAAGAAAGCTGGGTCCAGACATGATAAGATACATTG	56º	**pDONR221**	Recombination - BP reaction; 2h RT
PMENTR CamPARI	**PCR from pcDNA3 CamPARI (Fosque 2015)** GGGGACCACTTTGTACAAGAAAGCTGGGTCTTATGAGCTCAGCCGACCTA GGGGACAAGTTTGTACAAAAAAGCAGGCTGGgccaccATGCTGCAGAACGAGCTTG	67º	**pDONR221**	Recombination - BP reaction; 2h RT

Table 8 GW reactions for the final plasmids of ongoing projects

Final Plasmid	middle plasmids	Cloning
Minos 3xP3::GFP, Ph-HS::Integrase	pDest minos 3xP3::GFP R4R3	Recombination - LR reaction; ON RT
	P5ENTR Ph-HS ATTB	
	PMENTR IntegraseNLS	
	P3ENTR Psl Polylinker	
Minos 3xP3::dsRed, Ph-HS ATTB H2BRFP, RAEPPLI	pDest minos 3xP3::dsRed R4R3	Recombination - LR reaction; ON RT
	P5ENTR Ph-HS ATTB	
	pMENTR H2B RFP (Norden Lab)	
	P3ENTR RAEPPLI	
Minos DC5 ATTB:: Integrase, RAEPPLI	pDest minos R4R3	Recombination - LR reaction; ON RT
	P5ENTR DC5 ATTB	
	PMENTR IntegraseNLS	
	P3ENTR RAEPPLI	
Minos Ph-Ops1 ATTB:: Integrase, RAEPPLI	pDest minos R4R3	Recombination - LR reaction; ON RT
	P5ENTR Ph-Ops1 ATTB	
	PMENTR IntegraseNLS	
	P3ENTR RAEPPLI	
Minos 3xP3::GFP,Ph-Ops1::Campari	pDest minos 3xP3::GFP R4R3	Recombination - LR reaction; ON RT
	P5ENTR Ph-Ops1	
	PMENTR CamPARIV39	
	P3ENTR polyA (Norden Lab)	
Minos 3xP3::GFP,Ph-DC5::Campari	pDest minos 3xP3::GFP R4R3	Recombination - LR reaction; ON RT
	P5ENTR DC5 ATTB	
	PMENTR CamPARIV39	
	P3ENTR polyA (Norden Lab)	

References

Alwes, F., Hinchen, B., and Extavour, C.G. (2011). Patterns of cell lineage, movement, and migration from germ layer specification to gastrulation in the amphipod crustacean Parhyale hawaiensis. Dev. Biol. *359*, 110–123.

Alwes, F., Enjolras, C., and Averof, M. (2016). Live imaging reveals the progenitors and cell dynamics of limb regeneration. Elife *5*.

Arikawa, K. (2003). Spectral organization of the eye of a butterfly, Papilio. J. Comp. Physiol. A Sensory, Neural, Behav. Physiol. *189*, 791–800.

Arikawa, K., Inokuma, K., and Eguchi, E. (1987). Pentachromatic visual system in a butterfly. Naturwissenschaften *74*, 297–298.

Arikawa, K., Mizuno, S., Scholten, D.G., Kinoshita, M., Seki, T., Kitamoto, J., and Stavenga, D.G. (1999). An ultraviolet absorbing pigment causes a narrow-band violet receptor and a single-peaked green receptor in the eye of the butterfly Papilio. Vision Res. *39*, 1–8.

Blythe, M.J., Malla, S., Everall, R., Shih, Y., Lemay, V., Moreton, J., Wilson, R., and Aboobaker, a A. (2012). High through-put sequencing of the Parhyale hawaiensis mRNAs and microRNAs to aid comparative developmental studies. PLoS One *7*, e33784.

Briscoe, A.D. (2001). Functional Diversification of Lepidopteran Opsins Following Gene Duplication. Mol. Biol. Evol. *18*, 2270–2279.

Briscoe, A.D., Bernard, G.D., Szeto, A.S., Nagy, L.M., and White, R.H. (2003). Not all butterfly eyes are created equal: Rhodopsin absorption spectra, molecular identification, and localization of ultraviolet-, blue-, and green-sensitive rhodopsin-encoding mRNAs in the retina ofVanessa cardui. J. Comp. Neurol. *458*, 334–349.

BROWN, P.K., and BROWN, P.S. (1958). Visual Pigments of the Octopus and Cuttlefish. Nature *182*, 1288–1290.

Browne, W.E., Price, A.L., Gerberding, M., and Patel, N.H. (2005). Stages of embryonic development in the amphipod crustacean, Parhyale hawaiensis. Genesis *42*, 124–149.

Budd, G.E., and Telford, M.J. (2009). The origin and evolution of arthropods. Nature *457*, 812–817.

Capella-Gutiérrez, S., Silla-Martínez, J.M., and Gabaldón, T. (2009). trimAl: a tool for automated alignment trimming in large-scale phylogenetic analyses. Bioinforma. Appl. NOTE *25*, 1972–197310.

Chaw, R.C., and Patel, N.H. (2012). Independent migration of cell populations in the early gastrulation of the amphipod crustacean Parhyale hawaiensis. Dev. Biol. *371*, 94–109.

Chen, T.-W., Wardill, T.J., Sun, Y., Pulver, S.R., Renninger, S.L., Baohan, A., Schreiter, E.R., Kerr, R.A., Orger, M.B., Jayaraman, V., et al. (2013). Ultrasensitive fluorescent proteins for imaging neuronal activity. Nature *499*, 295–300.

Chiou, T.-H., Kleinlogel, S., Cronin, T., Caldwell, R., Loeffler, B., Siddiqi, A., Goldizen, A., and Marshall, J. (2008). Circular Polarization Vision in a Stomatopod Crustacean. Curr. Biol. *18*, 429–434.

Chittka, L., Beier, W., Hertel, H., Steinmann, E., and Menzel, R. (1992). Opponent colour coding is a universal strategy to evaluate the photoreceptor inputs in Hymenoptera. J. Comp. Physiol. A *170*, 545–563.

Clandinin, T.R., and Zipursky, S.L. (2002). Making connections in the fly visual system. Neuron *35*, 827–841.

Cohen, J.H., and Putts, M.R. (2013). Polarotaxis and scototaxis in the supratidal amphipod Platorchestia platensis. J. Comp. Physiol. A. Neuroethol. Sens. Neural. Behav. Physiol. *199*, 669–680.

Cohen, J.H., Cronin, T.W., Lessios, N., and Forward, R.B. (2010). Visual physiology underlying orientation and diel behavior in the sand beach amphipod Talorchestia longicornis. J. Exp. Biol. *213*, 3843–3851.

Cong, P., Ma, X., Hou, X., Edgecombe, G.D., and Strausfeld, N.J. (2014). Brain structure resolves the segmental affinity of anomalocaridid appendages. Nature *513*, 538–542.

Crandall, K.A., and Cronin, T.W. (1997). The Molecular Evolution of Visual Pigments of Freshwater Crayfishes (Decapoda: Cambaridae). J. Mol. Evol. *45*, 524–534.

Cronin, T.W. (1982). Photosensitivity spectrum of crayfish rhodopsin measured using fluorescence of metarhodopsin. J. Gen. Physiol. *79*, 313–332.

Cronin, T.W. (2006). Invertebrate Vision in Water. In Invertebrate Vision, E. Warrant, and D.-E. Nilsson, eds. (Cambridge University Press), p.

Cronin, T., and Marshall, N.J. (1989a). Multiple spectral classes of photoreceptors in the retinas of gonodactyloid stomatopod crustaceans. J. Comp. Physiol. A *166*, 261–275.

Cronin, T.W., and Hariyama, T. (2002). Spectral Sensitivity in crustaceans. In The Crustacean Nervous System, K. Wiese, ed. (Berlin: Springer-Verlag), pp. 499–511.

Cronin, T.W., and Marshall, N.J. (1989b). A retina with at least ten spectral types of photoreceptors in a mantis shrimp. Nature *339*.

Cronin, T.W., Caldwell, R.L., and Marshall, J. (2001). Sensory adaptation. Tunable colour vision in a mantis shrimp. Nature *411*, 547–548.

Cronin, T.W., Johnsen, S., Marshall, N.J., and Warrant, E.J. (2014). Visual Ecology. (Princeton University Press).

Dacke, M., Byrne, M., Smolka, J., Warrant, E., and Baird, E. (2013). Dung beetles ignore landmarks for straight-line orientation. J. Comp. Physiol. A Neuroethol. Sensory, Neural, Behav. Physiol. *199*, 17–23.

Do, M.T.H., Kang, S.H., Xue, T., Zhong, H., Liao, H.-W., Bergles, D.E., and Yau, K.-W. (2009). Photon capture and signalling by melanopsin retinal ganglion cells. Nature *457*, 281–287.

Dohle, W., and Scholtz, G. (1988). Clonal analysis of the crustacean segment: the discordance between genealogical and segmental borders. Development *104*.

Dohle, W., Gerberding, M., Hejnol, A., and Scholtz, G. (2004). Cell lineage, segment differentiation, and gene expression in crustaceans. Crustac. Issues *15*, 95–133.

Domingos, P.M., Brown, S., Barrio, R., Ratnakumar, K., Frankfort, B.J., Mardon, G., Steller, H., and Mollereau, B. (2004). Regulation of R7 and R8 differentiation by the spalt genes. Dev. Biol. *273*, 121–133.

Dube, C., and Fleissner, G. (1986). Circadian rhythms in the compound eyes of the carabid beetle Pachymorpha (Anthia) sexguttata. II. Retinomotoric mechanisms of exogenous and endogenous senitivity control. Carabid Beetles Their Adapt. Dyn. XVIIth Int. Congr. Entomol. Hamburg, 1984 / Ed. by P.J. Den Boer ... [et Al.].

Eguchi, E., Watanabe, K., Hariyama, T., and Yamamoto, K. (1982). A comparison of electrophysiologically determined spectral responses in 35 species of Lepidoptera. J. Insect Physiol. *28*, 675–682.

Feiler, R., Harris, W.A., Kirschfeld, K., Wehrhahn, C., and Zuker, C.S. (1988). Targeted misexpression of a Drosophila opsin gene leads to altered visual function. Nature *333*, 737–741.

Feiler, R., Bjornson, R., Kirschfeld, K., Mismer, D., Rubin, G.M., Smith, D.P., Socolich, M., and Zuker, C.S. (1992). Ectopic expression of ultraviolet-rhodopsins in the blue photoreceptor cells of Drosophila: visual physiology and photochemistry of transgenic animals. J. Neurosci. *12*, 3862–3868.

Fischbach, K.-F., and Dittrich, a P. (1989). The optic lobe of Drosophila melanogaster. I: A. Golgi analysis of wild-type structure. Cell Tissue Res *258*, 441–475.

Fleissner, G., and Fleissner, G. (2006). Endogenous control of visual adaptation in invertebrates. In Invertebrate Vision, E. Warrant, and D.-E. Nilsson, eds. (Cambridge University Press), pp. 127–166.

Forward, R.B., Bourla, M.H., Darnell, M.Z., and Cohen, J.H. (2009). Entrainment of the circadian rhythm of the supratidal amphipod Talorchestia longicornis by light and temperature: mechanisms of detection and hierarchical organization. Mar. Freshw. Behav. Physiol. *42*, 233–247.

Forward, R.B., Bourla, M.H., Lessios, N.N., and Cohen, J.H. (2009). Orientation to shorelines by the supratidal amphipod Talorchestia longicornis: Wavelength specific behavior during sun compass orientation. J. Exp. Mar. Bio. Ecol. *376*, 102–109.

Fosque, B.F., Sun, Y., Dana, H., Yang, C.-T., Ohyama, T., Tadross, M.R., Patel, R., Zlatic, M., Kim, D.S., Ahrens, M.B., et al. (2015). Neural circuits. Labeling of active neural circuits in vivo with designed calcium integrators. Science *347*, 755–760.

Frank, T.M., and Widder, E.A. (1999). Comparative study of the spectral sensitivities of mesopelagic crustaceans. J. Comp. Physiol. A Sensory, Neural, Behav. Physiol. *185*, 255–265.

Gambineri, S., and Scapini, F. (2008). Importance of orientation to the sun and local landscape features in young inexpert Talitrus saltator (Amphipoda: Talitridae) from two Italian beaches differing in morphodynamics, erosion or stability. Estuar. Coast. Shelf Sci. *77*, 357–368.

Garbers, C., and Wachtler, T. (2016). Wavelength Discrimination in Drosophila Suggests a Role of Rhodopsin 1 in Color Vision. PLoS One *11*, e0155728.

Gärtner, W., and Towner, P. (1995). Invertebrate visual pigments. Photochem. Photobiol. *62*, 1–16.

Gehring, W.J., and Ikeo, K. (1999). Pax 6: Mastering eye morphogenesis and eye evolution. Trends Genet. *15*, 371–377.

Gerberding, M. (2002). Cell lineage analysis of the amphipod crustacean Parhyale hawaiensis reveals an early restriction of cell fates. Development *129*, 5789–5801.

Goldman, L. (1975). Microspectrophotometry of rhodopsin and metarhodopsin in the moth Galleria. J. Gen. Physiol. *66*, 383–404.

Goldsmith, T.H. (1978). The spectral absorption of crayfish rhabdoms: Pigment, photoproduct and pH sensitivity. Vision Res. *18*, 463–473.

Hadjieconomou, D., Timofeev, K., and Salecker, I. (2011a). A step-by-step guide to visual circuit assembly in Drosophila. Curr. Opin. Neurobiol. *21*, 76–84.

Hadjieconomou, D., Rotkopf, S., Alexandre, C., Bell, D.M., Dickson, B.J., and Salecker, I. (2011b). Flybow: genetic multicolor cell labeling for neural circuit analysis in Drosophila melanogaster. Nat. Methods *8*, 260–266.

Hallberg, E., and Nilsson, H.L. (1980). Classification of Amphipod Compound Eyes - the Fine Structure of the Ommatidial Units (Crustacea, Amphipoda). Zoomorphologie *306*, 279–306.

Hardie, R.C. (1985). Functional Organization of the Fly Retina. (Springer, Berlin, Heidelberg), pp. 1–79.

Hardie, R.C. (1986). The photoreceptor array of the dipteran retina. Trends Neurosci. *9*, 419–423.

Harzsch, S., and Glötzner, J. (2002). An immunohistochemical study of structure and development of the nervous system in the brine shrimp Artemia salina Linnaeus, 1758 (Branchiopoda, Anostraca) with remarks on the evolution of the arthropod brain. Arthropod Struct. Dev. *30*, 251–270.

Harzsch, S., and Hansson, B.S. (2008). Brain architecture in the terrestrial hermit crab Coenobita clypeatus (Anomura, Coenobitidae), a crustacean with a good aerial sense of smell. BMC Neurosci. *9*, 58.

Harzsch, S., Vilpoux, K., Blackburn, D.C., Platchetzki, D., Brown, N.L., Melzer, R., Kempler, K.E., and Battelle, B. a (2006). Evolution of arthropod visual systems: development of the eyes and central visual pathways in the horseshoe crab Limulus polyphemus Linnaeus, 1758 (Chelicerata, Xiphosura). Dev. Dyn. *235*, 2641–2655.

Hayashi, T., Kojima, T., and Saigo, K. (1998). Specification of primary pigment cell and outer photoreceptor fates by BarH1 homeobox gene in the developing Drosophila eye. Dev. Biol. *200*, 131–145.

Heinze, S., and Homberg, U. (2007). Maplike Representation of Celestial E-Vector Orientations in the Brain of an Insect. Science (80-.). *431*, 2004–2006.

Henze, M.J., Oakley, T.H., C, D., SE, F., HM, R., DW, H., SM, B., TW, C., A, G., and AR, L. (2015). The dynamic evolutionary history of pancrustacean eyes and opsins. Integr. Comp. Biol. *55*, 830–842.

Higashijima, S.I., Kojima, T., Michiue, T., Ishimaru, S., Emori, Y., and Saigo, K. (1992). Dual Bar homeo box genes of Drosophila required in two photoreceptor cells, R1 and R6, and primary pigment cells for normal eye development. Genes Dev. *6*, 50–60.

Hoglund, G., Struwe, G., and G., H.G.; S. (1969). Pigment Migration and Spectral sensitivity in the compound eye of Moths. Z. Vergl. Physiol.

HUBBARD, R., and WALD, G. (1960). Visual Pigment of the Horseshoe Crab, Limulus Polyphemus. Nature *186*, 212–215.

Ichikawa, T., and Tateda, H. (1982). Distribution of color receptors in the larval eyes of four species of lepidoptera. J. Comp. Physiol. ? A *149*, 317–324.

Ito, K., Shinomiya, K., Ito, M., Armstrong, J.D., Boyan, G., Hartenstein, V., Harzsch, S., Heisenberg, M., Homberg, U., Jenett, A., et al. (2014). A systematic nomenclature for the insect brain. Neuron *81*, 755–765.

Kanca, O., Caussinus, E., Denes, A.S., Percival-Smith, A., and Affolter, M. (2014). Raeppli: a whole-tissue labeling tool for live imaging of Drosophila development. Development *141*, 725–725.

Kao, D., Lai, A.G., Stamataki, E., Rosic, S., Konstantinides, N., Jarvis, E., Di Donfrancesco, A., Pouchkina-Stancheva, N., Sémon, M., Grillo, M., et al. (2016). The genome of the crustacean *Parhyale hawaiensis,* a model for animal development, regeneration, immunity and lignocellulose digestion. Elife *5*.

Karman, S., Diah, S., and Gebeshuber, I. (2012). Bio-Inspired Polarized Skylight-Based Navigation Sensors: A Review. Sensors *12*, 14232–14261.

Katoh, K., Rozewicki, J., and Yamada, K.D. (2017). MAFFT online service: multiple sequence alignment, interactive sequence choice and visualization. Brief. Bioinform.

Kelber, A., and Henze, M.J. (2013). Colour Vision: Parallel Pathways Intersect in Drosophila. Curr. Biol. *23*, R1043–R1045.

KELBER, A., VOROBYEV, M., and OSORIO, D. (2003). Animal colour vision – behavioural tests and physiological concepts. Biol. Rev. Camb. Philos. Soc. *78*, S1464793102005985.

Keskinen, E., Takaku, Y., Meyer-rochow, V.B., and Hariyama, T. (2002). Postembryonic Eye Growth in the seashore Isopod Ligia exotica (Crustacea, Isopoda). Biol. Bull. *202*, 223–231.

KIRK, M.D. (1982). THE CRAYFISH VISUAL SYSTEM: INTRACELLULAR STUDIES AND MORPHOLOGIES OF IDENTIFIED INTERNEURONS.

Kirschfeld, K. (1972). The Visual System of Musca: Studies on Optics, Structure and Function. In Information Processing in the Visual Systems of Anthropods, (Berlin, Heidelberg: Springer Berlin Heidelberg), pp. 61–74.

Kirshner, H., Aguet, F., Sage, D., and Unser, M. (2013). 3-D PSF fitting for fluorescence microscopy: Implementation and localization application. J. Microsc. *249*, 13–25.

Konstantinides, N., and Averof, M. (2014). A Common Cellular Basis for Muscle Regeneration in Arthropods and Vertebrates. Science (80-.). *343*, 788–791.

Kontarakis, Z., and Pavlopoulos, A. (2014). Hox Genes. In Hox Genes. Methods in Molecular Biology, G. Y, and R. R, eds. (Humana Press, New York, NY), p.

Kontarakis, Z., Pavlopoulos, A., Kiupakis, A., Konstantinides, N., Douris, V., and Averof, M. (2011). A versatile strategy for gene trapping and trap conversion in emerging model organisms. Development *138*, 2625–2630.

Koutalos, Y., Ebrey, T.G., Tsuda, M., Odashima, K., Lien, T., Park, M.H., Shimizu, N., Derguini, F., and Nakanishi, K. (1989). Regeneration of bovine and octopus opsins in situ with natural and artificial retinals. Biochemistry *28*, 2732–2739.

Kwan, K.M., Fujimoto, E., Grabher, C., Mangum, B.D., Hardy, M.E., Campbell, D.S., Parant, J.M., Yost, H.J., Kanki, J.P., and Chien, C.-B. (2007). The Tol2kit: a multisite gateway-based construction kit for Tol2 transposon transgenesis constructs. Dev. Dyn. *236*, 3088–3099.

Langer, H., Hamann, B., and Meinecke, C.C. (1979). Tetrachromatic visual system in the mothSpodoptera exempta (Insecta: Noctuidae). J. Comp. Physiol. ? A *129*, 235–239.

Larsson, A. (2014). AliView: a fast and lightweight alignment viewer and editor for large datasets. Bioinformatics *30*, 3276–3278.

Legg, D.A., Sutton, M.D., and Edgecombe, G.D. (2013). Arthropod fossil data increase congruence of morphological and molecular phylogenies. Nat. Commun. *4*, 1–7.

Lesser, M.P., Carleton, K.L., Böttger, S.A., Barry, T.M., and Walker, C.W. (2011). Sea urchin tube feet are photosensory organs that express a rhabdomeric-like opsin and PAX6. Proceedings. Biol. Sci. *278*, 3371–3379.

Liubicich, D.M., Serano, J.M., Pavlopoulos, A., Kontarakis, Z., Protas, M.E., Kwan, E., Chatterjee, S., Tran, K.D., Averof, M., and Patel, N.H. (2009). Knockdown of Parhyale Ultrabithorax recapitulates evolutionary changes in crustacean appendage morphology. Proc. Natl. Acad. Sci. U. S. A. *106*, 13892–13896.

Livet, J., Weissman, T.A., Kang, H., Draft, R.W., Lu, J., Bennis, R.A., Sanes, J.R., and Lichtman, J.W. (2007). Transgenic strategies for combinatorial expression of fluorescent proteins in the nervous system. Nature *450*, 56–62.

Macpherson, B.R. (1977). Microanatomy of the central nervous system of Gammarus Setosus Dementieva (amphipoda). THe supraoesophageal Ganglion (brain).

Marshall, N.J. (1988). A unique colour and polarization vision system in mantis shrimps. Nature *333*, 557–560.

Marshall, N.J., Cronin, T.W., and Frank, T.M. (2003). Visual Adaptations in Crustaceans: Chromatic, Developmental, and Temporal Aspects. In Sensory Processinf in Aquatic Environments, (Springer-Verlag), pp. 129–145.

Martin, A., Serano, J.M., Jarvis, E., Bruce, H.S., Wang, J., Ray, S., Barker, C.A., O'Connell, L.C., and Patel, N.H. (2016). CRISPR/Cas9 Mutagenesis Reveals Versatile Roles of Hox Genes in Crustacean Limb Specification and Evolution. Curr. Biol. *26*, 14–26.

Meyer-Rochow, V.B., Towers, D., and Ziedins, I. (1990). Growth patterns in the eye of Petrolisthes elongatus (Crustacea; Decapoda; Anomura). Exp. Biol. *48*, 329–340.

Miyawaki, A., Llopis, J., Heim, R., McCaffery, J.M., Adams, J.A., Ikura, M., and Tsien, R.Y. (1997). Fluorescent indicators for Ca2+based on green fluorescent proteins and calmodulin. Nature *388*, 882–887.

Mlodzik, M., Hiromi, Y., Weber, U., Goodman, C.S., and Rubin, G.M. (1990). The Drosophila seven-up gene, a member of the steroid receptor gene superfamily, controls photoreceptor cell fates. Cell *60*, 211–224.

Morris, A., Bowmaker, J.K., and Hunt, D.M. (1993). The Molecular Basis of a Spectral Shift in the Rhodopsins of Two Species of Squid from Different Photic Environments. Proc. R. Soc. B Biol. Sci. *254*, 233–240.

Naito, T., Nashima-Hayama, K., Ohtsu, K., and Kito, Y. (1981). Photoreactions of cephalopod rhodopsin. Vision Res. *21*, 935–941.

Narendra, A., Alkaladi, A., Raderschall, C. a, Robson, S.K. a, and Ribi, W. a (2013). Compound eye adaptations for diurnal and nocturnal lifestyle in the intertidal ant, Polyrhachis sokolova. PLoS One *8*, e76015.

Nässel, D.R. (1976). The retina and retinal projection on the lamina of the crayfish Pacifastacus leniusculus(Dana). J Comp Neurol *167*.

Nässel, D.R., Rolf, E., Rolf, O., R, N.D., Elofsson, R., and Odselius, R. (1978). Neuronal Connectivity Patterns in the Compound Eyes of Artemia salina and Daphnia magna (Crustacea : Branchiopoda)*. Cell Tissue Res. *457*, 435–457.

Nestorov, P., Battke, F., Levesque, M.P., and Gerberding, M. (2013). The maternal transcriptome of the crustacean Parhyale hawaiensis is inherited asymmetrically to invariant cell lineages of the ectoderm and mesoderm. PLoS One *8*, e56049.

Nilsson, D.-E. (2009). The evolution of eyes and visually guided behaviour. Philos. Trans. R. Soc. Lond. B. Biol. Sci. *364*, 2833–2847.

Nilsson, D.-E., and Kelber, A. (2007). A functional analysis of compound eye evolution. Arthropod Struct. Dev. *36*, 373–385.

Nolte, J. (1972). Electrophysiological Properties of Cells in the Median Ocellus of Limulus. J. Gen. Physiol. *59*, 167–185.

Oakley, T.H. (2003). On homology of arthropod compound eyes. Integr. Comp. Biol. *43*, 522–530.

Omoto, J.J., Keleş, M.F., Nguyen, B.C.M., Bolanos, C., Lovick, J.K., Frye, M.A., and Hartenstein, V. (2017). Visual Input to the Drosophila Central Complex by Developmentally and Functionally Distinct Neuronal Populations. Curr. Biol. *27*, 1098–1110.

Özhan-Kizil, G., Havemann, J., and Gerberding, M. (2009). Germ cells in the crustacean Parhyale hawaiensis depend on Vasa protein for their maintenance but not for their formation. Dev. Biol. *327*, 230–239.

Parchem, R.J., Poulin, F., Stuart, A.B., Amemiya, C.T., and Patel, N.H. (2010). BAC library for the amphipod crustacean, Parhyale hawaiensis. Genomics *95*, 261–267.

Paterson, J.R., García-Bellido, D.C., Lee, M.S.Y., Brock, G.A., Jago, J.B., and Edgecombe, G.D. (2011). Acute vision in the giant Cambrian predator Anomalocaris and the origin of compound eyes. Nature *480*, 237–240.

Paul, R., Steiner, A., and Gemperlein, R. (1986). Spectral sensitivity ofCalliphora erythrocephala and other insect species studied with Fourier Interferometric Stimulation (FIS). J. Comp. Physiol. A *158*, 669–680.

Pavlopoulos, A., and Averof, M. (2005). Establishing genetic transformation for comparative developmental studies in the crustacean Parhyale hawaiensis. Proc. Natl. Acad. Sci. U. S. A. *102*, 7888–7893.

Pavlopoulos, A., Kontarakis, Z., Liubicich, D.M., Serano, J.M., Akam, M., Patel, N.H., and Averof, M. (2009). Probing the evolution of appendage specialization by Hox gene misexpression in an emerging model crustacean. Proc. Natl. Acad. Sci. U. S. A. *106*, 13897–13902.

Peitsch, D., Fietz, A., Hertel, H., de Souza, J., Ventura, D.F., and Menzel, R. (1992). The spectral input systems of hymenopteran insects and their receptor-based colour vision. J. Comp. Physiol. A *170*, 23–40.

Perry, M., Kinoshita, M., Saldi, G., Huo, L., Arikawa, K., and Desplan, C. (2016). Molecular logic behind the three-way stochastic choices that expand butterfly colour vision. Nature *535*, 280–284.

Pirovano, W., Feenstra, K.A., and Heringa, J. (2008). PRALINETM: a strategy for improved multiple alignment of transmembrane proteins. Bioinformatics *24*, 492–497.

Popp, M.P., Grisshammer, R., Hargrave, P.A., and Smith, W.C. (1996). Ant opsins: Sequences from the Saharan silver ant and the carpenter ant. Invertebr. Neurosci. *1*, 323–329.

Porter, M.L., Cronin, T.W., McClellan, D. a., and Crandall, K. a. (2007). Molecular characterization of crustacean visual pigments and the evolution of pancrustacean opsins. Mol. Biol. Evol. *24*, 253–268.

Porter, M.L., Blasic, J.R., Bok, M.J., Cameron, E.G., Pringle, T., Cronin, T.W., and Robinson, P.R. (2012a). Shedding new light on opsin evolution. Proc. Biol. Sci. *279*, 3–14.

Porter, M.L., Bok, M.J., Robinson, P.R., and Cronin, T.W. (2012b). Molecular diversity of visual pigments in Stomatopoda (Crustacea). Vis. Neurosci. *26*, 255–265.

Price, A.L., Modrell, M.S., Hannibal, R.L., and Patel, N.H. (2010). Mesoderm and ectoderm lineages in the crustacean Parhyale hawaiensis display intra-germ layer compensation. Dev. Biol. *341*, 256–266.

Ramm, T., and Scholtz, G. (2017). No sight, no smell? - Brain anatomy of two amphipod crustaceans with different lifestyles. Arthropod Struct. Dev. 1–15.

Regier, J.C., Shultz, J.W., Zwick, A., Hussey, A., Ball, B., Wetzer, R., Martin, J.W., and Cunningham, C.W. (2010). Arthropod relationships revealed by phylogenomic analysis of nuclear protein-coding sequences. Nature *463*, 1079–1083.

Rehm, E.J., Hannibal, R.L., Chaw, R.C., Vargas-Vila, M. a, and Patel, N.H. (2009a). Fixation and dissection of Parhyale hawaiensis embryos. Cold Spring Harb. Protoc. *2009*, pdb.prot5127.

Rehm, E.J., Hannibal, R.L., Chaw, R.C., Vargas-Vila, M.A., and Patel, N.H. (2009b). In situ hybridization of labeled RNA probes to fixed Parhyale hawaiensis embryos. Cold Spring Harb. Protoc. *2009*, pdb.prot5130.

Reisenman, C.E., Insausti, T.C., and Lazzari, C.R. (2002). Light-induced and circadian changes in the compound eye of the haematophagous bug Triatoma infestans (Hemiptera : Reduviidae). *210*, 201–210.

Ro, A., and Nilsson, D. (1995). Pupil adjustments in the eye of the common backswimmer. *77*, 71–77.

Rossel, S. (1979). Regional differences in photoreceptor performance in the eye of the praying mantis. J. Comp. Physiol. ? A *131*, 95–112.

Sage, D., Donati, L., Soulez, F., Fortun, D., Schmit, G., Seitz, A., Guiet, R., Vonesch, C., and Unser, M. (2017). DeconvolutionLab2: An open-source software for deconvolution microscopy. Methods *115*, 28–41.

Sakamoto, Hisatomi, Tokunaga, and Eguchi (1996). Two opsins from the compound eye of the crab Hemigrapsus sanguineus. J. Exp. Biol. *199*, 441–450.

Salcedo, E., Huber, A., Henrich, S., Chadwell, L. V, Chou, W.H., Paulsen, R., and Britt, S.G. (1999). Blue- and

green-absorbing visual pigments of Drosophila: ectopic expression and physiological characterization of the R8 photoreceptor cell-specific Rh5 and Rh6 rhodopsins. J. Neurosci. *19*, 10716–10726.

Sandeman, D., Sandeman, R.E., Derby, C., and Schmidt, M. (1992). Morphology of the brain of Crayfish, Crabs and Spiny lobsters: A common nomenclature for homologous structures. Biol. Bull. MBL *183*, 304–326.

Satoh, A.K., Li, B.X., Xia, H., and Ready, D.F. (2008). Calcium-activated Myosin V closes the Drosophila pupil. Curr. Biol. *18*, 951–955.

Schindelin, J., Arganda-Carreras, I., Frise, E., Kaynig, V., Longair, M., Pietzsch, T., Preibisch, S., Rueden, C., Saalfeld, S., Schmid, B., et al. (2012). Fiji: an open-source platform for biological-image analysis. Nat. Methods *9*, 676–682.

Schindelin, J., Rueden, C.T., Hiner, M.C., and Eliceiri, K.W. (2015). The ImageJ ecosystem: An open platform for biomedical image analysis. Mol. Reprod. Dev. *82*, 518–529.

Schnaitmann, C., Garbers, C., Wachtler, T., and Tanimoto, H. (2013a). Color discrimination with broadband photoreceptors. Curr. Biol. *23*, 2375–2382.

Schnaitmann, C., Garbers, C., Wachtler, T., and Tanimoto, H. (2013b). Color discrimination with broadband photoreceptors. Curr. Biol. *23*, 2375–2382.

Schwind, R. (1984). Evidence for true polarization vision based on a two-channel analyzer system in the eye of the water bug,Notonecta glauca. J. Comp. Physiol. A *154*, 53–57.

Shaw, S. (1984). Early visual processing in insects. J. Exp. Biol. *112*.

Shaw, S.R., Fröhlich, A., and Meinertzhagen, I.A. (1989). Direct connections between the R7/8 and R1-6 photoreceptor subsystems in the dipteran visual system. Cell Tissue Res. *257*, 295–302.

Sims, S.J., and Macagno, E.R. (1985). Computer reconstruction of all the neurons in the optic ganglion of Daphnia magna. J. Comp. Neurol. *233*, 12–29.

Sinakevitch, I., Douglass, J.K., Scholtz, G., Loesel, R., and Strausfeld, N.J. (2003). Conserved and Convergent Organization in the Optic Lobes of Insects and Isopods, with Reference to Other Crustacean Taxa. J. Comp. Neurol. *467*, 150–172.

Smith, K.C., and Macagno, E.R. (1990). UV photoreceptors in the compound eye of Daphnia magna (Crustacea, Branchiopoda). A fourth spectral class in single ommatidia. J. Comp. Physiol. A *166*, 597–606.

Smith, W.C., Ayers, D.M., Popp, M.P., and Hargrave, P.A. (1997). Short wavelength-sensitive opsins from the Saharan silver and carpenter Ants. Invertebr. Neurosci. *3*, 49–56.

Sombke, A., and Harzsch, S. (2015). Immunolocalization of histamine in the optic neuropils of Scutigera coleoptrata (Myriapoda: Chilopoda) reveals the basal organization of visual systems in Mandibulata. Neurosci. Lett. *594*, 111–116.

Sommer, E.W., and Wehner, R. (1975). The retina-lamina projection in the visual system of the bee, Apis mellifera. Cell Tissue Res. *163*, 45–61.

Stowe, S. (1977). The retina-lamina projection in the crab Leptograpsus variegatus. Cell Tissue Res. *185*, 515–525.

Strausfeld, N.J. (2005). The evolution of crustacean and insect optic lobes and the origins of chiasmata. Arthropod Struct. Dev. *34*, 235–256.

Strausfeld, N.J., and Lee, J.-K. (1991). Neuronal basis for parallel visual processing in the fly. Vis. Neurosci. *7*, 13–33.

Strausfeld, N.J., Douglass, J.K., Campbell, J., and Higgins, C. (2006). Parallel processing in the optic lobes of flies and the ocurrence of motion computing circuits. In Invertebrate Vision, E.J. Warrant, and D.-E. Nilsson, eds. (Cambridge University Press), p.

Strausfeld, N.J., Ma, X., Edgecombe, G.D., Fortey, R.A., Land, M.F., Liu, Y., Cong, P., and Hou, X. (2016). Arthropod eyes: The early Cambrian fossil record and divergent evolution of visual systems. Arthropod Struct. Dev. *45*, 152–172.

Struwe, G. (1972). Spectral sensitivity of the compound eye in butterflies (Heliconius). J. Comp. Physiol. *79*, 191–196.

Takemura, S.-Y., Lu, Z., and Meinertzhagen, I.A. (2008). Synaptic circuits of the Drosophila optic lobe: the input terminals to the medulla. J. Comp. Neurol. *509*, 493–513.

Takemura, S.Y., Kinoshita, M., and Arikawa, K. (2005). Photoreceptor projection reveals heterogeneity of lamina cartridges in the visual system of the Japanese yellow swallowtail butterfly, Papilio xuthus. J. Comp. Neurol. *483*, 341–350.

Thisse, C., and Thisse, B. (2008). High-resolution in situ hybridization to whole-mount zebrafish embryos. Nat. Protoc. *3*, 59–69.

Tomlinson, A., Kimmel, B.E., and Rubin, G.M. (1988). rough, a Drosophila homeobox gene required in photoreceptors R2 and R5 for inductive interactions in the developing eye. Cell.

Townson, S.M., Chang, B.S., Salcedo, E., Chadwell, L. V, Pierce, N.E., and Britt, S.G. (1998). Honeybee blue- and ultraviolet-sensitive opsins: cloning, heterologous expression in Drosophila, and physiological characterization. J. Neurosci. *18*, 2412–2422.

Trifinopoulos, J., Nguyen, L.-T., von Haeseler, A., and Minh, B.Q. (2016). W-IQ-TREE: a fast online phylogenetic tool for maximum likelihood analysis. Nucleic Acids Res. *44*, W232–W235.

Ugolini, a, Borgioli, G., Galanti, G., Mercatelli, L., and Hariyama, T. (2010). Photoresponses of the compound eye of the sandhopper Talitrus saltator (Crustacea, Amphipoda) in the ultraviolet-blue range. Biol. Bull. *219*, 72–79.

Vanhoutte, K.J.A., Eggen, B.J.L., Janssen, J.J.M., and Stavenga, D.G. (2002). Opsin cDNA sequences of a UV and green rhodopsin of the satyrine butterfly Bicyclus anynana. Insect Biochem. Mol. Biol. *32*, 1383–1390.

Varela, F.G. (1969). Fine structure of the visual system of the honeybee (Apis mellifera): I. The retina. J. Ultrastruct. Res. *29*, 236–259.

Varela, F.G. (1970). Fine structure of the visual system of the honey bee (Apis mellifera) II. The Lamina. J. Ultrastruct. Res. *31*, 178–194.

Velez, M.M., Wernet, M.F., Clark, D.A., and Clandinin, T.R. (2014). Walking Drosophila align with the e-vector of linearly polarized light through directed modulation of angular acceleration. J. Comp. Physiol. A. Neuroethol. Sens. Neural. Behav. Physiol. *200*, 603–614.

Vitzthum, H., Müller, M., and Homberg, U. (2002). Neurons of the central complex of the locust Schistocerca gregaria are sensitive to polarized light. J. Neurosci. *22*, 1114–1125.

Wakakuwa, M., Kurasawa, M., Giurfa, M., and Arikawa, K. (2005). Spectral heterogeneity of honeybee ommatidia. Naturwissenschaften *92*, 464–467.

Wardill, T.J., List, O., Li, X., Dongre, S., McCulloch, M., Ting, C.-Y., O'Kane, C.J., Tang, S., Lee, C.-H., Hardie, R.C., et al. (2012). Multiple Spectral Inputs Improve Motion Discrimination in the Drosophila Visual System. Science (80-.). *336*, 925–932.

Waterman, T.H. (1981). Polarization Sensitivity. In Handbook of Sensory Physiology, H. Autrum, ed.

(Springer Berlin Heidelberg, New York), pp. 281–469.

Wehner, rudiger (2001). POLARIZATION VISION – A UNIFORM SENSORY CAPACITY? J. Exp. Biol. *204*.

Wehner, R. (1976). Polarized-Light Navigation by Insects insects have evolved for the purpose is remarkably sophisticated. Sci. Am. *235*, 106–115.

Wehner, R., Bernard, G.D., and Geiger, E. (1975). Twisted and non-twisted rhabdoms and their significance for polarization detection in the bee. J. Comp. Physiol. ? A *104*, 225–245.

Wernet, M.F., Velez, M.M., Clark, D.A., Baumann-Klausener, F., Brown, J.R., Klovstad, M., Labhart, T., and Clandinin, T.R. (2012). Genetic dissection reveals two separate retinal substrates for polarization vision in Drosophila. Curr. Biol. *22*, 12–20.

White, R.H., Brown, P.K., Hurley, A.K., and Bennett, R.R. (1983). Rhodopsins, retinula cell ultrastructure, and receptor potentials in the developing pupal eye of the mothManduca sexta. J. Comp. Physiol. ? A *150*, 153–163.

Wolff, C., and Gerberding, M. (2015). "Crustacea": Comparative Aspects of Early Development. In Evolutionary Developmental Biology of Invertebrates 4: Ecdysozoa II: "Crustacea," A. Wanninger, ed. (Springer- Verlag Wien), pp. 1–190.

Wolff, C., Tinevez, J.-Y., Pietzsch, T., Stamataki, E., Harich, B., Preibisch, S., Shorte, S., Keller, P.J., Tomancak, P., and Pavlopoulos, A. (2017). Reconstruction of cell lineages and behaviors underlying arthropod limb outgrowth with multi-view light-sheet imaging and tracking. bioRxiv.

Yang, E.C., and Osorio, D. (1996). Spectral responses and chromatic processing in the dragonfly lamina. J. Comp. Physiol. A *178*, 543–550.

Young, S. (1974). DIRECTIONAL DIFFERENCES IN THE COLOUR SENSITIVITY OF DAPHNIA MAGNA. 3» Exp. Biol *61*, 261–267.

Zeiger, J., and Goldsmith, T.H. (1994). Behavior of crayfish rhodopsin and metarhodopsin in digitonin: the 510 and 562 nm "visual pigments" are artifacts. Vision Res. *34*, 2679–2688.

Zelhof, A.C., Hardy, R.W., Becker, A., and Zuker, C.S. (2006). Transforming the architecture of compound eyes. Nature *443*, 696–699.

Zeng, V., Villanueva, K.E., Ewen-Campen, B.S., Alwes, F., Browne, W.E., and Extavour, C.G. (2011). De novo assembly and characterization of a maternal and developmental transcriptome for the emerging model crustacean Parhyale hawaiensis. BMC Genomics *12*, 581.

Zheng, L., de Polavieja, G.G., Wolfram, V., Asyali, M.H., Hardie, R.C., and Juusola, M. (2006). Feedback Network Controls Photoreceptor Output at the Layer of First Visual Synapses in *Drosophila*. J. Gen. Physiol. *127*, 495–510.

Zhu, Y. (2013). The Drosophila visual system From neural circuits to behavior. 333–344.